Biomedical Research Institute (BRI) - Foundation for Research and Technology-Hellas (FORTH), Ioannina, Greece

Laboratory of Biological Chemistry, Department of Medicine, University of Ioannina, Greece

Master's thesis

Inter-institutional Interdepartmental Program of Postgraduate Studies
"Molecular and Cellular Biology and Biotechnology"

Unraveling the role of endocytic pathways of amyloid-beta clearance in brain endothelial cells as a protective mechanism against Alzheimer's disease.

Martha Kontostathi

Supervisor: Savvas Christoforidis, Professor of Biological Chemistry, Department of Medicine, University of Ioannina

Ioannina 2025

ACKNOWLEDGEMENTS

This Master's thesis was carried out at the Biomedical Research Institute (BRI) at Ioannina, of the Foundation for Research and Technology (FORTH), and the Laboratory of Biological Chemistry withing the Department of Medicine at the University of Ioannina.

I would like to thank Professor Savvas Christoforidis for giving me the opportunity to work in his lab and for his invaluable supervision. His guidance, insights, and support have contributed significantly to my personal and academic growth. I would especially like to thank the postdoctoral researcher Dr. Evi Vasili, for her daily assistance and dedicated guidance, which were crucial for the successful completion of this thesis and my academic development. I am also grateful to Professors Efstathios Friligkos, Dimitris Liakopoulos, Michaela Filiou, and Christos Gogas for kindly agreeing to serve as members of the evaluation committee.

I would also like to thank all the members of the lab — research scientist Alexandra Papafotika, PhD candidate Panagiotis Lentzaris, postdoctoral researcher Dr. Evangelia Goula, and postgraduate student Natalia Tsironi — for their collaboration and support during my thesis. Finally, I would like to thank all my friends and my family who supported me during my studies.

Contents

LIST OF ABBREVIATIONS

Abbreviation	Definition
ABC	ATP binding cassette
Aβ	Beta-amyloid
AD	Alzheimer's disease
AICD	APP intracellular domain
AJs	Adherens junctions
Ang-1	Angiopoetin-1
ApoE	Apolipoprotein E
APP	Amyloid precursor protein
BACE-1	β-amyloid cleaving enzyme / β-secretase
BBB	Blood-brain barrier
BCRP	Breast cancer resistance protein
BECs	Brain endothelial cells
bFGF	basic fibroblast growth factor
BM	Basement membrane
BSA	Bovine serum albumin
CaSRs	Calcium-sensing receptors
Cdc42	Cell division control protein 42
CLU	Clusterin
CME	Clathrin-mediated endocytosis
CNS	Central nervous system
C83	C-terminal fragment 83
C99	C-terminal fragment 99
ECM	Extracellular matrix
ECs	Endothelial cells
EIPA	5-N-Ethyl-N-isopropyl amiloride
ELISA	Enzyme-linked immunosorbent assay
EOAD	Early-onset Alzheimer's disease
ESAM	Endothelial cell-selective adhesion molecules
E6	Essential 6
E8	Essential 8
FAD	Familiar Alzheimer’s disease
GDNF	Glial-derived neurotrophic factor
HRP	Horseradish peroxidase
HUVEC	Human umbilical vein endothelial cells
ICC	Immunocytochemistry
IDE	Insulin-degrading enzyme
JAM	Junctional adhesion molecules
kDa	Kilodaltons
LOAD	Late-onset Alzheimer's disease
LRP1/2	Lipoprotein receptors 1/2
MRPs	Multidrug resistance proteins
NVU	Neurovascular unit
NFTs	Neurofibrillary tangles
OD	Optical density

PA	Phosphatidic acid
PBS	Phosphate buffer saline
PECAM-1	Platelet endothelial cell adhesion molecule-1
PFA	Paraformaldehyde
P-gp	P-glycoprotein
PICALM	Phosphatidylinositol-binding clathrin assembly protein
PIP_3	Phosphatidylinositol-(3,4,5)-trisphosphate
PI3K	Phosphatidylinositol-3-kinase
RA	all-trans retinoic acid
Rac1	Ras-related C3 botulinum toxin substrate 1
RPM	revolutions per minute
RT	Room temperature
sAPPa	Soluble APP alpha
sAPPβ	Soluble APP beta
SD	Standard deviation
siRNA	Small interfering RNA
TEER	Transendothelial electrical resistance
iPSCs/hiPSCs	Induced pluripotent stem cells/ human induced pluripotent stem cells
ISF	Interstitial fluid
TJs	Tight junctions
VEGF	Vascular endothelial growth factor
VEGFR	Vascular endothelial growth factor receptor
VE-cadherin	Vascular endothelial cadherin
VLDLR	Very low-density lipoprotein receptor
VWF	von Willebrand factor
WB	Western blotting
WPB	Weibel-Palade body
WT	Wild-type
ZOs	Zonula occludens

ABSTRACT

Alzheimer's disease is a neurodegenerative disease characterized by progressive memory loss and cognitive decline. The neuropathological hallmark of this condition is the accumulation of amyloid-β (Aβ) plaques and neurofibrillary tangles in the brain. Aβ deposition results primarily from impaired clearance of Aβ from the brain, a process that is largely facilitated by the brain endothelial cells (BECs) of the blood-brain barrier (BBB). It is already known that BECs utilize clathrin-mediated endocytosis to internalize Aβ and transport it across the BBB into the bloodstream. Since endothelial cells employ several distinct endocytosis pathways to uptake extracellular cargo, our focus shifted to exploring the previously uncharacterized endocytic pathways that may facilitate Aβ uptake and clearance by BECs, with particular emphasis on macropinocytosis. In parallel, another aim of the study was to establish a robust human in vitro BBB model using induced pluripotent stem cells (iPSCs), as a tool to investigate the endocytic pathways of BECs.

In the first part of the study, we utilized primary BECs to investigate the role of macropinocytosis in $A\beta_{42}$ uptake. Inhibition of this endocytic pathway through siRNAs targeting known modulators of macropinocytosis resulted in a significant reduction in $A\beta_{42}$ internalization. To further validate this finding in an in vivo system, we employed 5XFAD transgenic mice as an AD model, which exhibits early accumulation of Aβ plaques in the brain. Inhibition of macropinocytosis in this model using the chemical inhibitor EIPA led to increased accumulation of Aβ in the brain, highlighting the significant role of macropinocytosis in Aβ clearance. However, because EIPA inhibits macropinocytosis in multiple cell types rather than exclusively targeting BECs, it was not possible to precisely determine the specific contribution of impaired macropinocytosis in BECs in the observed effect.

In the second part of the study, we established an in vitro human BBB model using iPSCs derived from a healthy individual (WT) and from an AD patient carrying the ApoE ε4/ε4 genotype. To achieve this, we differentiated the iPSC lines into a mature and homogeneous population of BECs with a robust BBB phenotype, using a facile, reproducible and highly efficient differentiation protocol with fully defined components. The success of differentiation and acquisition of BBB properties was confirmed by the expression of tight and adherens junction proteins, endothelial markers and increased TEER values (>1000 $\Omega x cm^2$). The successful differentiation of both healthy- and patient-derived iPSCs into BECs provides a scalable and robust in vitro transwell BBB model for the investigation of endocytic pathways of BECs under physiological and diseased conditions. To further improve the model and enhance its physiological relevance, it is highly recommended to incorporate additional cellular components of the neurovascular unit into the transwell model in a coculture with iPSC-derived BECs. Moreover, iPSC-derived neurons with amyloidogenic properties can be utilized in this transwell setup to investigate Aβ transcytosis across BECs. Overall, comparing BECs derived from healthy individuals and AD patients can reveal cellular phenotypes associated with BBB dysfunction in AD, as well as potential endocytic abnormalities that contribute to impaired Aβ clearance across the BBB.

Περίληψη

Η νόσος Αλτσχάιμερ (ΝΑ) είναι μια νευροεκφυλιστική ασθένεια που χαρακτηρίζεται από προοδευτική απώλεια μνήμης και γνωστική έκπτωση. Το νευροπαθολογικό χαρακτηριστικό της πάθησης είναι η συσσώρευση πλακών βητα αμυλοειδούς (Αβ) και νευροϊνιδιακών δεματίων στον εγκέφαλο. Η συσσώρευση του Αβ προκύπτει κυρίως από τη μειωμένη κάθαρση του από τον εγκέφαλο —μια διαδικασία που μεσολαβείται σε μεγάλο βαθμό από τα ενδοθηλιακά κύτταρα του αιματεγκεφαλικού φραγμού (ΑΕΦ). Είναι ήδη γνωστό ότι τα ενδοθηλιακά κύτταρα χρησιμοποιούν την ενδοκυττάρωση μέσω κλαθρίνης για την πρόσληψη του Αβ και τη μεταφορά του διαμέσου του ΑΕΦ προς την κυκλοφορία του αίματος. Δεδομένου ότι τα ενδοθηλιακά κύτταρα χρησιμοποιούν διάφορες διακριτές οδούς ενδοκυττάρωσης για την πρόσληψη εξωκυττάριων μορίων, η έρευνά μας επικεντρώθηκε στη διερεύνηση άλλων, μέχρι τώρα μη χαρακτηρισμένων, ενδοκυτταρικών οδών που μπορεί να διευκολύνουν την πρόσληψη και κάθαρση του Αβ από τα ενδοθηλιακά κύτταρα, με ιδιαίτερη έμφαση στη μακροπινοκυττάρωση. Παράλληλα, ένας ακόμη στόχος της μελέτης ήταν η δημιουργία ενός αξιόπιστου ανθρώπινου in vitro μοντέλου του BBB, χρησιμοποιώντας επαγόμενα πολυδύναμα βλαστικά κύτταρα (iPSCs), ως εργαλείο για τη μελέτη των ενδοκυτταρικών οδών των ενδοθηλιακών κυττάρων.

Στο πρώτο μέρος της μελέτης, χρησιμοποιήθηκαν πρωτογενή εγκεφαλικά ενδοθηλιακά κύτταρα για τη διερεύνηση του ρόλου της μακροπινοκυττάρωσης στην πρόσληψη του $Aβ_{42}$. Η αναστολή αυτής της οδού ενδοκυττάρωσης μέσω siRNAs που στοχεύουν γνωστούς ρυθμιστές της μακροπινοκυττάρωσης οδήγησε σε σημαντική μείωση της πρόσληψης του Αβ42. Για την περαιτέρω επιβεβαίωση του ευρήματος αυτού in vivo, χρησιμοποιήθηκαν διαγονιδιακά ποντίκια 5XFAD ως μοντέλο της ΝΑ, το οποίο εμφανίζει πρώιμη συσσώρευση πλακών αμυλοειδούς στον εγκέφαλο. Η αναστολή της μακροπινοκυττάρωσης σε αυτό το μοντέλο με τη χρήση του χημικού αναστολέα EIPA οδήγησε σε αυξημένη συσσώρευση Αβ στον εγκέφαλο, γεγονός που υπογραμμίζει τον σημαντικό ρόλο της μακροπινοκυττάρωσης στην κάθαρση του Αβ. Ωστόσο, δεδομένου ότι το EIPA αναστέλλει τη μακροπινοκυττάρωση σε πολλούς τύπους κυττάρων και όχι αποκλειστικά στα ενδοθηλιακά, δεν ήταν εφικτό να προσδιοριστεί με ακρίβεια ο βαθμός συμβολής της αναστολής της μακροπινοκυττάρωσης στα ενδοθηλιακά κύτταρα στο παρατηρούμενο αποτέλεσμα.

Στο δεύτερο μέρος της μελέτης, εγκαθιδρύσαμε ένα in vitro ανθρώπινο μοντέλο του ΑΕΦ χρησιμοποιώντας iPSCs που προέρχονται από ένα υγιές άτομο (WT) και από έναν ασθενή με ΝΑ που φέρει το γονότυπο ApoE ε4/ε4. Για την επίτευξη αυτού, διαφοροποιήσαμε τα iPSCs σε έναν ώριμο και ομοιογενή πληθυσμό εγκεφαλικών ενδοθηλιακών κυττάρων με ισχυρό φαινότυπο ΑΕΦ, χρησιμοποιώντας ένα απλό, αναπαραγώγιμο και υψηλής απόδοσης πρωτόκολλο διαφοροποίησης με πλήρως καθορισμένα συστατικά. Η επιτυχία της διαφοροποίησης και η απόκτηση χαρακτηριστικών του ΑΕΦ επιβεβαιώθηκαν από την έκφραση πρωτεϊνών στενών συνδέσεων, ενδοθηλιακών δεικτών, καθώς και από αυξημένες τιμές TEER (>1000 $Ωxcm^2$). Η επιτυχής διαφοροποίηση τόσο των υγιών όσο και των προερχόμενων από ασθενή iPSCs προς ενδοθηλιακά κύτταρα παρέχει ένα επεκτάσιμο και αξιόπιστο in vitro μοντέλο του ΑΕΦ για τη μελέτη των ενδοκυτταρικών οδών των ενδοθηλιακών κυττάρων υπό φυσιολογικές και παθολογικές συνθήκες. Για τη βελτίωση του μοντέλου και την ενίσχυση της φυσιολογικής του συνάφειας, συνιστάται έντονα η

ενσωμάτωση επιπλέον κυτταρικών συστατικών της νευροαγγειακής μονάδας σε συνεκκαλλιέργεια με τα ενδοθηλιακά κύτταρα που προέρχονται από iPSCs. Επιπλέον, νευρώνες που προέρχονται από iPSCs και διαθέτουν αμυλοειδογενείς ιδιότητες μπορούν να χρησιμοποιηθούν στο ίδιο σύστημα για τη μελέτη της διακυττάρωσης του Αβ μέσω των ενδοθηλιακών κυττάρων. Συνολικά, η σύγκριση ενδοθηλιακών κυττάρων που προέρχονται από υγιή άτομα και από ασθενείς με ΝΑ μπορεί να αποκαλύψει κυτταρικούς φαινοτύπους που σχετίζονται με τη δυσλειτουργία του ΑΕΦ στη νόσο, καθώς και δυσλειτουργίες μονοπατιών ενδοκυττάρωσης που συμβάλλουν στη μειωμένη κάθαρση του Αβ διαμέσου του ΑΕΦ.

1. INTRODUCTION

1.1 Alzheimer's disease: prevalence, symptoms, risk factors.

Alzheimer's disease (AD) is the most prevalent neurodegenerative disease, responsible for 60-80% of dementia cases (Barker, Luis et al. 2002). This disease was named after the German psychiatric Alois Alzheimer in 1906, when he described the case of a 51-year-old woman who suffered from impaired memory and personality disorder before dying. This disease is defined as a severe pathology of the cerebral cortex that causes mental and cognitive deficits, such as memory loss, impairment of language and motor skills, loss of perception and physical disability in people older that 65 years of age (Breijyeh and Karaman 2020). In 2020, there were around 50 million patients with AD worldwide and by 2050 this number is estimated to reach 152 million. AD burden affects not only the patients and their families but also the global economy, as the estimated cost for the welfare of the patients reaches $1 trillion globally every year (Breijyeh and Karaman 2020). Currently, there is no cure for Alzheimer's disease, but only treatments alleviate the symptoms (Livingston, Huntley et al. 2020, Yiannopoulou and Papageorgiou 2020).

AD is a slowly progressive disease that can be classified into many clinical stages. At the pre-clinical stage, biological changes start to appear at the cortex and the hippocampus of the brain, with no detectable symptoms, but only a mild memory loss (De-Paula, Radanovic et al. 2012, Dubois, Hampel et al. 2016, Kumar, Sidhu et al. 2025). After several years, at the mild or early stage of AD, symptoms that impair daily life of the patients start to appear. These include distractibility, memory deficits, disorientation to place and time, mood swings and the onset of depression (Wattmo, Minthon et al. 2016, Kumar, Sidhu et al. 2025) . At the moderate stage of AD, patients exhibit increased memory loss, lose impulse control and have difficulty in reading, writing and speaking (Kumar, Sidhu et al. 2025). Finally, at the severe or late-stage of AD, the whole cerebral cortex is pathologically affected resulting in functional and cognitive impairment, that includes total disability in recognizing familiar faces, difficulties in swallowing and urinating, and eventually death, due to these complications (De-Paula, Radanovic et al. 2012, Apostolova 2016).

Several risk factors are related to the development of AD. Aging is one of the most prevalent risk factors, as in most cases AD pathology starts after 65 years of age (Guerreiro and Bras 2015). Aging is a process accompanied by impaired brain function and the loss of neuronal synapses, which can result in many medical conditions, including AD (Riedel, Thompson et al. 2016, Hou, Dan et al. 2019). AD can be classified into two types, considering the age of onset. Early-onset AD (EOAD) which is rare (1-6% of cases), affects individuals between 30 and 65 years old and is often hereditary. On the other hand, the more prevalent late-onset form (LOAD) begins after age 65 and can occur in individuals with or without family history (Tcw and Goate 2017). Apart from aging, genetic factors play a crucial role in the development of the disease. Approximately 70% of EOAD cases are inherited in an autosomal dominant manner. Genes associated with AD include Amyloid precursor protein (APP), Presenilin-1 (PSEN-1), Presenilin-2 (PSEN-2), and apolipoprotein E (ApoE).

While aging and genetics are the primary risk factors for Alzheimer's disease (AD), they do not account for all cases. Several environmental factors, including air pollution, diet, metals and infections, can contribute to the onset of the disease. These factors are known to induce oxidative stress and neuroinflammation, which are well-established risk factors for AD. Moreover, medical conditions, such as cardiovascular disease, obesity and diabetes, are also widely reported to be linked to an increased risk of developing AD (de Bruijn and Ikram 2014, Santos, Snyder et al. 2017).

1.2 Pathophysiological changes in the brain associated with AD.

Alzheimer's disease is characterized by two neuropathological hallmarks: the accumulation of extracellular senile plaques composed of amyloid-beta (Aβ) protein and intracellular neurofibrillary tangles (NFTs) (Butterfield and Boyd-Kimball 2004, Ittner, Ke et al. 2010). The brain regions most affected by these pathologies are the neocortex, hippocampus and other subcortical parts that are critical for cognitive function (Moreira, Carvalho et al. 2010). These pathological features are significant biomarkers for early detection of AD, as they emerge several years before clinical symptoms appear. Aβ protein is the most important risk factor and plays major role in the onset and progression of the disease (Findeis 2007). While this protein is produced in normal conditions, in some cases Aβ may aggregate, leading to the progression of AD. There are several types of Aβ aggregates, including soluble oligomers or protofibrils, that can easily spread throughout the brain, as well as large insoluble amyloid fibrils which further accumulate to form amyloid (or senile) plaques (Fig.1.1) (Breijyeh and Karaman 2020). The aggregated forms of Aβ, particularly soluble oligomers, are neurotoxic and can induce neuronal dysfunction (Moreira, Carvalho et al. 2010, Bao, Wicklund et al. 2012, Esparza, Zhao et al. 2013). Increased concentrations of these toxic aggregates lead to impaired synaptic activity (Shankar and Walsh 2009), alterations in synaptic proteins (Hardy and Selkoe 2002), and the degeneration of neural axons, dendritic spines (Breijyeh and Karaman 2020), and ultimately, neuronal death(Kihara and Shimohama 2004). Furthermore, amyloid plaques can activate astrocytes and microglia, triggering neuroinflammatory processes that contribute to neurodegeneration in brain regions critical for cognitive and memory functions (Tabaton and Piccini 2005, Armstrong 2009, Chen, Xu et al. 2017). The second hallmark of AD is the formation of neurofibrillary tangles (NFTs), which are structurally paired helical filaments of hyperphosphorylated tau protein (Goedert and Spillantini 2006, Moreira, Carvalho et al. 2010). Tau is a tubulin-associated protein in neurons, localized in the cell body and axons (Buee, Bussiere et al. 2000). Under physiological conditions, it promotes the formation of microtubules and contributes to their stability (Gotz, Probst et al. 1995). The hyperphosphorylation of tau protein and the formation of NFTs can cause loss of cytoskeletal microtubules (Breijyeh and Karaman 2020), disruption in axonal transport (Uddin, Kabir et al. 2020) and ultimately neuronal cell death. In AD, the development of NFTs impairs neuronal function, while the quantity of these tangles determines the degree of dementia (Brion 1998).

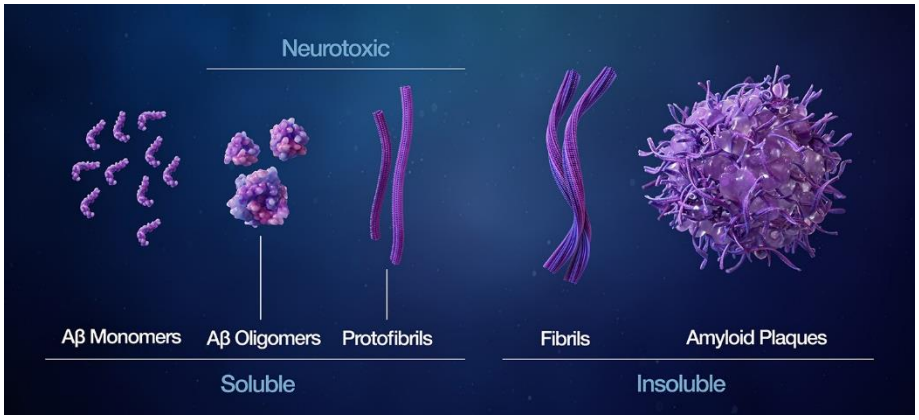

Figure 1.1: Five main conformations of amyloid beta protein. *Amyloid-beta (Aβ) can appear as a monomer or in aggregated forms such as soluble oligomers, protofibrils, and insoluble fibrils within amyloid plaques. (Figure adopted from: https://www.nature.com/articles/d43747-023-00119-8)*

1.2.1 Amyloid cascade hypothesis.

According to the "amyloid cascade hypothesis", first proposed by Hardy and Higgins in 1992 (Hardy and Higgins 1992) , the central and causative event that initiates AD pathogenesis is the deposition of Aβ protein in the brain parenchyma. The overproduction of Aβ peptides, derived from the cleavage of Amyloid Precursor Protein (APP), coupled with impaired Aβ clearance, leads to the accumulation of Aβ in the form of soluble oligomers or insoluble fibrils and plaques. These Aβ aggregates, particularly the soluble oligomers, exhibit synaptotoxic properties, causing defects in neuronal communication, cytoskeletal abnormalities, altered receptor localization, and the inhibition of synaptic plasticity, and ultimately triggering a neurodegenerative cascade responsible for memory deficits (Ferreira and Klein 2011, Koffie, Hyman et al. 2011, Ferreira, Lourenco et al. 2015). Furthermore, Aβ accumulation induces the hyperphosphorylation of tau protein, leading to the formation of neurofibrillary tangles (NFTs), widespread neuronal cell death, and the subsequent cognitive decline and dementia that characterize AD. Consequently, according to this hypothesis, Aβ deposition is the primary driver that induces the downstream neurodegenerative mechanisms of AD.

1.2.2 Production of Aβ protein

Aβ protein is generated from the abnormal proteolytic processing of amyloid precursor protein (APP) (Weggen and Beher 2012). APP is a type I transmembrane glycoprotein of 695-770 amino acids (Uddin, Kabir et al. 2020). It contains the sequence encoding Aβ peptides (d'Uscio, He et al. 2018) within its transmembrane and extracellular domains. According to the "amyloid cascade hypothesis" the APP protein can be processed through two main pathways: the non-amyloidogenic and the amyloidogenic (Fig. 1.2). The balance between these two determines whether Aβ peptides are produced and accumulated in the brain. In the non-amyloidogenic pathway, APP is cleaved by α-secretase, which is a metalloprotease, in the middle of the Aβ domain (MacLeod, Hillert et al. 2015). This cleavage prevents the formation of intact Aβ peptides and generates a soluble APPα fragment (sAPPα) and a membrane bound C-terminal fragment (C83). C83 fragment is cleaved by γ-secretase, an

enzymatic complex of four proteins including presenilin enhancer 2, presenilins (PSEN), anterior pharynx defective 1, and nicastrin, producing a small p3 fragment and the APP intracellular domain (AICD). By contrast, in the amyloidogenic pathway, which is critical in AD, the processing of APP involves different initial cleavage enzymes. Instead of α-secretase, APP is firstly cleaved by β-secretase (BACE1), an aspartic protease with high sequence specificity. β-secretase cleaves APP at the N-terminal of the Aβ domain either at residues Glu682 or Asp672 (MacLeod, Hillert et al. 2015), generating the soluble APPβ fragment (sAPPβ) and a cell-membrane-bound C-terminal fragment 99 (C99). Afterwards, γ-secretase cuts the C99 fragment and generates Aβ peptides of various lengths, along with the AICD. The two primary Aβ isoforms are the Aβ1-40 peptide, which is the most abundant form, and the Aβ1-42 peptide, which is prone to aggregation and generation of oligomers, fibrils and eventually plaques, the pathological hallmark of AD (Ristori, Donnini et al. 2020, Uddin, Kabir et al. 2020).

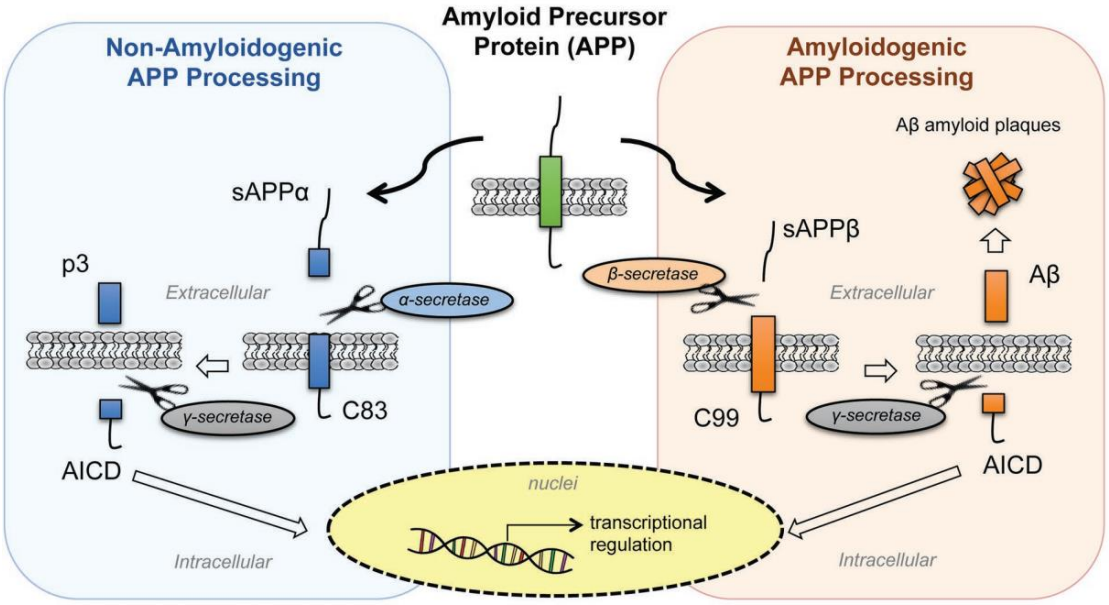

Figure 1.2: Pathways of amyloid precursor protein (APP) cleavage. *The non-amyloidogenic APP processing produces the extracellular sAPPα and p3 fragments, while the amyloidogenic processing releases sAPPβ and β-amyloid (Aβ) peptides. Aβ peptides accumulate and form amyloid plaques. Both pathways release APP intracellular domain (AICD), which translocate in the nuclei and regulate gene transcription (Ristori, Donnini et al. 2020).*

Under physiological conditions, APP is cleaved by the non-amyloidogenic pathway and Aβ is produced at low levels. The pathway by which APP is cleaved is influenced by the cellular distribution of APP. When APP is located at the cell membrane, it is more likely to be cleaved by α-secretase, favoring the non-amyloidogenic pathway. Conversely, when APP is internalized into acidic compartments like early endosomes, amyloidogenic pathway is induced (O'Brien and Wong 2011).

The critical role of Aβ production in AD, as proposed by the amyloid cascade hypothesis, is strongly validated by genetic evidence. Late onset AD (FAD) is caused by autosomal dominant mutations in APP gene itself or the genes encoding presenilin proteins (PSEN1 and PSEN2) of γ-secretase protein complex(Borchelt, Thinakaran et al. 1996, Ertekin-Taner 2007). Over 150 such mutations in PSEN genes have been identified. These mutations change γ-secretase

activity, increasing the production of aggregation-prone Aβ1-42 peptide(Radde, Bolmont et al. 2006). Mutations leading to increased production of Aβ and impaired clearance mechanisms are considered to contribute to the pathological buildup of Aβ in the brain (Uddin, Kabir et al. 2020).

1.2.3 Impaired clearance of Aβ

Growing evidence suggest that impaired clearance of Aβ from the brain is implicated in up to 30% of late-onset AD (LOAD) (Mawuenyega, Sigurdson et al. 2010). Clearance routes include proteolytic degradation intracellularly or extracellularly and Aβ removal from the brain to the blood circulation across the blood brain barrier (BBB). Apolipoprotein E (APOE), the predominant apolipoprotein in the brain, plays a crucial role in these processes. The APOE genotype is the strongest risk factor for AD, with three common isoforms- ApoE2, ApoE3, and ApoE4- differentially influencing risk. The ε4 allele is associated with a significantly increased risk (Farrer, Cupples et al. 1997) and accounts for approximately 50% of all AD cases(Ashford 2004), while the ε2 allele is considered protective (Corder, Saunders et al. 1994). The ε4 allele is responsible for increased Aβ deposition in animal models of AD (Bales, Liu et al. 2009, Castellano, Kim et al. 2011) and in human AD (Mann, Iwatsubo et al. 1997).

The proteolytic degradation of Aβ is one common clearance mechanism impaired in AD. This process is catalyzed by lipidated ApoE, which is produced through its interaction with the ATP-binding cassette A1 (ABCA1) transporter (Zelcer, Khanlou et al. 2007, Morales, Ballesteros et al. 2008). The efficiency of ApoE in facilitating Aβ proteolysis is highly dependent on its isoform and degree of lipidation. Highly lipidated isoforms, such as ApoE2 and ApoE3, are highly effective, whereas the poorly lipidated ApoE4 isoform is inefficient (Jiang, Lee et al. 2008). ABCA1-mediated lipidation of ApoE stimulates Aβ degradation through two primary pathways: extracellular degradation by insulin-degrading enzyme (IDE) or uptake by microglial cells and subsequent lysosomal degradation (Wildsmith, Holley et al. 2013).

The efflux of Aβ protein across the BBB into the bloodstream is the most prominent clearance route, accounting for an estimated 70-85% of Aβ removal (Tarasoff-Conway, Carare et al. 2015). The transport of Aβ across the brain endothelial cells (BECs) of BBB is mediated by receptors, as the passive diffusion at the BBB is allowed only for very small, nonpolar molecules. The ApoE receptor LRP1 (low-density lipoprotein receptor–related protein 1) plays major role in the export Aβ from the brain. On the abluminal (brain-facing) side of the BBB, Aβ binds to LRP1 expressed on endothelial cells. This interaction initiates receptor-mediated transcytosis, facilitating the transport of the Aβ-LRP1 complex across the endothelial cell to the luminal (blood-facing) side of the BBB (Shibata, Yamada et al. 2000, Van Uden, Mallory et al. 2002). Once at the luminal surface, the complex dissociates, allowing Aβ to be released into the circulation directing it to tissues like the liver for degradation (Nelson et al., 2016; Ramanathan et al., 2015). Markedly, BBB plays a major role in Aβ clearance through several endocytosis pathways, whose role and contribution to Aβ clearance remain unknown.

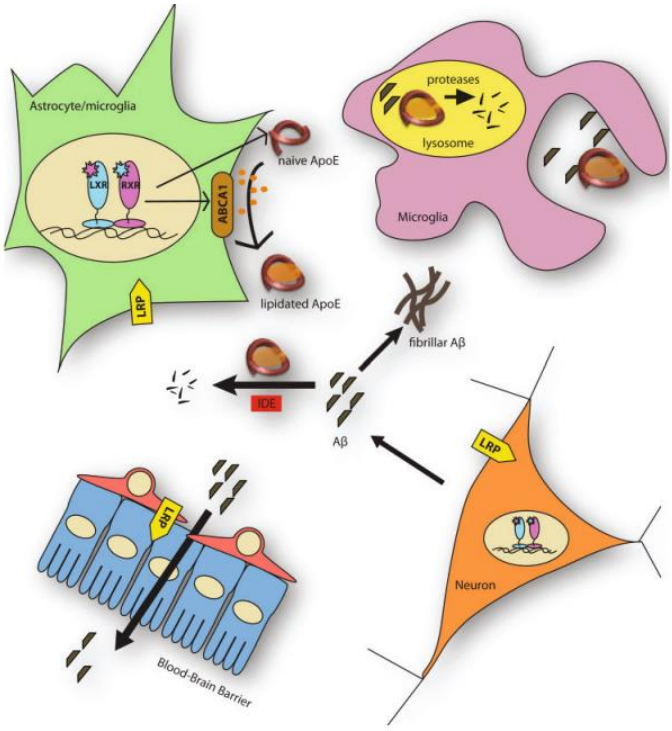

Figure 1.3: Mechanisms of Aβ clearance. *ApoE lipidation by ABCA1 promotes Aβ clearance through pathways, such as extracellular degradation by IDE, uptake by microglial cells for lysosomal degradation, LRP1-mediated efflux of Aβ across the BBB via endocytosis. Aβ clearance across the BBB represents the primary pathway for removing Aβ from the brain (Wildsmith et al., 2013).*

1.3 The Blood-Brain-Barrier (BBB) structure and cellular components.

The BBB is a highly selective, semi-permeable interface between the blood and the brain that regulates the exchange of material necessary for neural function (Dotiwala, McCausland et al. 2025) and restricts the invasion of toxins, pathogens and immune cells into the brain parenchyma. It plays an essential role in maintaining an optimal environment for central nervous system (CNS) function and homeostasis and, in normal conditions, it protects the brain from degeneration (Daneman and Prat 2015). The brain endothelial cells (BECs) are the anatomical site of the BBB and they associate with other brain cells, including pericytes, astrocytes, neurons, microglia and a basement membrane, forming a unique structure referred to as the neurovascular unit (NVU) (Iadecola 2017) (Fig. 1.4).

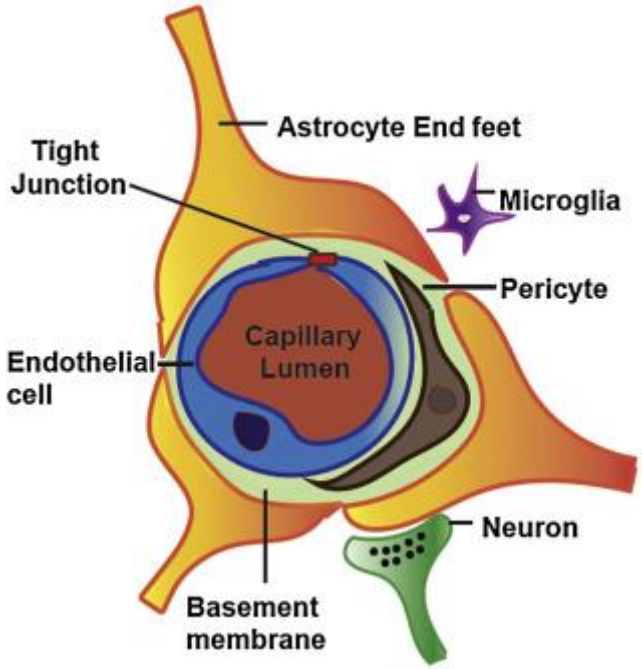

Figure 1.4: The neurovascular unit. *The neurovascular unit is a functional system composed of vascular cells (pericytes, endothelial cells), glial cells (astrocytes, microglia) and neurons, that interact and communicate with each other (Sumbria and Fisher 2017).*

Brain endothelial cells (BECs)

The physical integrity of the BBB is derived from the brain endothelial cells (BECs) that are tightly connected and line the brain microvasculature and strictly control paracellular and transcellular transport. Adjacent BECs are stitched together by tight and adherens junctions, eliminating paracellular flux of material between them(Brightman and Reese 1969). BECs also lack fenestrations and exhibit reduced transcytosis relative to non-brain ECs(Coomber and Stewart 1985), highly regulated by a combination of specialized transporters and efflux pumps. All these features of BECs form a highly selective anatomical barrier between blood circulation and the brain.

Pericytes

Pericytes are supportive cells embedded in the capillary basement membrane and in close contact with endothelial cells. Pericytes play a major role in BBB integrity by aiding vascular development, as they are recruited to stabilize nascent vessels and promote vascular maturation and stability (Kanekiyo and Bu 2014). Brain pericytes help in the formation of the BBB by controlling tight junction's formation and reducing the expression of factors that increase permeability. Notably, pericyte degeneration is observed in Alzheimer's disease (AD) and may contribute to BBB breakdown (Mantle and Lee 2019).

Astrocytes

Astrocytes, a type of glial cells, play a major role in inducing and maintaining BBB properties and integrity of BECs. Astrocytic end-feet enclose over 90% of the capillary surface and induce BBB function by enhancing tight junctions formation, polarizing localization of transporters and efflux pumps and secreting various factors (glial-derived neurotrophic factor (GDNF), basic fibroblast growth factor (bFGF), and angiopoetin-1 (Ang-1)), found to promote barrier tightness (Igarashi, Utsumi et al. 1999, Abbott, Ronnback et al. 2006). Moreover, astrocytes mediate communication between neurons and BECs, as a single astrocyte contacts on average five different blood vessels and four different neuronal somata. This positioning enables astrocytes to coordinate neurovascular coupling, regulating blood flow according to local neuronal activity (Jamieson, Searson et al. 2017). Thus, astrocyte end-feet themselves do not form a diffusion barrier, but they are crucial for the development and maintenance of functional BBB properties.

Microglia

While microglia are not a structural component of the neurovascular unit, they have a significant influence on barrier function and integrity in response to injury and disease. They are one of the main CNS immune cell types derived from myeloid lineage and differentiated in the brain parenchyma during embryonic development (Jamieson, Searson et al. 2017). Under normal conditions microglia's activity is suppressed by neurons (Engelhardt, Carare et al. 2016), but their activation upon neuronal or BBB damage releases pro-inflammatory cytokines, leading to increased BBB permeability by disrupting tight junctions and promoting macrophages recruitment. Therefore, microglia play a crucial role in CNS pathologies associated with neuroinflammation (Nian, Harding et al. 2020) .

Basement membrane(BM)

Basement membrane (BM) is a thin layer of extracellular matrix (ECM) surrounding the brain capillaries. The BM interacts with brain endothelial cells, pericytes, astrocytes and neurons through physical and biomolecular pathways and mediates cell attachment and differentiation. It is composed of proteins, such as collagen IV, laminin, elastin and fibronectin, secreted by these cells (Jamieson, Searson et al.

2017). These proteins create cross-linked networks that anchor BECs and pericytes by binding to transmembrane integrins. These networks also transmit signals to the actin cytoskeleton, regulating cell behavior and promoting a quiescent state (Wolburg, Noell et al. 2009). BM degradation can cause BBB dysfunction, as its disruption alters the endothelial cytoskeleton and tight junctions (Cardoso, Brites et al. 2010). Furthermore, BM thinning is an early event that triggers pericyte migration away from the endothelium (Dore-Duffy, Owen et al. 2000) and the detachment of astrocyte end-feet (Engelhardt, Carare et al. 2016). Therefore, BM is critical for maintaining BBB integrity.

Therefore, brain endothelial cells are supported structurally and functionally by astrocytes, pericytes and the basement membrane (NVU), forming a physical barrier. Adjacent BECs are sealed together with tight and adherens junctions restricting paracellular permeability and express specific transporters and enzymes that regulate transcytosis of metabolites across the BBB. The BBB thus tightly controls brain entry of nutrients and exits of waste, protecting neural tissue from toxins while supplying critical molecules.

1.4 Tight and adherens junctions of BECs.

Paracellular permeability is strictly regulated by complex tight junctions (TJs) between adjacent brain endothelial cells, that seal the paracellular space forming a continuous barrier. An intact BBB has very low paracellular permeability and high trans-endothelial electrical resistance (TEER). TJs of BECs are located at the limit between the apical membrane facing the bloodstream and the basolateral membrane facing the brain parenchyma. This transmembrane structure regulates the paracellular passage of ions and molecules depending on their size and charge. Besides this function, TJs restrict the free movement of lipids and proteins within the plasma membrane between the apical and basal surface, establishing cell polarity (Dragsten, Blumenthal et al. 1981, Mandel, Bacallao et al. 1993).

Brain endothelial tight junction proteins include claudins (claudin-1, −3, −5, −12), occludin, and zonula occludens (ZOs) (Fig. 1.5). The claudins and occludin are both transmembrane proteins, while ZOs are peripheral membrane proteins. Claudins belong to a family of more than 20 members. They possess four transmembrane domains with high variability in the amino acid sequence. This variability determines the selectivity in ionic paracellular passage across the BBB, with some claudins forming ion channels and others constitutive ion barriers. Claudin-5, a member of the claudin family expressed specifically in BECs, is the principal protein responsible for the sealing function of tight junctions (Stamatovic, Johnson et al. 2016), as it reduces ion movement paracellularly and narrows the cleft between neighboring BECs (Krause, Winkler et al. 2009). Occludin, another essential protein of TJs, enhances adhesion between BECs and interacts with intracellular scaffolding proteins and the actin cytoskeleton (Stamatovic, Johnson et al. 2016). ZOs (ZO-1, ZO-2 and ZO-3) are peripherally associated membrane proteins that interact with claudins and occludin and anchor them to the actin cytoskeleton, stabilizing the TJ structure (Gonzalez-Mariscal, Tapia et al. 2008).

Another category of brain endothelial junctions, that further stabilize the cell-cell contacts and attachment and regulate the paracellular permeability of substances, are the adherens junctions (AJ). AJ proteins include Vascular endothelial-cadherin (VE-cadherin), PECAM-1, the

junctional adhesion molecules (JAMs) -A, -B, -C and the endothelial cell-selective adhesion molecule (ESAM) (Sweeney, Zhao et al. 2019). They are located at the lateral membrane immediately underneath the tight junctions (Fig. 1.5). Vascular endothelial cadherin (VE-cadherin) is the major structural protein of AJ in endothelial cells (Mehta and Malik 2006). It is an endothelial-specific member of cadherins, one of the major families of cell adhesion transmembrane proteins. VE-cadherin possesses five extracellular cadherin domains (EC-domains) that mediate adhesion via homophilic, Ca_2-dependent interactions (Vestweber 2008). The cytoplasmic domain binds to β- or γ- catenin, which interacts with α-catenin, an actin-binding protein, stabilizing the AJ anchorage to the actin cytoskeleton. α-catenin can also bind to vinculin, which further stabilizes the AJ structure. VE-cadherin is essential for the formation of a normal vasculature and the integrity of BBB (Wang and Dudek 2009).

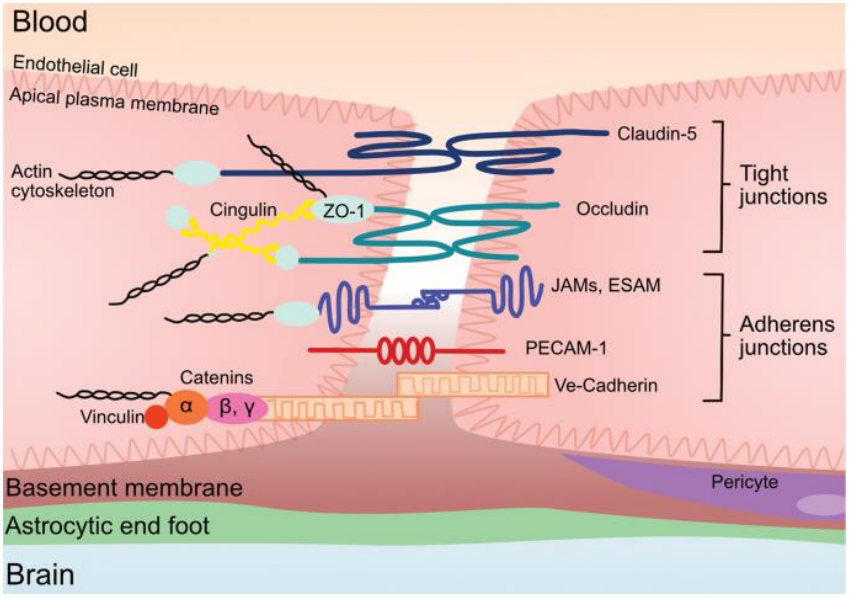

Figure 1.5: Tight and adherens junction proteins of BECs. *Tight junctions include transmembrane proteins, such as claudin-5 and accludin, and the intracellular membrane-associated zonula occludens (ZO-1,-2,-3) proteins. Adherens junction proteins are composed of the transmembrane proteins VE-cadherin, PECAM-1, JAMs, ESAM. VE-cadherin forms a complex with catenins and vinculin. Ultimately, the actin cytoskeleton provides structural anchorage for all of these junctional complexes within endothelial cells (Knox, Aburto et al. 2022).*

1.5 Transcellular molecular transport across BECs.

Brain endothelial cells (BECs) regulate molecular traffic across the BBB through multiple mechanisms. Only a limited number of molecules can cross the BBB with transcellular passive diffusion or paracellular transport (Fig. 1.6 A, B). Only gases, such as oxygen and carbon dioxide, and small lipid-soluble molecules can passively diffuse through BECs (Pardridge 2012), while the paracellular pathway is highly restricted by the presence of tight and adherens junctions. Most of the transport across the BBB is mediated by transporters that ensure that essential molecules can enter the brain. Active efflux transport (Fig. 1.6 C) is mediated by ATP binding cassette (ABC) transporters, who use energy from ATP to transport molecules according to the concentration gradient. ABC transporters, such as P-glycoprotein (P-gp), multidrug resistant proteins (MRPs), and breast cancer resistant protein (BCRP), prevent the accumulation of drugs, nucleosides and xenobiotics in the brain (Sweeney, Zhao et al. 2019). Carrier-mediated transport is highly selective and mediates the bidirectional transport of

several molecules, such as carbohydrates, amino acids, monocarboxylates, hormones, fatty acids, nucleotides, organic anions, and cations etc, across the BECs depending on the concentration gradient (Teixeira, Lopes et al. 2020). For larger molecules and proteins, transport is usually receptor-mediated or absorptive-mediated (Fig. 1.6 E, F). In receptor-mediated transport, the ligand binds to a receptor on the plasma membrane and is transferred into or out of the brain (Pardridge 2002, Jones and Shusta 2007). Usually, this transport takes place through clathrin-mediated endocytosis of the ligand-receptor complex and subsequent transcytosis across the BECs and exocytosis of the ligand. For instance, LRP1 receptor of BECs is responsible for the endocytosis of amyloid-beta protein and its transport across the BBB from the brain to the bloodstream. In the absorptive-mediated pathway, molecules are absorbed through charged interactions with the glycocalyx of the cell membrane of BECs, resulting in caveolae-dependent endocytosis (Langen, Ayloo et al. 2019) (Fig. 1.6 F). BECs are, also, equipped with ion transporters (Fig. 1.6 G), including sodium pumps, calcium transporters, and potassium channels, which are crucial for regulating ionic concentrations in the brain. These transporters influence neuronal activity and help establish the ionic gradient across the BBB that facilitates ion-dependent transport processes (Sweeney, Zhao et al. 2019).

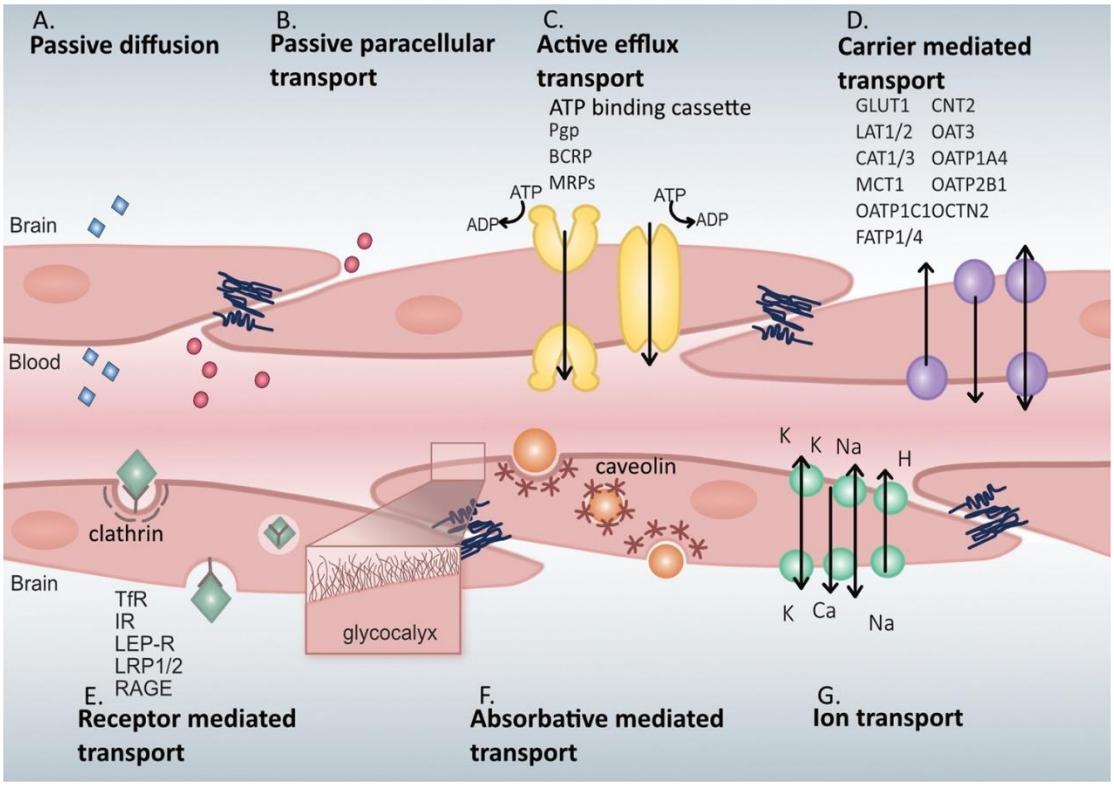

Figure 1.6: Transport mechanisms across the BBB. *The main transport mechanisms of molecules across the BECs are: (A) passive diffusion by limited number of small gas molecules (blue), (B) passive paracellular diffusion of limited water-soluble molecules between tight junctions, (C) active efflux transport that eliminates drugs and toxins from the brain, (D) carrier-mediated transport, (E) receptor-mediated transport that includes the interaction the ligand with a specific receptor and most frequently the clathrin-mediated endocytosis of the complex, (F) absorbative-mediated transport that facilitates the endocytosis of molecules that interact with the glycocalyx of the plasma membrane, and (G) ion transport that regulates the ion gradient between the barrier and includes sodium pumps, calcium transporters, and potassium channels (Knox, Aburto et al. 2022).*

Under normal conditions, BECs exhibit relatively low levels of transcytosis compared to peripheral endothelia (Kadry, Noorani et al. 2020). This strictly regulated transcytosis activity is a hallmark of the BBB, preventing unregulated entry of plasma proteins into the brain. Nevertheless, the BBB can mediate the transcytosis of Aβ protein from the brain parenchyma into the blood circulation, through a receptor-mediated transport mechanism, involving clathrin-mediated endocytosis.

1.6 Clathrin-mediated endocytosis facilitates Aβ clearance across the BBB

As mentioned above, one of the critical functions that are impaired in AD is the clearance of Aβ proteins from the brain. Studies indicate that Aβ is removed from the brain primarily through trans-vascular clearance across the BBB (70-80% of the cases), whereas a smaller proportion is cleared via interstitial fluid (ISF) flow (Tarasoff-Conway, Carare et al. 2015). Under physiological conditions, soluble Aβ levels in the brain are maintained at low levels by continuous clearance across the brain endothelial cells (BECs) of the blood–brain barrier (BBB), via clathrin-mediated endocytosis of Aβ, followed by transcytosis through the endothelial cells and exocytosis into the blood circulation.

The exact molecular pathway of Aβ clearance across the BECs via clathrin-mediated endocytosis has been recently elucidated (Fig. 1.7). The key player of this process is the low-density lipoprotein receptor–related protein 1 (LRP1), a membrane receptor highly expressed in BECs at the abluminal side facing the brain. Aβ binds to LRP1, triggering the rapid formation of clathrin-coated vesicles that engulf the Aβ-LRP1 complex and internalize it into the endothelial cells. Phosphatidylinositol-binding clathrin assembly protein (PICALM) is critical for clathrin/PICALM-mediated internalization of Aβ and guides intracellular trafficking of Aβ-containing endocytic vesicles across the endothelial cells. Once internalized, these vesicles fuse sequentially with Rab5-positive early endosomes and Rab11-positive sorting endosomes, enabling vesicular transport toward the luminal (blood-facing) membrane. Finally, the Aβ–LRP1 complex undergoes exocytosis at the luminal side, releasing Aβ into circulation. Through this receptor-mediated transcytosis, Aβ is efficiently transported across the BBB into the periphery, where it is subsequently degraded in the liver (Ramanathan, Nelson et al. 2015).

Several high risk genes for sporadic and familial AD play a crucial role in vascular-mediated clearance of Aβ and, especially, through the pathway of clathrin-mediated endocytosis (CME). APOE gene is associated with AD, as its ε4 allele is the strongest genetic risk factor for late-onset AD (Zlokovic 2013). ApoE can bind to Aβ protein and form a complex with LRP1. While the ε2 and ε3 isoforms of APOE gene bind with Aβ and facilitate its rapid removal from the brain, the ε4 isoform forms a complex with Aβ that is internalized and cleared from brain endothelial cells (BECs) more slowly, as it is associated with the very low-density lipoprotein receptor (VLDLR) (Bell, Sagare et al. 2007, Deane, Sagare et al. 2008). Other common AD related genes are PICALM and Clusterin (CLU/apoJ). PICALM, highly expressed in brain endothelium, regulates Aβ endocytosis and trafficking across the BBB. Variants in PICALM reduce endothelial expression and Aβ clearance (Zhao, Sagare et al. 2015). Clusterin (CLU/apoJ) also binds Aβ, preventing aggregation and facilitating its clearance across the BBB

(Bell, Sagare et al. 2007). Mutations in CLU are associated with sporadic AD (Harold, Abraham et al. 2009).

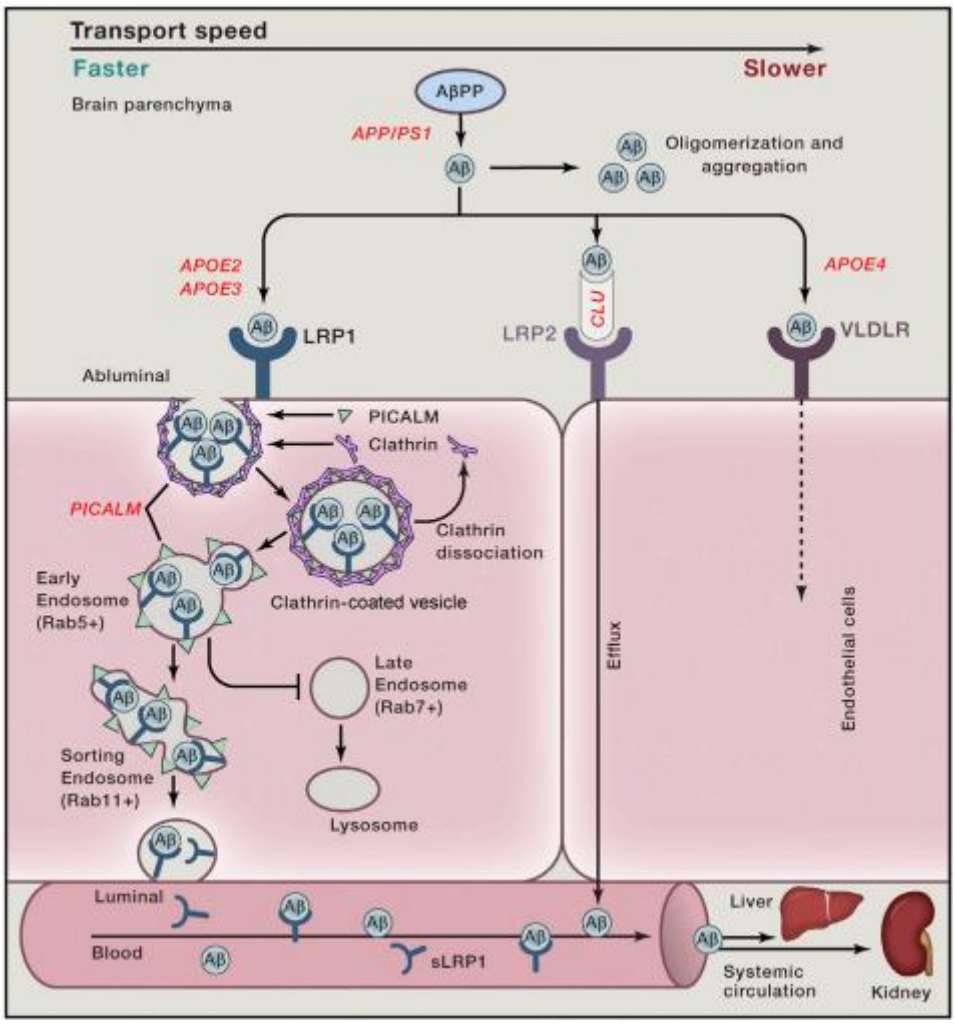

Figure 1.7: Aβ clearance across the BBB through clathrin-mediated endocytosis. *LRP1 binds Aβ at the abluminal side of the brain endothelium and mediates its internalization via the recruitment of PICALM and clathrin, leading to the formation of endocytic vesicles containing LRP1–Aβ complexes. Next, PICALM directs the trafficking of these vesicles to Rab5+ early endosomes and then to Rab11+ sorting endosomes for exocytosis at the luminal side of the BBB, resulting in Aβ transcytosis. Importantly, PICALM prevents Aβ from being targeted to lysosomal degradation. In addition, CLU mediates Aβ transcytosis across the BBB via LRP2. Aβ secreted into the bloodstream binds to soluble LRP1 (sLRP1) and is transported to the liver and kidneys for degradation. Several genetic risk factors are implicated in this clearance pathway. APOE2 and APOE3 alleles are associated with a lower risk of AD compared to APOE4. Although CLU variants influence AD risk, their precise role in Aβ clearance remains unclear. PICALM variants, on the other hand, can affect the efficiency of Aβ clearance across the BBB. In parallel, PSEN1 mutations causing autosomal-dominant AD lead to increased Aβ production, imposing an excessive Aβ burden on the clearance mechanisms (Zhao, Nelson et al. 2015).*

1.7 Distinct endocytic pathways of BECs- Macropinocytosis

Endothelial cells utilize multiple endocytic pathways to internalize molecules from the extracellular space. Among these, clathrin-mediated endocytosis is the most well characterized and plays a central role in Aβ uptake and clearance from the brain, as analyzed previously (Section 1.6). This pathway involves the internalization of receptors into endocytic vesicles coated with the protein clathrin and their intracellular trafficking (Scita and Di Fiore 2010). In addition to clathrin-mediated endocytosis, endothelial cells employ other endocytic routes, including macropinocytosis, caveolin-mediated endocytosis and several less well-characterized clathrin- and caveolin-independent pathways (Fig. 1.8). While the contribution

of these alternative pathways to Aβ clearance remains incompletely understood, they likely provide complementary or context-dependent routes for molecular transport across the blood–brain barrier.

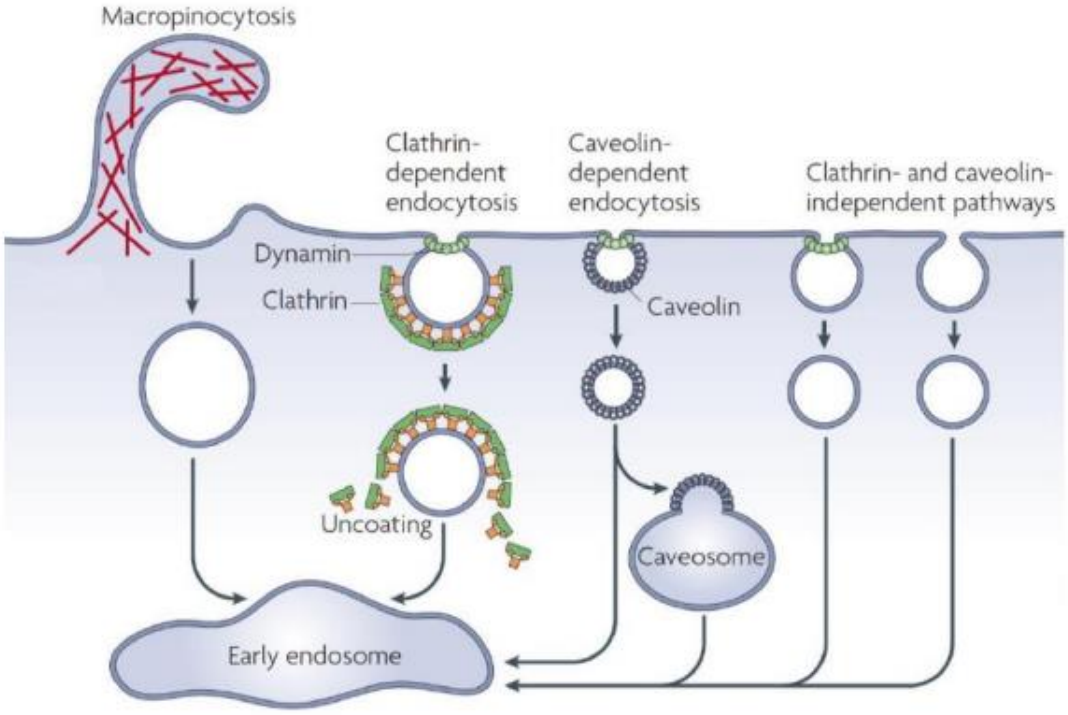

Figure 1.8: Distinct endocytic pathways performed by endothelial cells. *Endothelial cells internalize extracellular cargo through distinct pathways, such as macropinocytosis, clathrin-dependent endocytosis, caveolin-dependent endocytosis and other pathways independent of clathrin and caveolin (Mayor and Pagano 2007).*

Macropinocytosis is a non-selective, actin-driven endocytic pathway in which cells engulf extracellular fluid and its contents into large vesicles called macropinosomes. This process supports nutrient acquisition (Commisso, Davidson et al. 2013), receptor recycling and bulk membrane retrieval (Bryant, Kerr et al. 2007). Macropinosome formation can be induced by receptor signaling triggered by growth factors, such as vascular endothelial growth factor (VEGF) (Basagiannis, Zografou et al. 2016), or constitutive. In the constitutive pathway, macropinocytosis is dependent on extracellular calcium (Ca^{2+}) sensation by calcium-sensing receptors (CaSRs). Activation of macropinocytosis results in the accumulation of phosphatidic acid (PA) and phosphatidylinositol-(3,4,5)-trisphosphate (PIP_3) at the membrane after the activation of phosphatidylinositol-3-kinase (PI3K)(Canton, Schlam et al. 2016). Subsequently, PIP_3 activates and recruits GEFs and the RhoG GTPase, which activate Rac1. Rac1 is an essential GTPase for the induction of macropinocytosis (Redka, Gutschow et al. 2018). It recruits the SCAR/WAVE complex that drives the actin polymerization and the formation of macropinosomes (Veltman, Williams et al. 2016). Cdc42 has also been detected in macropinocytic cups, playing mainly a supporting role (West, Prescott et al. 2000) (Fig. 1.9).

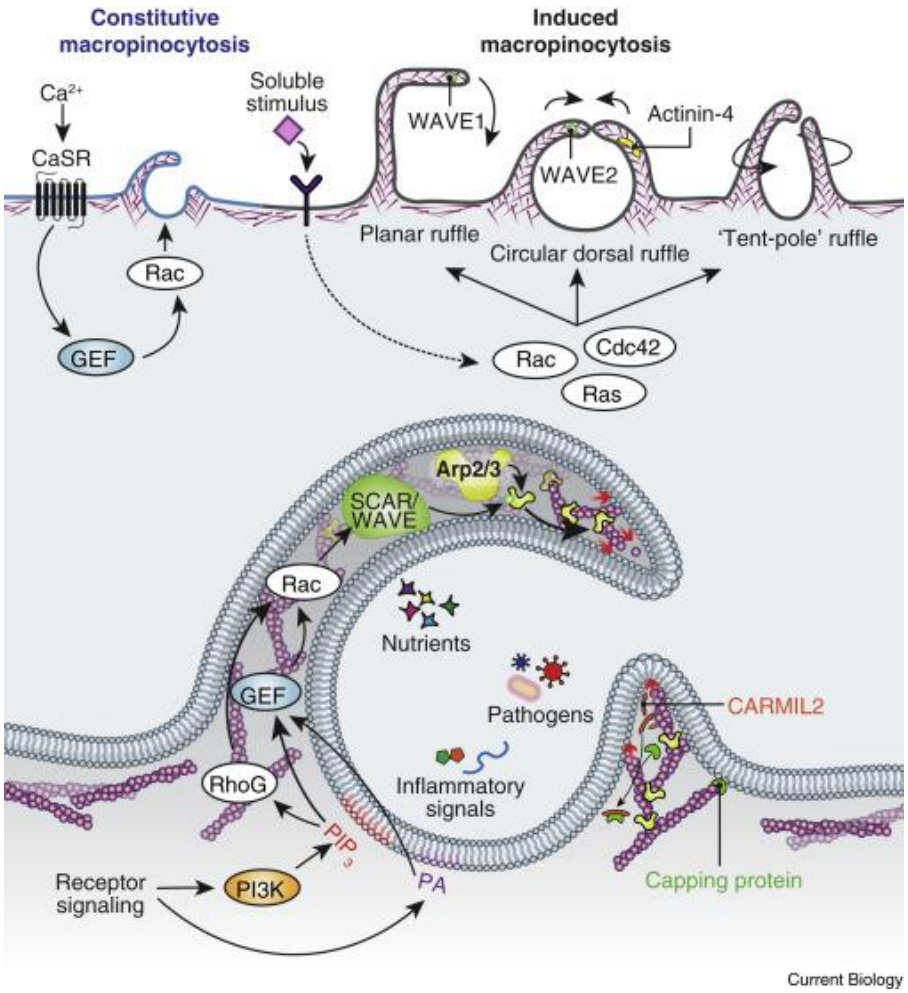

Figure 1.9: Molecular and membrane changes during macropinocytosis. *The pathway can be either constitutive, that depends on the extracellular calcium (Ca^{2+}) or induced by growth factors. Activation of receptor results in the accumulation of phosphatidic acid (PA) or phosphatidylinositol-(3,4,5)-trisphosphate (PIP3) in a phosphatidylinositol-3-kinase (PI3K)-dependent manner. Then, GEF and RhoG are recruited and activate Rac, that drives the Arp2/3-dependent formation of ruffles. Ruffles can display three main morphologies: planar, circular and pent-pole ruffles. The sources of this variability remain unclear(Mylvaganam, Freeman et al. 2021).*

Whether macropinocytosis contributes to Aβ clearance from the brain is still an open question. Under normal conditions, macropinocytosis at the BBB is not prominent, but it may be stimulated in disease states(Mantle and Lee 2019). Interestingly, very recent studies suggest that in AD there are increased levels of VEGF (Cho, Park et al. 2017), a growth factor that induces internalization via macropinocytosis. This finding suggests that macropinocytosis may be involved in Aβ transcytosis and clearance from the brain. Investigating the possible contribution of macropinocytosis and other endocytic pathways to Aβ clearance and its underlying molecular mechanisms is crucial, as it could serve as an alternative pathway to reduce the excess Aβ in early stages of AD. Enhancing clearance across the BBB represents a promising therapeutic strategy to slow or prevent the progression of AD.

1.8 Aim of the thesis

Given that Aβ clearance across the BBB is the prevalent protective mechanism against AD, and that endocytosis in BECs is the major route of Aβ transport from the brain to the bloodstream, it is crucial to investigate the unexplored endocytic pathways in BECs that may

contribute to Aβ uptake and clearance. Clathrin-mediated endocytosis in BECs is already known to participate in Aβ clearance through transcytosis and secretion into the bloodstream. However, it remains unclear whether macropinocytosis, or other endocytic pathways in endothelial cells, are also involved in Aβ transcytosis across BECs (Fig. 1.10). Macropinocytosis is the pathway that warrants close attention, as it is activated by VEGF/VEGFR pathway(Basagiannis, Zografou et al. 2016), the dominant regulator of angiogenesis. Therefore, this study focuses on elucidating the role of macropinocytosis in Aβ uptake and clearance by BECs.

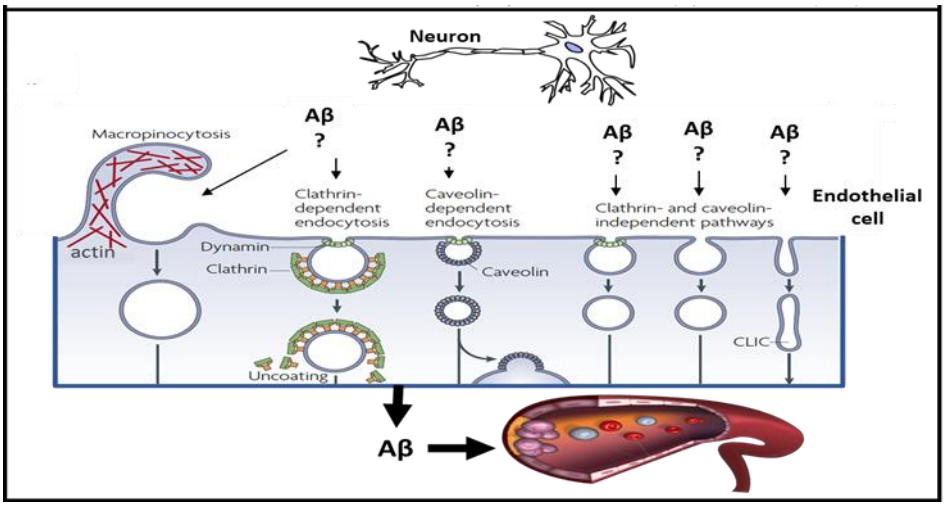

Figure 1.10: Overview of known endocytic pathways, whose role in Aβ clearance from the brain to the blood circulation across BECs remains to be addressed.

To address this question, we employed three complementary experimental models. First, we used commercially available primary human BECs to investigate the role of macropinocytosis in Aβ uptake. Due to the limitation that these cells exhibit poor BBB phenotype (Weksler, Subileau et al. 2005, Bicker, Alves et al. 2014) and undergo senescence after only a few passages, we proceeded in establishing an alternative in vitro BBB model using human induced pluripotent stem cell (hiPSC)-derived BECs. hiPSCs provide an unlimited, self-renewable, and scalable source of human cells for research (Lippmann, Al-Ahmad et al. 2013). hiPSCs derived from patients with AD and healthy individuals can be differentiated into BECs, allowing us to compare healthy and diseased versions of this cell type and to identify possible defects in endocytic pathways related to Aβ uptake and clearance in patient-derived cells. Finally, in vivo validation of our findings in a transgenic mouse model of AD is essential.

Therefore, the primary objectives of this thesis were to:

1. Investigate the role of macropinocytosis in Aβ uptake by primary BECs through blockage of the pathway using siRNAs targeting known modulators of macropinocytosis.
2. Examine the role of macropinocytosis in Aβ clearance in a transgenic mouse model of AD that produces amyloid plaques, through chemical inhibition of macropinocytosis and subsequent measurement of Aβ levels in the brain.
3. Differentiate iPSCs derived from a healthy donor and an AD patient with the ApoE ε4/ε4 genotype, the strongest genetic factor for AD, into a mature and pure

population of BECs, using an already established protocol (Neal, Marinelli et al. 2019) (Fig. 1.11).

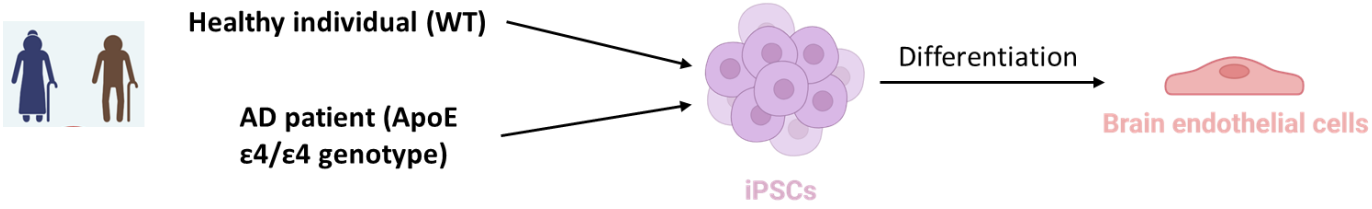

Figure 1.11: Differentiation of iPSCs derived from an AD patient carrying the ApoE ε4/ε4 genotype and an age matched healthy individual (WT) into BECs

2. MATERIALS & METHODS

2.1 Antibodies

The primary antibodies used in this study are summarized in the table below (Table 2.1), summarizing details about the host species, antibody class, source company, catalog number, and the specific dilutions employed for Western blotting (WB) and/or immunocytochemistry (ICC) applications.

Primary antibodies						
Protein target	**Host**	**Class**	**Company**	**Catalog number**	**Dilution for WB**	**Dilution for ICC**
β-amyloid (D54D2)	rabbit	monoclonal	Cell Signaling Technology	#8243	1:1000	1:700
RAC1	mouse	monoclonal	Santa Cruz Biotechnology	Sc-514583	1:200	-
RAC1	mouse	monoclonal	Developmental Studies Hybridoma Bank (DSHB)	CPTC-RAC1-1	1:500	-
CDC42	mouse	monoclonal	Santa Cruz Biotechnology	sc-8401	1:200	-
ZO-1	rabbit	polyclonal	Invitrogen	61-7300	-	1:50
VE-cadherin	mouse	monoclonal	(production in Dr. Kouklis's laboratory)	-	-	1:50
VE-cadherin	mouse	monoclonal	Santa Cruz Biotechnology	sc-9989	-	1:100
claudin-5	mouse	monoclonal	Invitrogen	35-2500	1:1000	-
von Willebrand factor (vwf)	rabbit	polyclonal	Dako/Agilent	A0082	-	1:200
β-actin	mouse	monoclonal	Developmental Studies Hybridoma Bank (DSHB)	224-236-1	1:500	-

Table 2.1 Overview of the primary antibodies used for Western Blotting (WB) and/or Immunocytochemistry (ICC)

The secondary antibodies used for Western Blotting or immunocytochemistry are summarized in Table 2.2, including details such as conjugate type, source company, catalog number, and the specific dilutions used.

Secondary antibodies				
Species reactivity	**Conjugate**	**Company**	**Catalog number**	**Dilution**
a-mouse	Alexa 594	ThermoFisher Scientific	A21203	1:200
a-mouse	Alexa 488	Biotium		1:200
a-rabbit	Alexa 594	ThermoFisher Scientific	A21207	1:200
a-rabbit	Alexa 488	ThermoFisher Scientific	A21206	1:200
a-mouse	HRP	Jackson ImmunoResearch	165373	1:5000
a-rabbit	HRP	Jackson ImmunoResearch	163676	1:5000

Table 2.2 Overview of secondary antibodies used for immunochemistry (Alexa 594 or 488 conjugated) or Western Blotting (HRP conjugated).

2.2 Primary BECs, as experimental model

2.2.1 Culture of primary BECs

Primary BECs were commercially purchased from Pelobiotech (Catalog number: PB-CH-110-4011). BECs were cultured in Microvascular Endothelial Cell Growth Medium enhanced from Pelobiotech (Catalog number: PB-MH-100-4099). Cells with passages between 1-8 were used in all experimental setups.

Cells were handled in a laminar flow and class II safety cabinet and were maintained in an incubator at 37°C in a humidified atmosphere with 5% CO2. Confluent cells were split every 2-3 days. After rinsing with PBS, the cells were detached using a Trypsin-EDTA 1X in PBS (BioSera) and transferred to new plates coated with Speed Coating Solution (Pelobiotech, Catalog number: PB-LU-000-0002-00). Cells were replated in a ratio depending on the confluency required for the particular experiment. For the experiments of the present study BECs were seeded on 12-well plates and on suitable microscopy plates, such as Culture-Insert 3 Well in μ-Dishes 35 mm, high (Ibidi, Catalog number: 80366).

2.2.2 Knock down of modulators of macropinocytosis in BECs

Expression of Rac1 and CDC42 proteins was silenced with siRNA transfection in BECs. Cells were cultured in 12-well plates and ibidi microscopy plates. When cells reached 50-70% confluency, were transfected with siRNAs complementary to the target mRNA (siRac1 or siCDC42) or with scrambled siRNAs (si-control). siRNAs were supplied by OriGene Technologies. A unique 27-mer siRNA duplex was used for Rac1 (OriGene, SR321562) and CDC42 (OriGene, SR319646) respectively and the used transfection reagent was RNAiMAX (Lipofectamine) diluted in Optimem. The mixtures were added dropwise onto cells, after 1 hour of serum starvation. The concentration of siRNAs during cell transfection was 50nM. 4-5

hours post-transfection, transfection complex-containing medium was replaced with Full Medium. 72 hours post-transfection, cells from 12-well plate were processed for protein extraction and cells from microscopy plates were treated with Aβ42 and Dextran70 and fixed for immunofluorescence.

2.2.3 Aβ42 and Dextran70 internalization assay in primary BECs

BECs seeded on microscopy plates were serum starved for 1 hour with serum-free medium. After serum starvation, serum-free medium was removed and replaced with fresh full media containing Aβ42 peptide (working concentration: 2 μM) and FITC-Dextran 70 kDa (working concentration: 1 mg/mL) for a 15-minute co-incubation. After 15 minutes incubation, the cells were washed once with PBS, incubated with an acidic buffer (0.2M glycine-0,15M NaCl, pH 2.2) for 2 minutes and washed again with PBS. Finally, cells were fixed in 4% paraformaldehyde (PFA) for 20 minutes, washed twice with PBS and underwent immunofluorescence staining.

2.2.4 Immunocytochemistry for BECs

Following fixation with 4% paraformaldehyde, cells were permeabilized with 0.1% Triton X-100 (ThermoFisher Scientific) for 10 minutes at RT. After another three washes with PBS, cells were blocked in 10% FCS in PBS for 1 hour at RT. The cells were then incubated overnight at 4°C with the primary antibody (listed in Table 2.1) solution diluted in blocking buffer. Next day, cells were washed 3 times for 5 minutes each in PBS and then incubated with Alexa fluorochrome-conjugated secondary antibodies (listed in Table 2.2) diluted in blocking solution for 1 hour at RT in the dark. The samples were washed again 3 times for 5 minutes each in PBS. Nuclei were stained with Hoechst 33342 trihydrochloride trihydrate (Thermo Fisher Scientific) for 10 minutes, followed by 3 more washes with PBS, each for 5 minutes. Samples were mounted in ibidi Mounting Medium (Ibidi, 50001).

2.3 Transgenic mice, as an experimental model of AD pathology

2.3.1 EIPA Treatment of 5XFAD transgenic mice to inhibit macropinocytosis

The in vivo experiments described here were conducted in collaboration with the group of Professor I. Charalampopoulo's lab (IMBB-FORTH). The 5XFAD transgenic mouse model of Alzheimer's disease was generated by introducing five mutations into APP/PS1 double-transgenic mice: the Swedish (KM670/671NL), Florida (I716V), and London (V717I) mutations in the APP gene, and the M146L (A > C) and L286V mutations in the PSEN1 gene. This mouse model develops Aβ plaques in the brain by 2 months of age. To investigate the role of macropinocytosis in Aβ clearance from the brain, 1.5-month-old 5XFAD transgenic mice were intraperitoneally injected with 3 mg/kg of EIPA (chemical inhibitor of macropinocytosis) or vehicle (DMSO) every three days. A second group of WT mice received the same treatment. Each experimental group consisted of n=3 WT mice, n=5 5XFAD mice, with an equal number of males and females. A summary of the experimental groups is provided in Table 2.3. At 3 months of age, mice were sacrificed, and brain samples were collected, and analyzed with Western blotting or immunocytochemistry.

Animal strains	WT mice	5XFAD transgenic mice
group 1	vehicle (no drug treatment)	
group 2	treatment with EIPA	

Table 2.3: Experimental groups of mice used to study the contribution of macropinocytosis to Aβ clearance, using EIPA as a chemical inhibitor.

2.4 iPSC-derived BECs, as an in vitro human model of BBB

2.4.1 iPSCs maintenance

iPSCs lines were generated at the Johns Hopkins School of Medicine, under the supervision of V. Machairaki. Briefly, the JHUi002-A iPSC cell line was generated from culture-expanded peripheral blood mononuclear cells (PBMNCs) from a 80 year old patient who has the APOE E4/E4 phenotype, the strongest genetic risk factor for Alzheimer's disease. Isogenic lines with genotypes APOE 3/4 and APOE 3/3 were generated from the parental JHUi002-A line. An iPSCs line was generated from a healthy donor, as control (iPSCs WT4 NgN2). iPSCs were cultured in E8 medium (Gibco, Catalog number: A1517001), on plates coated with vitronectin (VTN-N, Gibco, Catalog number: A14700). iPSCs were passaged every 3 days, when they reach 80-90% confluency. For passaging, iPSCs were washed once with DPBS (Thermo Fisher Scientific) and incubated with TrypLE (Gibco, Catalog number: 12604013) for 1-2 minutes. The resultant single cell suspension was collected via centrifugation (1000 RPM, 5 minutes), resuspended in fresh E8 medium and density was counted using a Countess II (Thermo Fisher Scientific). Viability of cells was measured with Trypan blue and cells were seeded according to the measured live cell count. New plates were coated with VNT-N 1% overnight. Cells were seeded on new plates at a density of 26,041 cells/cm^2 (e.g. 250,000 cells/well of a 6-well plate) in E8 medium containing 10 μM Y-27632. Next day, Y-27632 was removed and substituted with E8 medium without additions.

2.4.2 iPSCs differentiation into BECs

Differentiation of iPSCs into BECs was performed according to the protocol described by Neal et al., 2019. One day before the initiation of differentiation (Day -1), iPSCs were passaged to a 6 well plate at a density of 15,800 cells/cm^2 (150,000 cells/well) in E8 medium containing 10 μM Y-27632. Next day (Day 0), differentiation started by changing medium to E6 medium (Gibco, #A1516401). E6 medium was changed daily for 4 days. At day 5 of differentiation, cells were given human endothelial cell medium (hESFM supplemented with B-27 supplement), 20 ng/mL bFGF and 10 μM RA. Medium was not changed for 2 days. Following this treatment, mature BECs were purified through a process referred to as subculture. Cells were washed once with DPBS and treated with Accutase (StemPro™ Accutase™, Gibco #A1110501) for 15-20 minutes, until a single cell suspension was formed. Following centrifugation at 1000 RPM for 4 minutes, cells were resuspended in human endothelial cell medium containing 20 ng/mL bFGF and 10 μM RA and plated onto substrates coated with in a mixture of 400 μg/mL collagen IV (Sigma Aldrich, #C5533) and 100 μg/mL fibronectin (Corning, #354008). Coating of substrates was performed overnight. For subculture, substrates used were either tissue culture polystyrene plates (12-well, 24-well plates or ibidi plates for immunofluorescence) or Transwell filters with 1.1 cm^2 polyethylene terephthalate membranes and 0.4 μm pores. Cells were replated at a density of 2,2 million cells/well of a 6-well plate, 1,1 million cells/well of a 12-well plate, 1,1 million cells on transwell filters, 300,000 cells on 35 mm μ-Dish (Ibidi), and

500,000 cells/well of a 24-well plate. Next day, media was changed to basal endothelial medium with desired supplement but lacking bFGF and RA. 24 hours after removal of bFGF and RA, TEER was measured daily using STX2 chopstick electrodes and an EVOM2 voltohmeter (World Precision Instruments), and reported values were corrected for the resistance of an empty Transwell filter. At day 10 of differentiation, cells were fixed and stained for BBB-specific markers. The differentiation process is summarized in Figure 2.1.

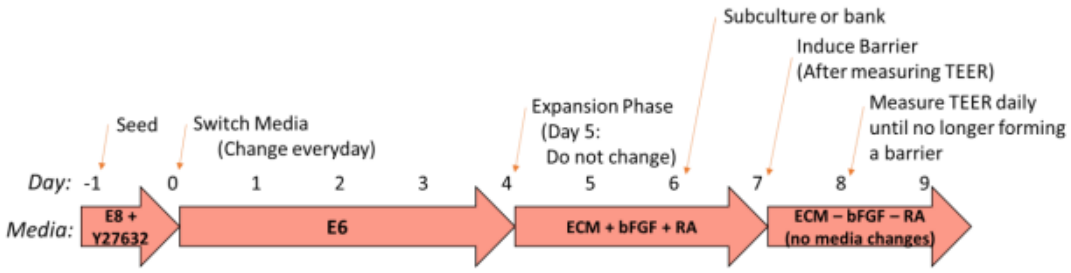

Figure 2.1: Scheme of protocol of differentiation of iPSCs into BECs. (Lippmann et al., 2011–2019, Unpublished lab protocol)

2.4.3 TEER measurement

Trans-epithelial electrical resistance (TEER) assay measured the resistance across differentiated BECs forming a monolayer on a transwell filter. This measurement is indicative of the tightness of the monolayer and barrier formation. TEER measurement does not destroy cells.

One day after subculture (Day 7), TEER was measured daily using STX2 chopstick electrodes and an EVOM2 voltohmeter (World Precision Instruments). Electrodes were positioned with the long side in the basolateral chamber and the short side into the apical chamber, and an electric current was applied. The measurement procedure included measuring the blank resistance (RBLANK) of an empty filter (without cells) and measuring the resistance across the BECs monolayer on the semi-permeable membrane (RTOTAL). The cell specific resistance (RTISSUE) in units of Ω, was obtained as: RTISSUE(Ω) = RTOTAL – RBLANK. The resulting value was multiplied by the surface area of the filter to express the result as Ω×cm^2 : $TEER_{REPORTED}$ = R_{TISSUE} (Ω) × A(cm^2).

Maximum TEER values were expected after Day 7, when RA and bFGF were removed and cells began to form a tight barrier. Typically, the BEC monolayer should exhibit a barrier above 1000 Ωxcm^2. TEER was measured daily until the cells no longer formed a barrier. Finally, filters were fixed and stained for markers of differentiation.

2.4.4 Immunocytochemistry for iPSC-derived BECs

On day 10 of differentiation, cells were washed twice with PBS and fixed with 4% PFA for 20 minutes. After fixation, cells were washed 3 times with PBS for 5 minutes per wash and pre-blocked for a minimum of 1 hour at RT in PBS with 5% donkey serum and 0.3% Triton X-100, referred to as PBS-DT. Cells were then incubated with primary antibody (listed in Table 2.1) at the desired dilution in PBS-DT overnight at 4°C. Cells were rinsed once with PBS and washed five times with a minimum of 5 min per wash using PBS with 0.3% Triton X-100 (PBS-T). Secondary antibodies (listed in Table 2.2) were diluted in PBS-DT and incubated with cells for

1-2 h at room temperature in the dark. Then, nuclei were stained with Hoechst 33342 trihydrochloride trihydrate (Thermo Fisher Scientific) diluted in PBS-T for 10 minutes. Finally, cells rinsed once with PBS-T and were washed 4 times with PBS-T for a minimum of 5 minutes per wash. For ibidi plates, cells were mounted in ibidi Mounting Medium (Ibidi, 50001), while for Transwell filters, samples were mounted in a medium consisting of 50% glycerol and 100 mg/ml DABCO.

2.5 Biochemical methods

2.5.1 Protein extraction

2.5.1.1 Primary BECs culture

72 hours after transfection with siRNAs, cells cultured in 12-well plates were processed for protein extraction. Cells were washed with PBS and then lysed in 2% Triton and 1 mM EDTA for 20 minutes while agitating. Cell lysates were then centrifuged at 14000 RMP for 10 minutes at 4°C. Supernatant was collected and stored at -20°C.

2.5.1.2 Mice brain samples

3-months-old mice were sacrificed following 1.5 months of EIPA treatment. Brain tissues were collected, and brains were sectioned vertically along the midline to separate the left and right hemispheres. Each hemisphere was divided into four regions: cortex, hippocampus, cerebellum and remaining brain areas. Each region of the left hemisphere was lysed for protein extraction (lysis buffer: 50 mM Tris-HCl pH 7.4, 150 mM NaCl, 0.1% Triton X-100, 1 mM EDTA and protease inhibitors), and sonicated twice for 10 seconds at 13% amplitude. To further homogenize the tissues, 5 mL and 1 mL syringes were used. Lysates were centrifuged at 1000 RPM for 5 min at 4°C. The resulting supernatant contained both soluble and insoluble protein fractions, enabling detection of various forms of amyloid beta (Aβ) protein- including soluble Aβ and amyloid plaques- by Western blotting. Lysates and pellets were stored at -20°C.

2.5.1.2 iPSC-derived BECs

Cells were washed with PBS and then lysed in RIPA lysis buffer (50 mM Tris-HCl pH 7.4, 150 mM NaCl, 1% Triton X-100, 0.5% sodium deoxycholate, 0.1% SDS, 1 mM EDTA and protease inhibitors) for 20 minutes while agitating. Cell lysates were then centrifuged at 14000 RMP for 10 minutes at 4°C. Supernatant was collected and stored at -20°C.

2.5.2 Quantification of total protein

The protein content of the samples was determined using the BCA Protein Assay Kit (ThermoFisher Scientific, 23225) according to the manufacturer's instructions. Specifically, Reagent A and Reagent B were combined in a 50:1 ratio to create the working reagent. To 1 ml of the working reagent, 5 µl of cell lysate was added. The mixture was incubated at 60°C for 30 minutes to allow the colorimetric reaction to occur. Following incubation, the absorbance was measured at 562 nm using a Jenway 630 501 Visible Spectrophotometer (Cole-Parmer). The protein content was calculated based on a Bovine Serum Albumin (BSA) standard curve that was previously constructed in our laboratory.

2.5.3 Western Blot analysis

Protein lysates (20μg to 40μg) were boiled at 95^{o}C for 5 minutes and separated by electrophoresis on 8%, 10% or 12% SDS-polyacrylamide gels, depending on the size of the protein of interest. Every gel was run at 35 mA. Proteins were transferred to nitrocellulose membranes (GE Healthcare Life Sciences) for 60 minutes up to 5 hours at 180-200 mA, depending on the size of protein of interest, using wet blotting in a Biorad chamber. Membranes were, then, blocked for 1 hour in 5% milk/PBS-Tween and incubated overnight at 4^{o}C with the primary antibodies (listed in Table 2.1) diluted in 2% gelatin solution. The next day, membranes were washed three times for 5 minutes each in PBS-Tween and then incubated for 1 hour with HRP-conjugated secondary antibodies (listed in Table 2.2) diluted in 5% milk/PBS-Tween. Membranes were washed again three times for 5 minutes each in PBS-Tween. Finally, membranes were incubated for 2 minutes with Enhanced Chemiluminescence (ECL) (Roche Diagnostics GmbH) or SuperSignal™ West Femto Maximum Sensitivity Substrate (ThermoFisher Scientific). The signal was developed using the Azure 600 device (Azure Biosystems).

2.6 Laser Scanning Confocal Microscopy

Microscopic observations of fixed cells was carried out in a Leica TCS SP5 Confocal microscope (BRI/FORTH, Ioannina, Greece) equipped with Argon/SS561/HeNe lasers. Data acquisition and analysis was conducted by using the accompanying software, LAS AF. The scanning frequency was performed at 400 Hz and an image resolution of 512x512 pixels was used. A Leica 63x 1.4 NA oil UV lens was used for the observation of the samples.

2.7 Quantification and statistical analysis

The quantification of immunoblots and immunofluorescence images was performed using the ImageJ software. Statistical analysis was performed using an unpaired, two-tailed, Student's t-test (parametric test), for two-group comparison. Data were collected from at least three independent replicates of each experimental setting and presented in graphs with standard deviation (SD) values. P values <0.05 were considered to indicate significant differences, with levels of significance as follows: *p≤0.05; **p≤0.01; ***p≤0.001; ****p≤0.0001.

3. RESULTS

3.1 Investigation of the role of macropinocytosis in Aβ uptake by BECs

3.1.1 RNAi-mediated knock down of Rac1 and CDC42 in primary BECs

Previous experiments from members of our lab showed that macropinocytosis is involved in Aβ uptake by BECs. This conclusion was initially based on chemical inhibition of the pathway in primary BECs using EIPA. However, chemical inhibitors of endocytic pathways can produce off-target effects, limiting the specificity of such approaches (Ivanov 2014). To more specifically assess the role of macropinocytosis in Aβ uptake, we employed siRNAs targeting key molecular modulators of macropinocytosis.

Macropinocytosis is an endocytic pathway that relies on cytoskeletal remodeling, through actin polymerization, to form large vesicles that engulf extracellular material. Actin polymerization in this context requires the activity of the GTPases Rac1 and CDC42 (Swanson 2008) (Fig. 3.1, A). Knock down of these proteins is supposed to inhibit macropinocytosis in endothelial cells. Therefore, we used siRNAs targeting Rac1 and CDC42 mRNAs, respectively, to reduce their expression levels in BECs. A scrambled siRNA sequence was used as a negative control.

We optimized the siRNA transfection protocol and achieved approximately 70% knockdown of Rac1 and 95% knockdown of CDC42, as assessed by Western blot quantification of cell lysates following transfection (Fig. 3.1, C).

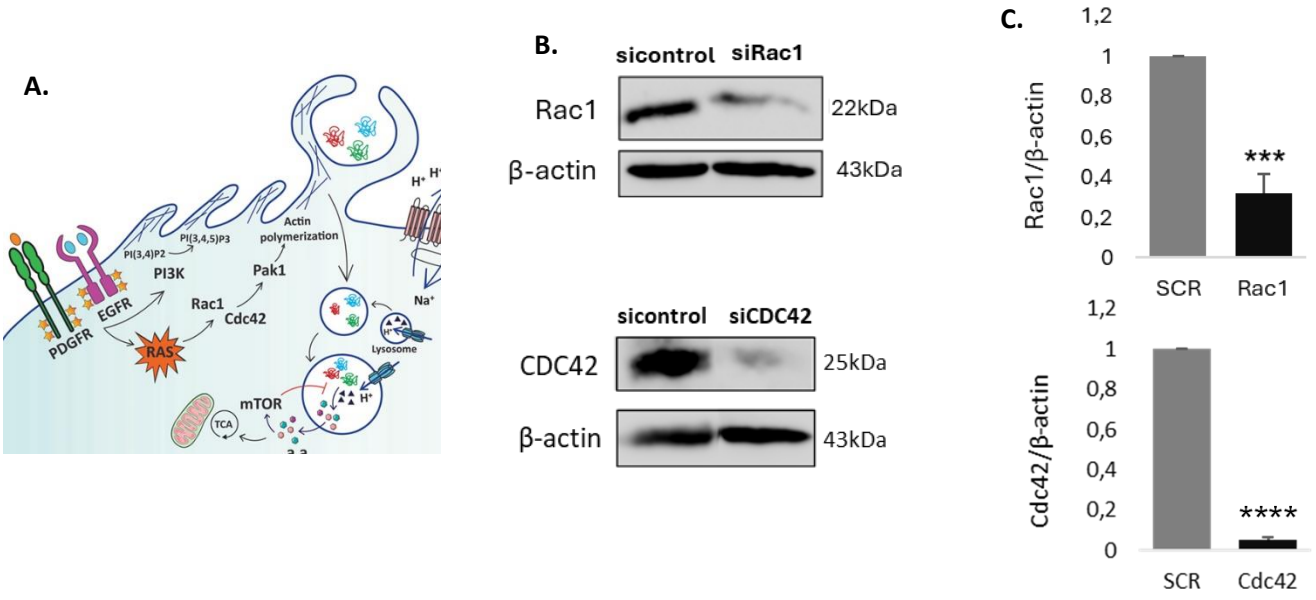

Figure 3.1: siRNA-mediated silencing of Rac1 and CDC42 expression in BECs. *(A)Macropinocytosis pathway relies on actin polymerization, to form large vesicles that engulf extracellular material and Rac1 and CDC42 are key molecular modulators of this pathway (Recouvreux and Commisso 2017). (B) BECs were transfected with siRNAs against Rac1 (siRac1) or CDC42 (siCDC42) or scrambled siRNA (sicontrol), at a final concentration of 50nM. Cells were incubated with siRNAs for 5 hours. 72 hours post-transfection cell lysates were analyzed with Western blotting, for the detection of Rac1 and CDC42 expression. β-actin was used as the loading control. (C) Quantification*

*of the blots showed 70% and 95% reduction of Rac1 and CDC42 expression, respectively, comparing with sicontrol (SCR) (n=3, mean ± S.D., *p ≤ 0.05; **p ≤ 0.01; ***p ≤ 0.001; ****p≤0.0001, student's t-test).*

After optimizing the siRNA-mediated silencing of Rac1 and CDC42 expression in primary BECs, the next step involved repeating the experiment with subsequent exogenous $A\beta_{42}$ treatment. This experiment aimed to determine the effect of macropinocytosis inhibition on Aβ uptake by BECs.

3.1.2 Aβ internalization assay following siRNA-mediated blockage of macropinocytosis in primary BECs.

Having successfully inhibited the macropinocytosis pathway using siRNAs targeting Rac1 or CDC42, we next performed an Aβ internalization assay to investigate whether macropinocytosis contributes to Aβ uptake by BECs. Following silencing of Rac1 or CDC42, cells were treated with Aβ42 and a high-molecular-weight dextran (Dextran 70 kDa). Dextran is a polysaccharide composed of glucose units connected by glycosidic bombs. High-molecular-weight dextran (70 kDa) is internalized by endothelial cells through macropinocytosis and is therefore commonly used as a marker for intracellular vesicles formed via this pathway, known as macropinosomes (Dharmawardhane, Schurmann et al. 2000).

Knockdown of Rac1 and CDC42 resulted in decreased uptake of Dextran 70 by BECs (Fig. 3.2, A), as quantified by the reduction in fluorescence intensity (Fig. 3.2, B), confirming successful inhibition of macropinocytosis. To test the hypothesis that Aβ is internalized through this pathway in BECs, we quantified Aβ fluorescence intensity and observed a decrease in uptake by approximately 50% and 57% following Rac1 and CDC42 silencing, respectively (Fig. 3.2, A, B). These findings indicate that macropinocytosis plays a significant role in the internalization of Aβ in BECs.

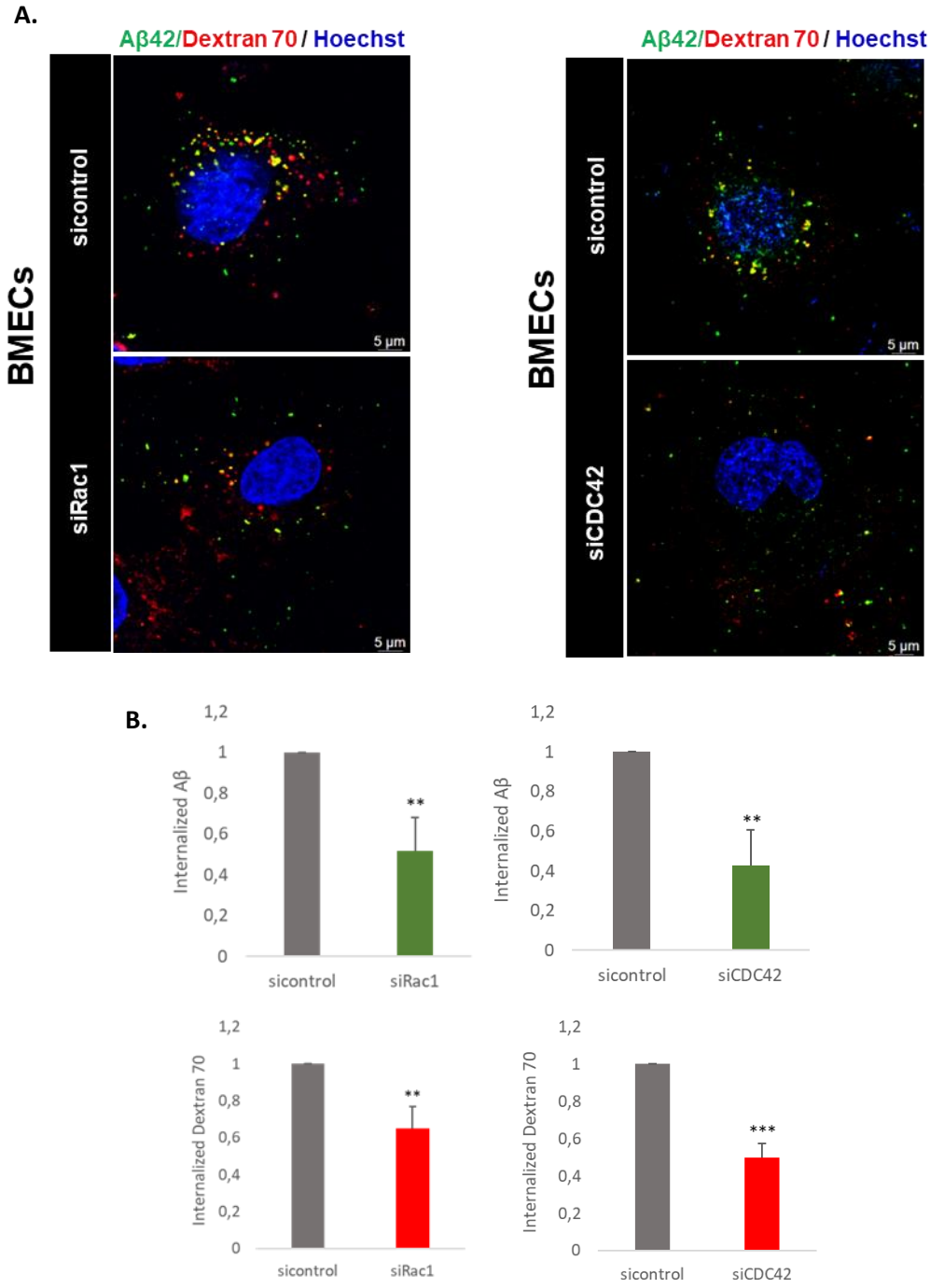

Figure 3.2: Aß uptake is decreased following knock down of molecular regulators of macropinocytosis in BECs. *(A)72 hours after transfection with siRNAs targeting Rac1 (siRac1), CDC42(siCDC42) or scrambled siRNA (sicontrol), BECs were serum-starved for 1 hour. Cells were then incubated for 15 minutes with 2 µmol/L Aß42 (green) and 1.5 mg/ml Dextran 70 kDa (red). Nuclei were stained with Hoechst (blue). Scale bar = 5 µm. (B) Quantification of the uptake of Aß42 and Dextran 70 by confocal microscopy based on the fluorescence intensity of each protein. Data are presented as mean fluorescence normalized to control (sicontrol). Aß42 and Dextran 70 uptake were decreased when Rac1 and CDC42 expression was silenced in BECs (n = 4, mean ± S.D., *p ≤ 0.05; **p ≤ 0.01; ***p ≤ 0.001; ****p≤0.0001, student's t-test).*

3.2 Investigation of the role of macropinocytosis in Aβ clearance from the brain in 5XFAD transgenic mice.

To validate our findings in vivo, we used 5XFAD transgenic mice that co-express a total of five AD-linked mutations [APP K670N/M671L (Swedish) + I716V (Florida) + V717I (London) and PS1 M146L + L286V], as an experimental model of AD. The 5xFAD transgenic mouse model is

widely used in Alzheimer's disease (AD) research due to its early and aggressive amyloid-beta (Aβ) deposition in the brain, particularly in the cortex and hippocampus. Specifically, these mice exhibit intraneuronal Aβ42 accumulation at approximately 1.5 months of age, cerebral amyloid plaque formation by 2 months, and measurable memory deficits by 4 months (Oakley, Cole et al. 2006) (Fig. 3.3).

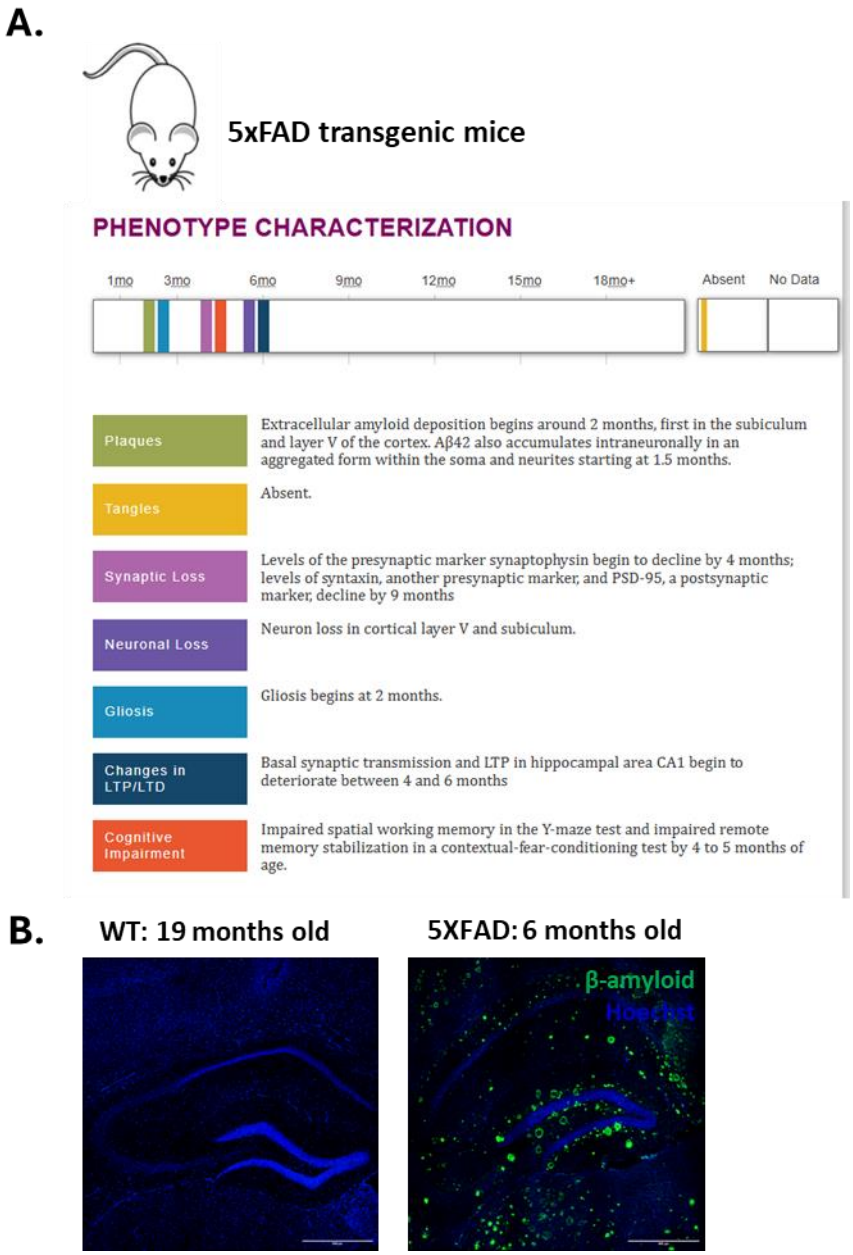

Figure 3.3: Experimental mouse model of AD. *(A) The 5XFAD mouse model is widely used in Alzheimer's disease (AD) research due to its early and aggressive amyloid-beta (Aβ) deposition in the brain, including the cortex and hippocampus. This model exhibits intraneuronal Aβ42 accumulation at 1.5 months, amyloid plaque formation at 2 months, and memory deficits by 4 months of age. (Figure adopted from: https://www.alzforum.org/research-models/5xfad-b6sjl) (B) 6 months old 5XFAD mice exhibit accumulation of Aβ protein in brain, while 19 months old WT mice show no detectable Aβ, as assessed by immunohistochemical analysis of brain sections.*

At 1.5 months of age, these mice were treated intraperitoneally with EIPA, a chemical inhibitor of macropinocytosis, every three days. At 3 months of age, mice brain samples were collected and analyzed by western blotting to detect Aβ protein levels. This experiment aimed

to determine whether inhibition of macropinocytosis impairs Aβ clearance across the BBB, thereby leading to increased accumulation of Aβ in the brain. Wild-type (WT) mice received the same treatment as 5XFAD mice, to assess whether inhibition of macropinocytosis leads to progressive abnormal accumulation of Aβ (Fig. 3.4).

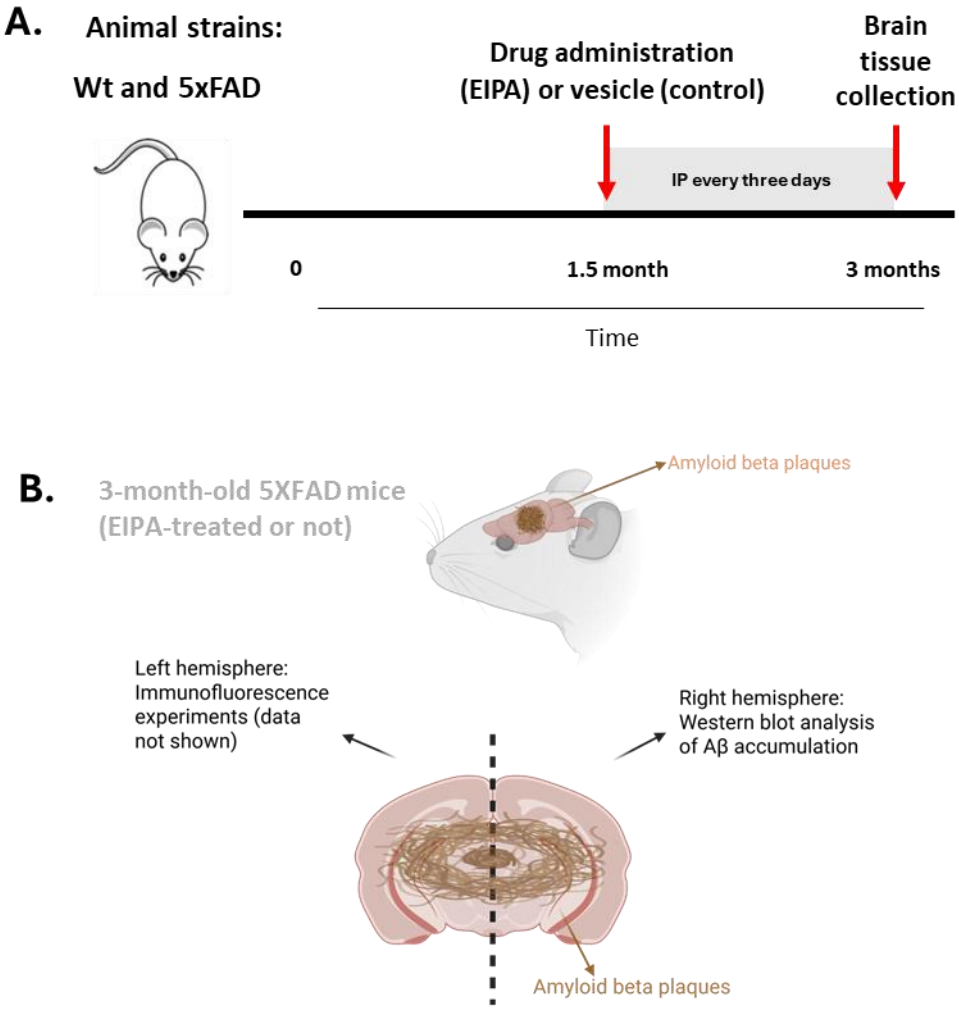

Figure 3.4: Experimental design for drug treatment in mice and subsequent brain tissue processing. *(A) 5XFAD and WT mice were treated intraperitoneally with EIPA, a chemical inhibitor of macropinocytosis, for 1.5 month starting at 1.5 months of age. At 3 months of age, mice were sacrificed, and brain tissues were collected. (B) The right hemisphere of each brain was homogenized and analyzed by Western blotting to quantify the levels of Aβ protein. The left hemisphere was processed for immunofluorescence experiments (data not shown). (Figures generated in Biorender)*

3.2.1 Aβ deposition in the cortex and hippocampus of 5XFAD mice is increased upon EIPA treatment.

Based on previous findings that macropinocytosis mediates Aβ uptake by endothelial cells, we hypothesized that its inhibition in 5XFAD transgenic mice would impair Aβ clearance from the brain. To test this, Aβ accumulation in the cortex and hippocampus of 5XFAD mice treated with EIPA or vehicle was analyzed by Western blotting. Wild-type (WT) mice treated with EIPA or vehicle served as controls.

As expected, Aβ accumulation was higher in both the cortex and hippocampus of 5XFAD mice following EIPA treatment compared to vehicle-treated controls. In addition, a substantial amount of high–molecular-weight Aβ species (>200 kDa), corresponding to amyloid plaques, was detected, and their accumulation was markedly increased upon EIPA treatment. Quantification of total Aβ levels in the cortex and hippocampus of five 5XFAD mice revealed that EIPA treatment resulted in approximately a 4-fold increase in cortical Aβ and a 1.5-fold increase in hippocampal Aβ. Predominantly, high–molecular-weight Aβ aggregates were observed, along with smaller, soluble Aβ oligomers (~28 kDa) (Fig 3.5, B).

The possible underlying mechanism suggests that inhibition of macropinocytosis in the brain impairs Aβ transcytosis across the BBB, leading to reduced clearance and subsequent accumulation of Aβ in the brain, thereby promoting plaque formation. However, as EIPA is expected to affect other cell types as well, we could not conclude that the effect is particularly because of the endothelial cells. Furthermore, Western blot analysis of cortex and hippocampus samples from WT mice treated with either EIPA or vehicle revealed only a single nonspecific band at 55 kDa, indicating that EIPA treatment does not induce abnormal Aβ production in wild-type animals (Fig. 3.6).

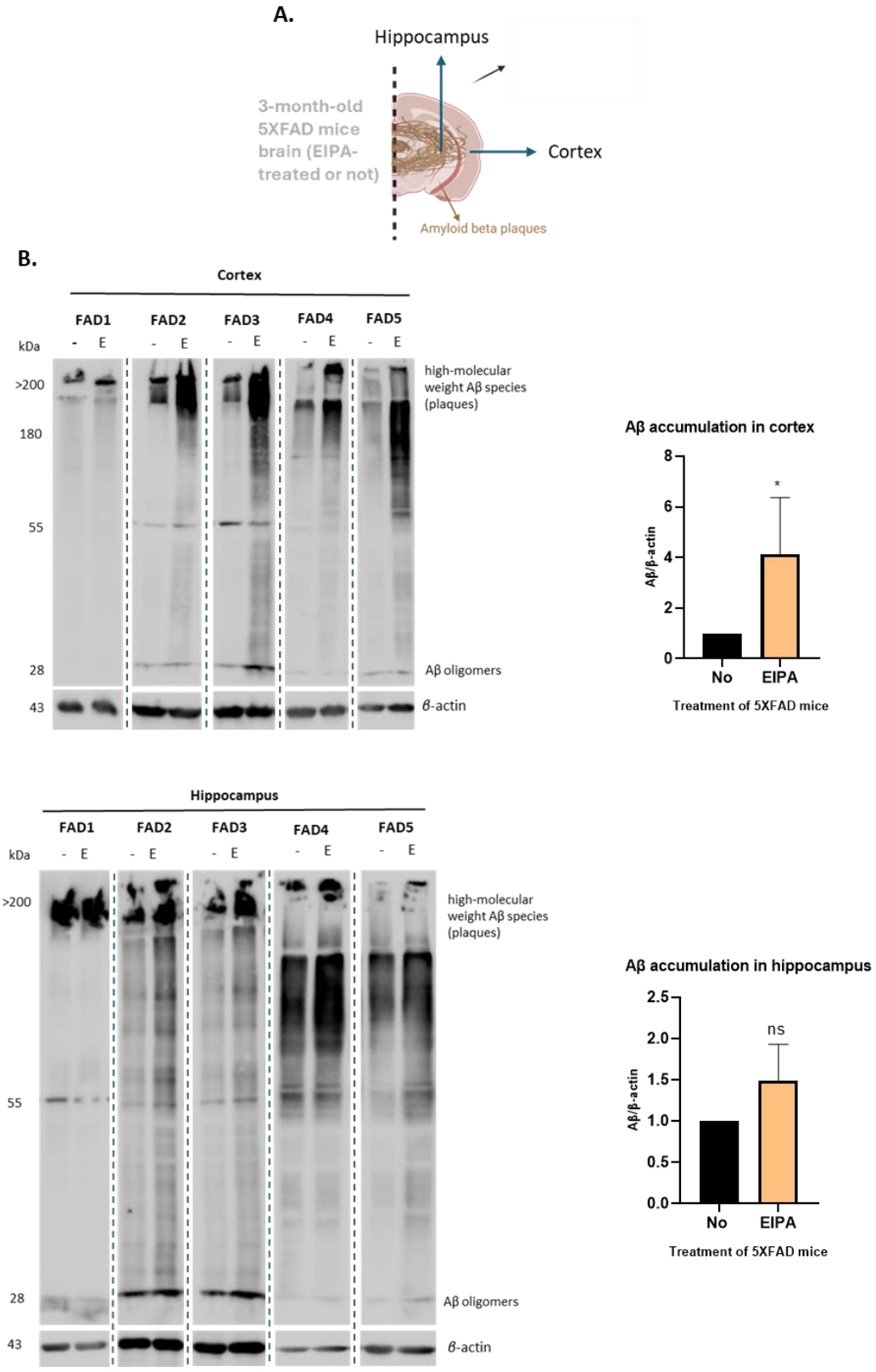

Figure 3.5: Western blot analysis of Aβ accumulation in 5XFAD mice upon EIPA treatment. *(A) Brain tissue from 5XFAD transgenic mice (EIPA-treated or not) was collected, and the cortex and hippocampus were separated for Aβ protein detection by Western blot. (B) Western blot analysis of Aβ protein in the cortex and hippocampus of five 5XFAD mice (FAD1-5), upon EIPA (E) or vehicle (-) treatment. Quantification of Aβ levels demonstrated that EIPA treatment resulted in a 4-fold and a 1.5-fold increase in Aβ accumulation upon EIPA treatment in the cortex and*

*the hippocampus, respectively, as compared to vehicle treated control (n = 5, mean ± S.D., ns, not significant; *p ≤ 0.05; **p ≤ 0.01; ***p ≤ 0.001; ****p≤0.0001, student's t-test).*

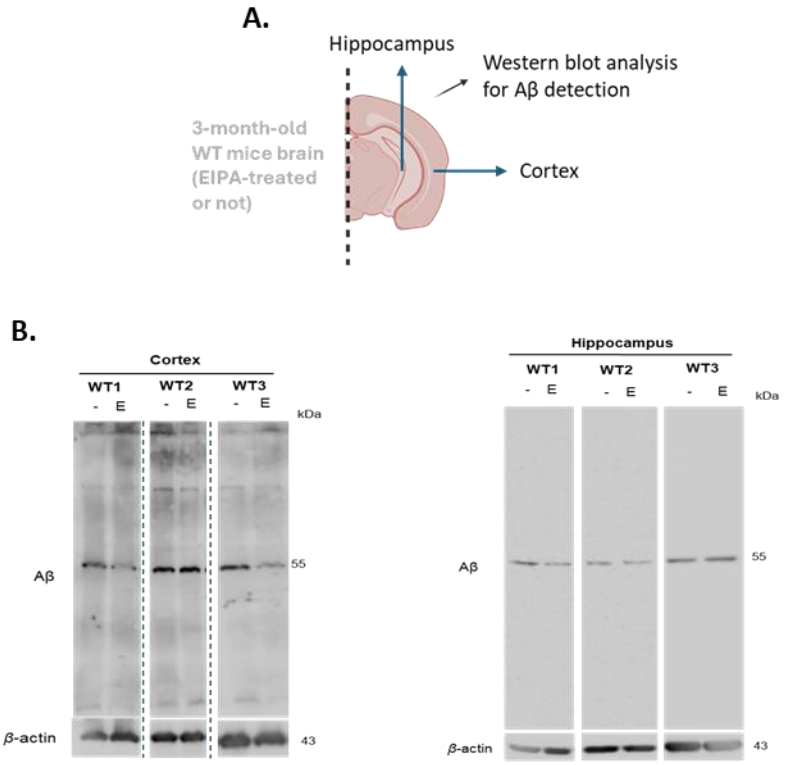

Figure 3.6: Western blot analysis in WT mice upon EIPA treatment. *(A) Brain tissue from WT mice (EIPA-treated or not) was collected, and the cortex and hippocampus were separated for Aβ protein detection by Western blot. (B) Western blot for Aβ detection in the cortex and hippocampus of three WT mice (WT1-3), EIPA-treated (E) or not (-). Only a non-specific band at the molecular weight of 55 kDa was detected.*

3.3 Establishment and characterization of an in vitro human model of Blood-Brain-Barrier derived from hiPSCs.

At the third part of the study, we aimed to establish a robust human in vitro model of the BBB derived from iPSCs. While primary BECs have been used previously, they exhibit poor BBB phenotype and senescence after few passages. In contrast, hiPSCs provide a scalable, renewable source of cells for BBB research (Jamieson, Searson et al. 2017).

Our aim was to differentiate iPSCs from a healthy donor (WT) and an age-matched AD patient carrying the APOE ε4/ε4 genotype into BECs, in order to generate a healthy and a diseased version of the in vitro model of BBB. The iPSC lines were generated from culture-expanded peripheral blood mononuclear cells and kindly provided by the group of PI V. Machairaki at Johns Hopkins School of Medicine (Das, Li et al. 2020).

Differentiation of iPSCs into brain endothelial cells was performed based on an already established protocol, using fully defined components (Neal, Marinelli et al. 2019). BEC differentiation occurs in a four-step process, beginning with the seeding of singularized iPSCs onto Vitronectin-coated plates in E8 medium containing 10 μM Rock inhibitor, for the maintenance of the pluripotency (Day -1). After seeding, iPSCs took neuroectodermal fate by switching medium to E6, a derivative of E8 medium composition lacking growth factors of pluripotency (Hollmann, Bailey et al. 2017), for 4 days (till Day 4). By day 4, a mixed population

of endothelial and neural progenitor cells was generated, and endothelial cells were next expanded by switching to endothelial cell (EC) medium, supplemented with bFGF and all-trans retinoic acid (RA). RA induces the brain endothelial specification and enhances the blood-brain barrier properties of the endothelial cells, through activation of BBB-specific gene expression (Lippmann, Al-Ahmad et al. 2014). By day 6 of differentiation, endothelial cells are expected to express all BBB-specific proteins, such as tight junction and adherens junction proteins. At day 6, BECs were purified from the mixed neuronal and endothelial population through subculture onto collagen IV/fibronectin-coated plates or filters. Brain endothelial cells selectively attach to this substate, while neural progenitor cells do not and are subsequently removed after medium exchange, yielding a pure population of BECs that form a tight monolayer. At day 7, purified BECs were shifted to EC medium lacking bFGF and RA. Finally, by the end of this differentiation procedure, we expect to generate a homogenous and scalable source of BECs derived from iPSCs (Fig. 3.7).

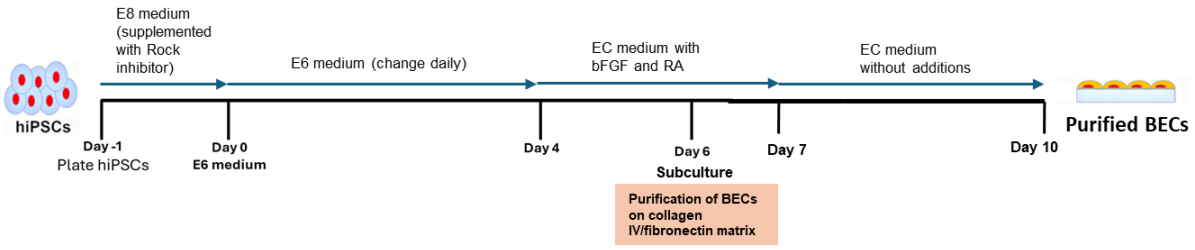

Figure 2.7: Differentiation scheme of hiPSCs into a purified population of BECs. *iPSCs were cultured in E6 medium for 4 days, followed by endothelial cell (EC) medium supplemented with bFGF and RA for 2 days. On day 6, differentiated BECs were purified by subculturing onto collagen IV/fibronectin-coated plates or transwells. Twenty-four hours after subculture, the medium was replaced with EC medium without supplements. By the end of the culture period (day 10), no further medium changes were performed.*

Following differentiation, we characterized the BBB model and assessed the quality of the iPSC-derived brain endothelium. Plate-cultured BECs were assessed by immunofluorescence and western blotting to confirm the expression of endothelial markers, adherens junction proteins, and tight junction proteins. BECs seeded on transwell inserts were evaluated for barrier formation through measurements of transendothelial electrical resistance (TEER), providing a quantitative assessment of tight junction integrity.

3.3.1 Morphological changes observed during the differentiation of healthy donor-derived iPSCs (WT) to BECs.

First, we applied the BEC differentiation protocol to iPSCs derived from a healthy donor (WT). We observed morphological changes and the formation of endothelial-like cells in phase-contrast images during the differentiation process. These images allowed us to monitor cell growth, cell viability and signs of cellular stress throughout the process.

Differentiation of iPSCs into brain endothelial cells (BECs) was initiated by switching medium to E6. By day 2, clusters of cells with cobblestone-like endothelial morphology appeared. To enrich the BEC population and promote barrier formation, at day 4 the medium was switched

to EC medium supplemented with bFGF and RA for two days. This resulted in overconfluent cultures by day 6, which were then subcultured onto collagen IV/fibronectin for purification. A confluent, endothelial-like monolayer formed by day 7, and by day 10, a dense, homogeneous culture of pure BECs with a tight, rounded morphology was obtained (Fig. 3.8).

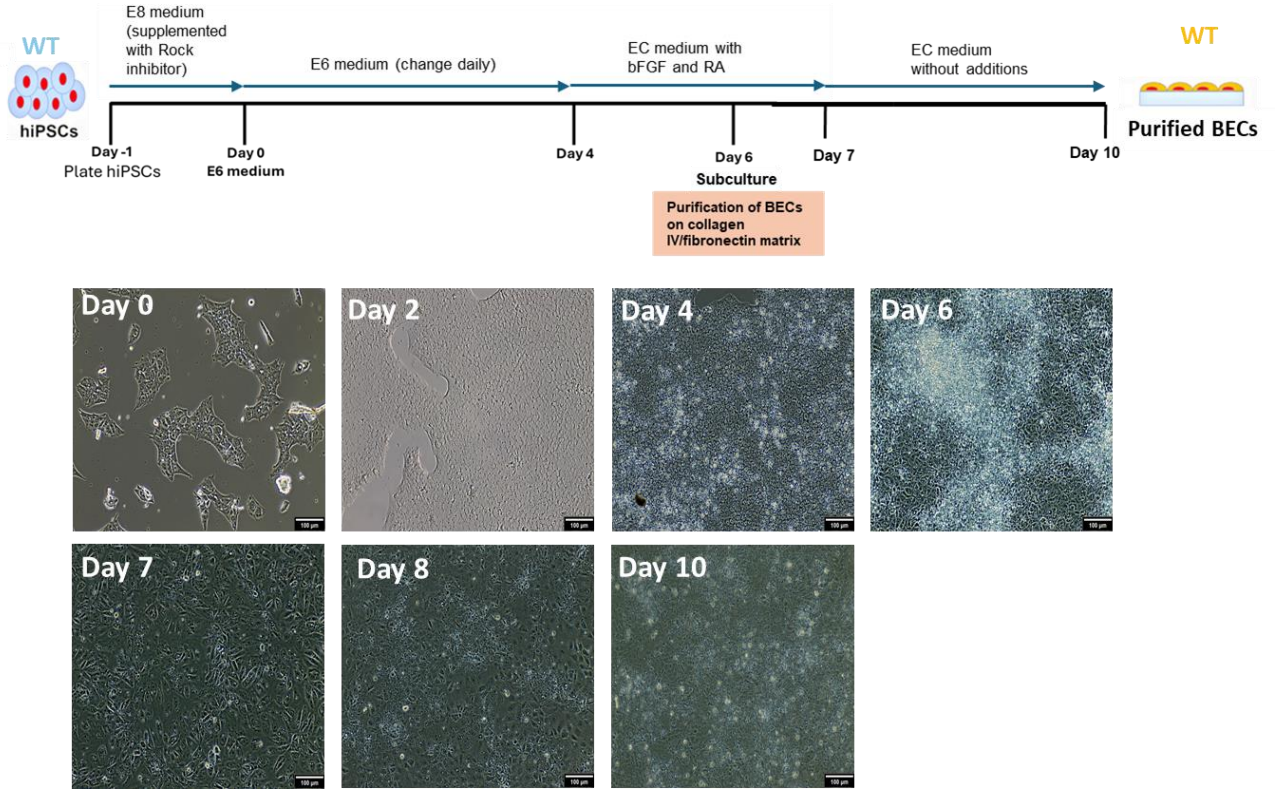

Figure 3.8: Phase contrast images of WT iPSCs during the differentiation process. *Light microscopy was used to visualize WT iPSCs differentiating into BECs with representative images shown from day 0 to day 10. Scale bar: 100 µm*

3.3.2 WT iPSC-derived BECs express BBB-specific tight junction and adherens junction proteins

The BBB integrity and quality of differentiated BECs, was, firstly, assessed by the expression of BBB-specific tight junction proteins. A metric of BBB integrity is the expression of tight junctions, which are multiprotein membrane complexes found in regions where two brain endothelial cells join together. Tight junctions between BECs seal the paracellular space forming a continuous and intact barrier with low paracellular permeability of ions and molecules (Campbell, Maiers et al. 2017, Knox, Aburto et al. 2022). Brain endothelial tight junctions include claudins (claudin-1, -3, -5, -12), occludin and the zonula occludens (ZO-1, ZO-2, ZO-3) (Fig. 3.9, A).

ZO-1 is an intracellular peripheral membrane protein of tight junctions that interact with the transmembrane proteins Claudin-5 and Occludin, anchoring them and connecting them to the actin cytoskeleton (Knox, Aburto et al. 2022). Thus, ZO-1 contributes to the sealing of neighboring brain endothelial cells and the establishment of the barrier. By day 10 of differentiation, we obtained a population of BECs that strongly expressed this protein, as

assessed by immunofluorescence microscopy. ZO-1 was continuously localized along the cell membranes without detectable gaps, indicating intact BBB formation (Fig. 3.9, Bi).

Claudin-5 is considered among the primary sealing components of the tight junctions and is a transmembrane protein. This protein reduces the paracellular ion movement and narrows the paracellular cleft between adjacent BECs (Knox, Aburto et al. 2022). By day 10 of differentiation, we detected strong expression of claudin-5 protein in iPSC-derived BECs, compared with the initial iPSC culture, using western blotting (Fig. 3.9, Bii)

Another set of cell junctions, the adherens, organize the intercellular connections at the brain endothelium and contribute to barrier properties. Adherens junctions include transcellular proteins such as cadherins, catenins, platelet endothelial cell adhesion molecule-1 (PECAM-1), junctional adhesion molecules (JAMs) and endothelial cell-selective adhesion molecule (ESAM) (Knox, Aburto et al. 2022). Cadherins represent one of the major families of transmembrane adhesion proteins that mediate strong cell-cell interactions through their extracellular domains, while intracellular domains interact with catenins, which connect cadherins with the actin cytoskeleton (Vestweber 2008).

Among the various cadherins, VE-cadherin is the only type selectively expressed by endothelial cells. It is crucial for the organization of the vasculature and the maintenance of endothelial cell integrity (Vestweber 2008). Thus, the expression of this protein in cell membranes indicates both the endothelial identity of the differentiated cells and the formation of an intact brain endothelium with strong intercellular contacts. Immunofluorescent staining of VE-cadherin confirmed its expression at the cell membrane (Fig. 3.9, C). The protein was already detectable by day 6 of differentiation, at which point the culture contained a mixed population of brain endothelial cells and neural progenitors. In other words, by day 6 we had obtained a population of endothelial cells with strong cell contacts. By day 10 of differentiation, VE-cadherin expression was still detectable in the differentiated cells; however, its levels were significantly reduced. VE-cadherin was no longer expressed uniformly, as only some cells retained detectable levels of the protein. Moreover, in cells that did express the protein, its localization at the cell membranes appeared discontinuous, indicating a loss of junctional integrity. This suggests that prolonged culture of differentiated cells, without medium changes, possibly stresses the cells, leading to a loss of barrier integrity.

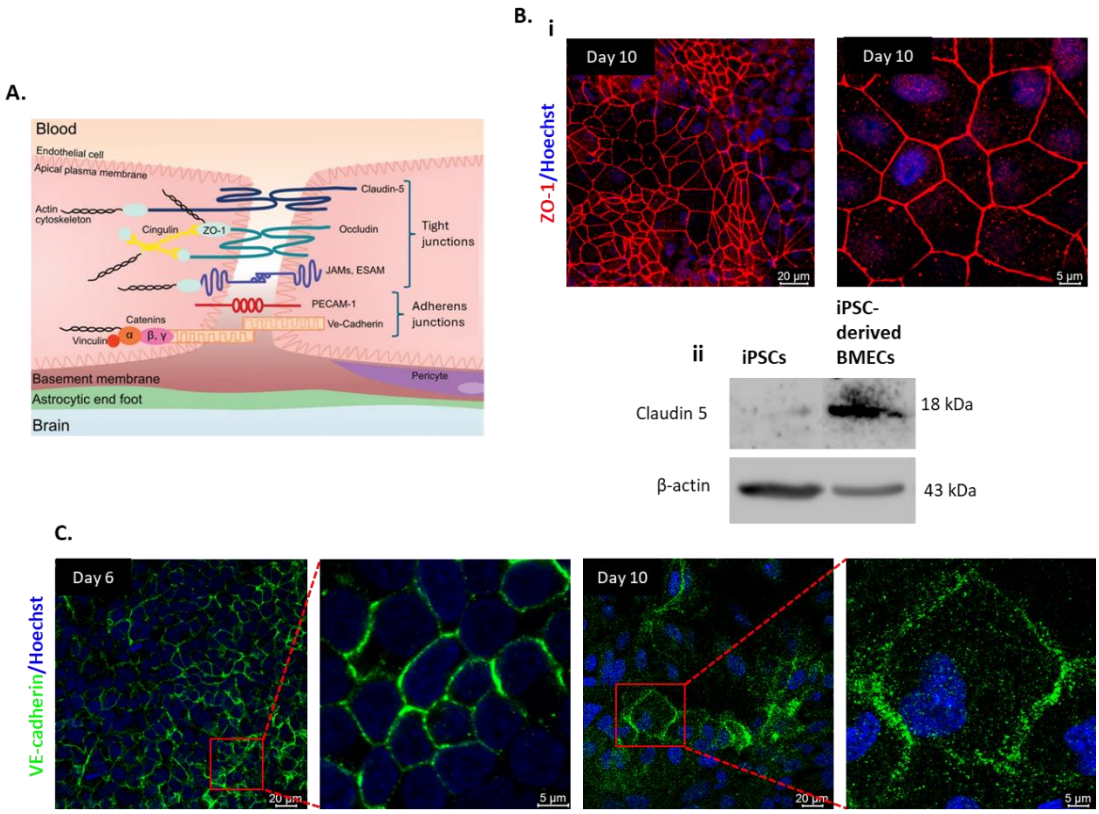

Figure 3.9: Differentiated BECs derived from WT iPSCs express BBB-specific tight junctions and adherens junctions proteins. *(A) Scheme of tight junction and adherens junction proteins expressed at the lateral membrane of adjacent BECs. (B) Differentiated BECs express tight junction proteins (ZO1: red, Claudin-5: green), as assessed by immunofluorescence and western blotting at day 10. (C) Differentiated BECs express VE-cadherin (green) at day 6 and day 10 of differentiation, as assessed by immunofluorescence. Nuclei were stained with Hoechst. Scale bars: 20 µm, 5 µm*

3.3.3 WT iPSC-derived BECs exhibit polarized expression of junctional proteins.

The junctional proteins of brain endothelial cells at the BBB exhibit a polarized distribution along the plasma membrane. The apical membrane of BECs faces the blood circulation, whereas the basal membrane faces the brain parenchyma. Junctional proteins that seal adjacent brain endothelial cells and restrict paracellular permeability are located at the lateral membrane. Specifically, tight junction proteins are located at the interface between apical membrane, facing the lumen, and the basolateral surface in contact with the brain. In addition to providing a barrier between blood and brain, tight junctions also limit the free diffusion of lipids and proteins between the apical and basal membrane, thereby establishing and maintaining cell polarity (Gonzalez-Mariscal, Tapia et al. 2008). According to this organization, adherens junction proteins are expected to localize underneath the tight junctions, closer to the basal membrane (Campbell, Maiers et al. 2017) (Fig. 3.10, A). Accordingly, in differentiated BEC cultures, tight junction proteins such as ZO-1 are anticipated near the apical membrane, while adherens junction proteins such as VE-cadherin localize underneath, closer to the basal membrane, though both remain confined to the lateral membrane. At day 10 of differentiation, immunostaining for VE-cadherin and ZO-1 followed by confocal microscopy and z-stack projections confirmed this polarized distribution, as shown in Fig. 3.9, B. ZO-1 (red) was detected closer to the apical membrane, whereas VE-cadherin (green) was localized

closer to the basal membrane. These findings demonstrate that the differentiated BECs exhibit the expected polarity.

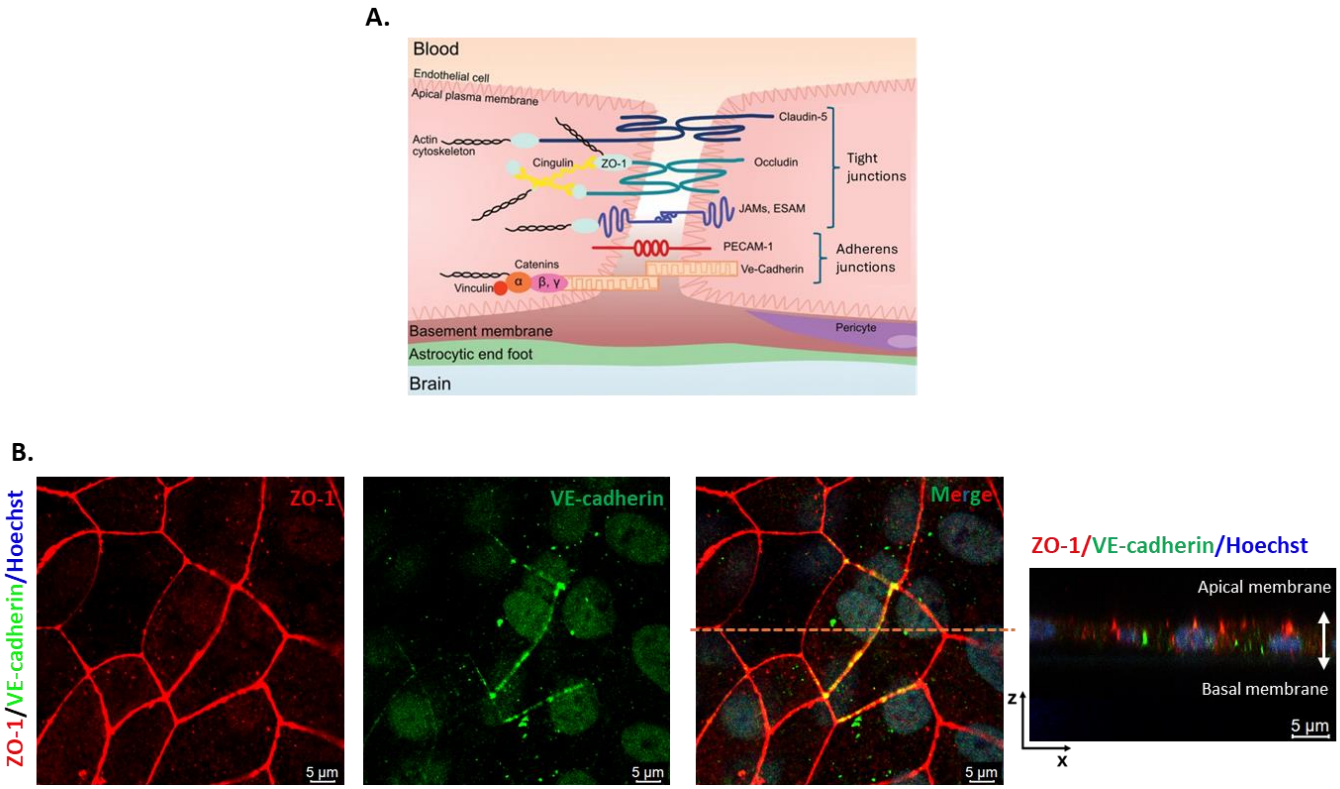

Figure 3.9: iPSC-derived BECs exhibit polarized expression of tight junctions and adherens junctions proteins. *(A) Scheme of tight junction and adherens junction proteins expressed at the lateral membrane of adjacent BECs. (B) Immunostaining for ZO-1 (red) and VE-cadherin (green). VE-cadherin is localized closer to the basal membrane and ZO-1 is closer to the apical membrane. Nuclei were stained with Hoechst. Scale bar: 5 µm.*

3.3.4 Differentiated BECs (WT) express the endothelial-specific von Willebrand factor (VWF).

To assess the successful differentiation of mature brain endothelial cells (BECs), it is necessary to examine endothelial-specific markers. A characteristic feature of endothelial cells is the presence of unique endocytic secretory vesicles called Weibel-Palade bodies (WPBs) (Weibel 2012). These vesicles are crucial for the rapid response to vascular damage, as they store and secrete prothrombotic, proinflammatory, and angiogenic biomolecules (Weibel and Palade 1964, Michaux and Cutler 2004). The main component of WBPs is von Willebrand factor (VWF), a large glycoprotein essential for blood clotting. VWF is essential for the formation of these vesicles through its polymerization. Therefore, the presence of VWF is a strong indicator of mature and functional endothelial cells.

On day 10 of differentiation, WT iPSC-derived BECs were fixed and immunostained for von-Willebrand factor (VWF) (Fig. 3.10). All cells expressed VWF, confirming their endothelial identity and the formation of a pure population. The staining pattern indicated the presence of Weibel-Palade bodies (WPBs), which were distributed as a network throughout the cells.

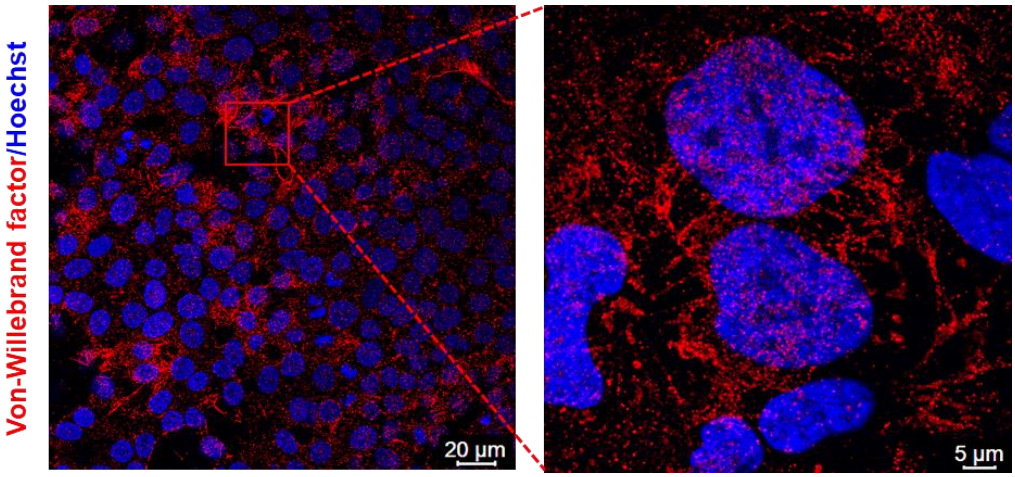

Figure 3.10: Differentiated BECs derived from WT iPSCs express the endothelial-specific marker von Willebrand factor. *At day 10 cells were stained for von Willebrand factor (red). Nuclei were stained with Hoechst. Scale bars: 20 µm, 5 µm.*

3.3.5 Evaluation of passive barrier properties of WT iPSC-derived BECs by TEER.

On day 6 of differentiation, the culture contained a mixed population of BECs and neural progenitors. Cells were subcultured onto collagen IV/fibronectin–coated transwell inserts, which selectively promoted BEC adhesion while non-adherent neural progenitors were removed. By day 7, a purified, mature BEC monolayer was obtained, and the medium was switched to EC medium without bFGF and RA to induce barrier formation (Fig. 3.11, A).

To monitor the development of the barrier properties in iPSC-derived BECs, transendothelial electrical resistance (TEER) was measured starting on day 7. TEER is a widely used quantitative technique for assessing tight junction integrity in endothelial and epithelial monolayers. Measurements were performed in real time using a pair of STX2 chopstick electrodes and an EVOM2 voltohmeter, with electrodes placed in the apical and basolateral compartments separated by the cellular monolayer. This non-invasive technique can be repeated without damaging the cells (Srinivasan, Kolli et al. 2015) and provides a reliable indicator of barrier integrity, reflecting the ability of iPSC-derived BECs to form tight junctions that restrict paracellular transport—a critical feature of the BBB.

On day 7, TEER values were very low (approximately 100 $\Omega x cm^2$). By day 8, BECs had formed a functional barrier, with TEER values rising to 1000 $\Omega \times cm^2$, which exceeds the commonly accepted threshold for a functional barrier (500-1000 $\Omega \times cm^2$) (Mantle, Min et al. 2016). Thus, on day 8 BECs formed a tightly sealed monolayer and a functional barrier, suitable for experimental assays. However, TEER significantly decreased on days 9 and 10 indicating a loss of barrier integrity (Fig. 3.11, B). This finding is consistent with immunofluorescence data showing a significant reduction in VE-cadherin expression by day 10 (Fig. 3.9, C). As previously suggested, this decline is likely due to the loss of brain endothelial phenotype caused by prolonged culture without medium changes.

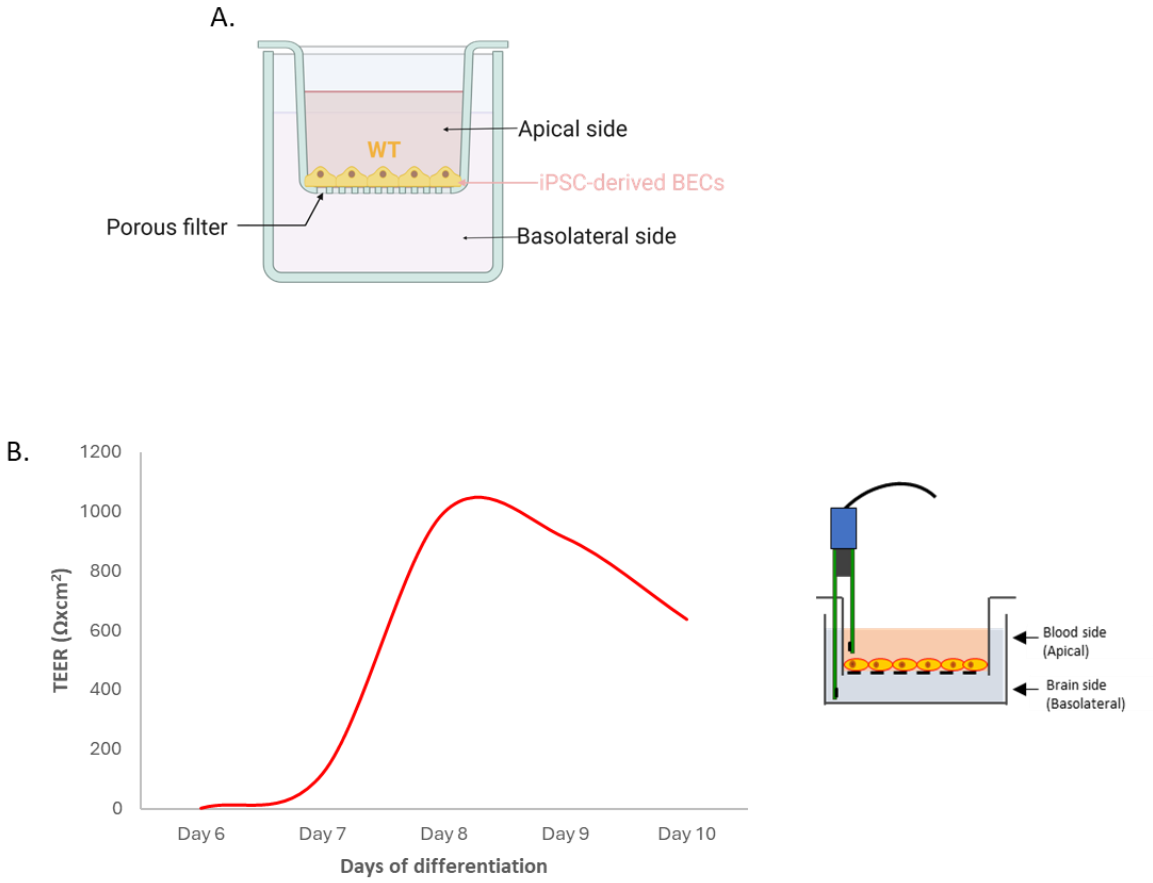

Figure 3.11: Evaluation of barrier integrity of WT iPSC-derived BECs by TEER measurement. *(A) At day 6 of differentiation, BECs were purified via replating onto collagen IV/fibronectin coated transwell inserts. (B) TEER was measured daily till day 10.*

On day 10, iPSC-derived BECs seeded on transwell inserts were analyzed by immunofluorescence to detect the expression and localization of tight and adherens junction proteins. The BEC monolayer showed a robust, continuous junctional network at cell-cell borders, with strong expression of both ZO-1 (a tight junction protein) and VE-cadherin (an adherens junction protein) without gaps (Fig. 3.12, A). Moreover, BECs exhibited polarity, as ZO-1 was localized near the apical membrane and VE-cadherin was expressed closer to the basal membrane. We also confirmed successful endothelial differentiation by detecting the expression of the endothelial-specific von Willebrand factor in all cells of the monolayer (Fig. 3.12, B).

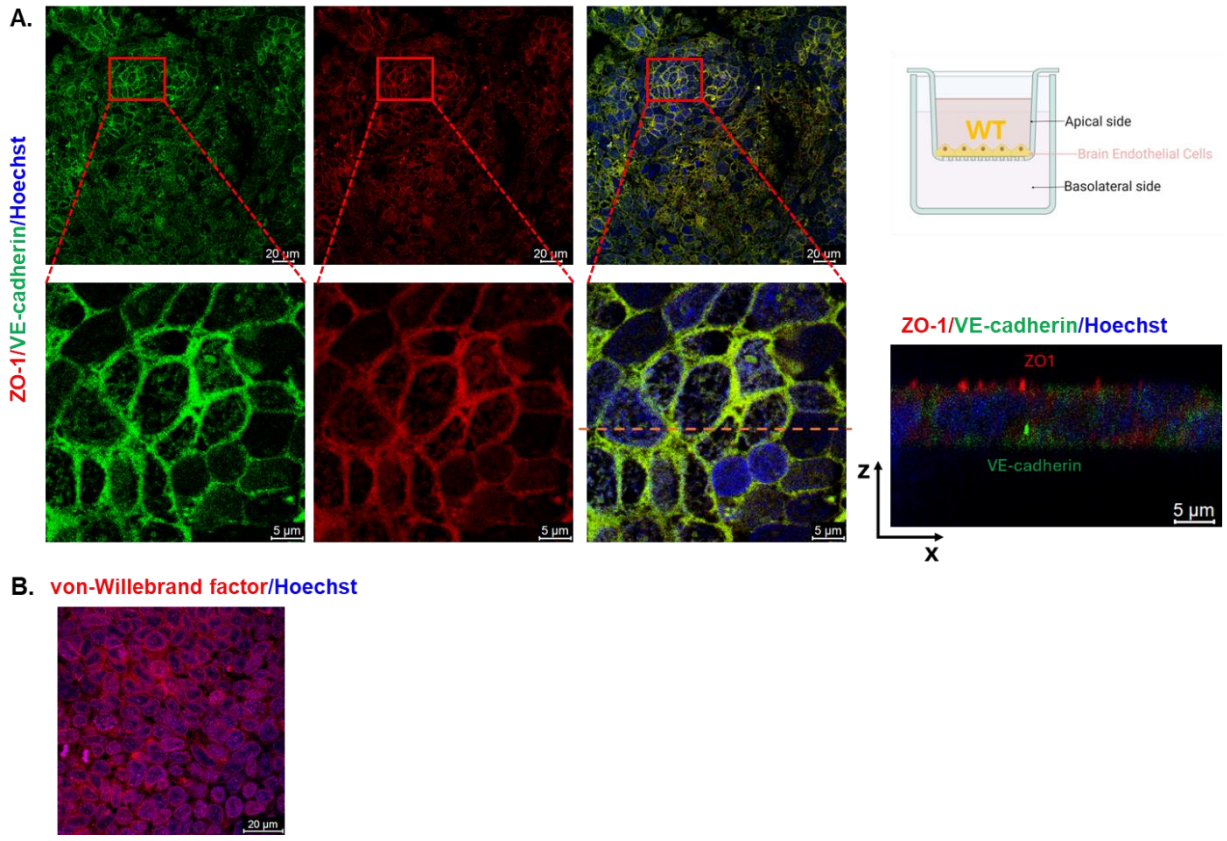

Figure 3.12: WT iPSC-derived BECs seeded onto transwell filters express tight and adherens junction proteins, as well as von Willebrand factor*. The monolayer of BECs purified on transwell inserts were fixed at day 10 and stained for BBB-specific and endothelial markers. (A) Immunofluorescence for ZO-1 (red), and VE-cadherin (green). (B) Immunofluorescence for von Willebrand factor (red). Nuclei were stained with Hoechst. Scale bars: 20 µm, 5 µm.*

These results indicate that the iPSC differentiation protocol generated a pure population of BECs with a robust BBB phenotype, confirmed by strong expression of tight junction (ZO-1, claudin-5), adherens junction (VE-cadherin), and endothelial (von Willebrand factor) markers. The cells also exhibited enhanced barrier function, as shown by elevated TEER values on transwell inserts, providing an effective in vitro BBB model for studying Aβ clearance.

Subsequently, to generate patient-derived brain endothelial cells for an Alzheimer's disease (AD) BBB model, we applied this differentiation protocol to an iPSC line (JHUi002-A) derived from an AD patient carrying the ApoE ε4/ε4 genotype, the strongest genetic risk factor for AD.

3.3.6 Morphological changes observed during the differentiation of AD patient-derived iPSCs to BECs.

Using phase-contrast microscopy, we monitored cell growth, viability, and stress throughout the differentiation process and confirmed the development of cells with an endothelial-like morphology (Fig. 3.13).

On day 0, the iPSC culture medium was switched to E6 to initiate differentiation. By day 2, we observed the emergence of endothelial-like cells, characterized by a small, rounded morphology. However, not all cells exhibited this typical morphology; cells with irregular shapes were also present. This morphological heterogeneity was the first observed difference between the differentiation of AD patient-derived iPSCs and the WT iPSC line into BECs. By

day 4, the cell density had increased, yielding large colonies of endothelial-like cells. These colonies displayed numerous projections at their edges and consisted of multiple cell layers. This contrasted with the WT line, where colonies formed a monolayer and lacked these projections. Cells became confluent by day 6. At this point, we obtained a mixed population of brain endothelial cells and neural progenitors. We therefore proceeded to purify the BECs by subculturing them onto plates or transwells coated with collagen IV and fibronectin. However, dissociation with Accutase induced cellular stress and death. Consequently, by day 7, the cultures had not reached confluence, and the cells were sparsely seeded on the plates. We then switched to EC medium, lacking bFGF and RA, and maintained the culture without further media changes until confluence was achieved. Finally, on day 11 a confluent monolayer of BEC-like cells was obtained.

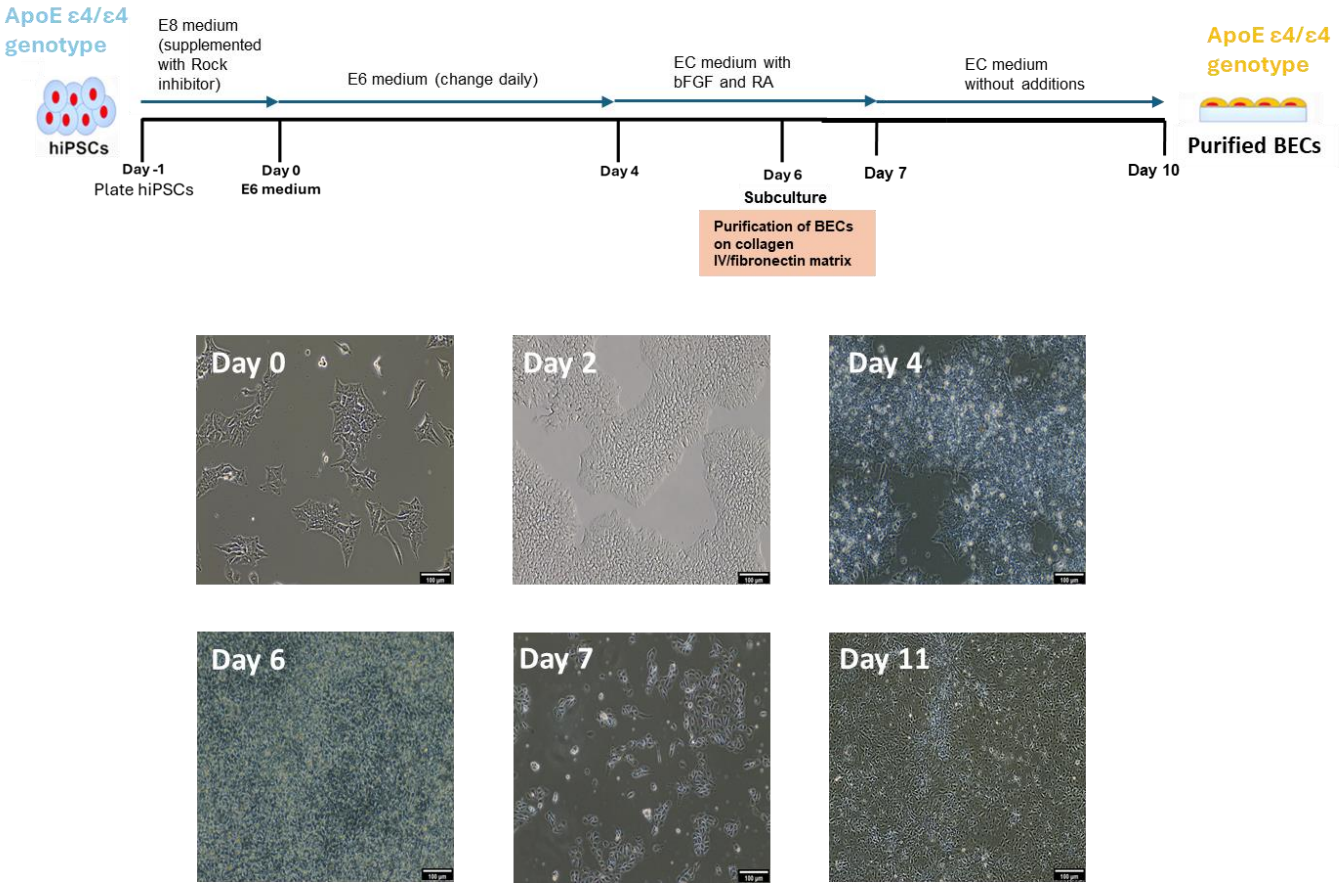

Figure 3.13: Phase contrast images of ApoE ε4/ε4 iPSCs during the differentiation process. *Light microscopy was used to visualize iPSCs differentiating into BECs with representative images shown from day 0 to day 11. Scale bar: 100 µm*

3.3.7 Differentiated BECs with ApoE ε4/ε4 genotype express adherens junction proteins and endothelial-specific markers.

During the differentiation of AD patient-derived iPSCs into BECs, we assessed the expression of BBB markers using immunofluorescence. By day 6 of differentiation, cells robustly expressed VE-cadherin, with continuous membrane localization and no gaps, indicating the formation of adherens junctions and confirming their endothelial identity (Fig. 3.14, A). This suggested successful generation of BECs by day 6 of differentiation. At this point,

we subcultured cells onto collagen IV/fibronectin-coated plates to purify the BECs from the mixed endothelial and neural population. On day 10, cells were subjected to immunofluorescence to detect the expression of endothelial-specific von-Willebrand factor (Fig. 3.14, B). All cells expressed this protein confirming the generation of a culture of

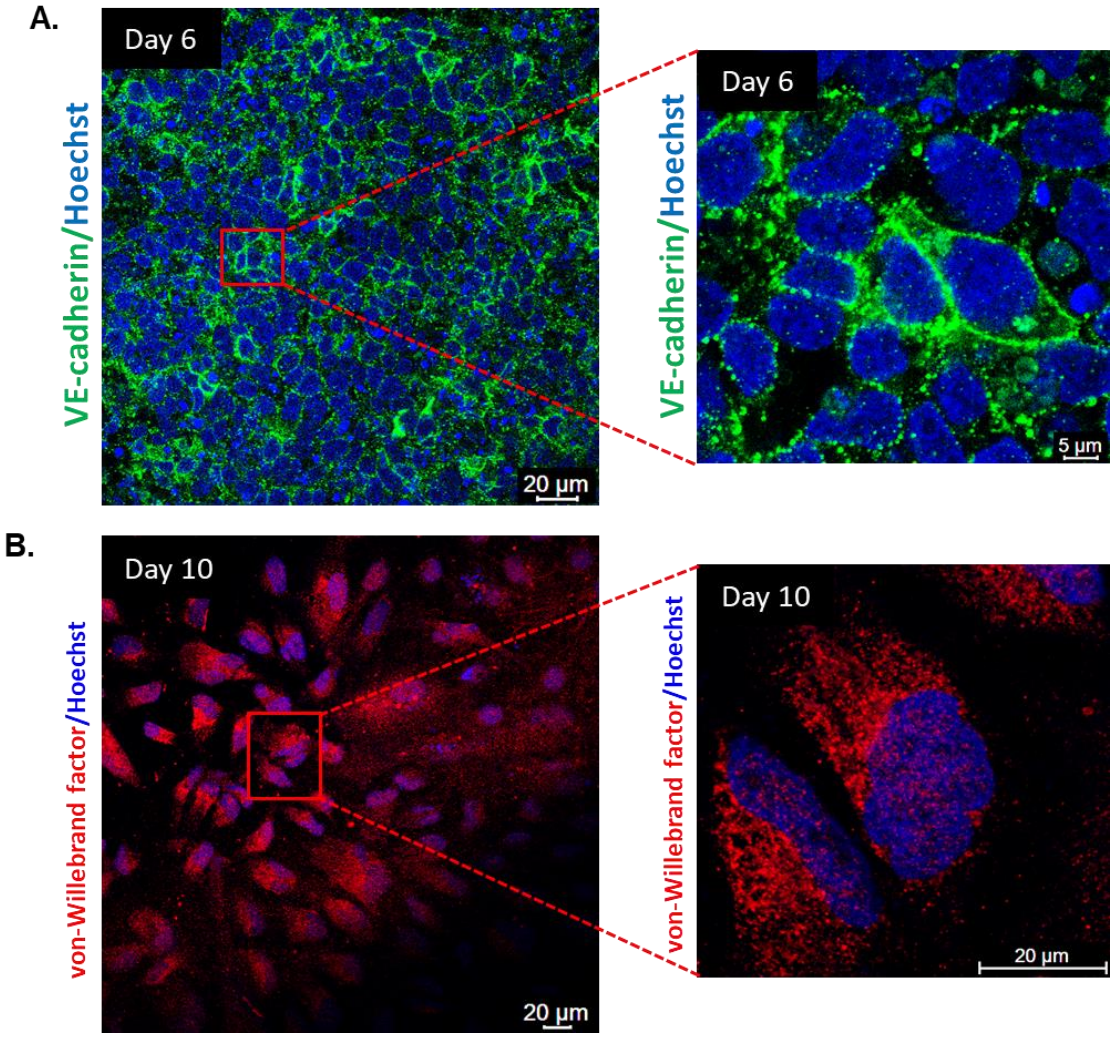

Figure 3.14: ApoE ε4/ε4 iPSC-derived BECs express the BBB-specific adherens junction protein VE-cadherin and the endothelial-specific marker von Willebrand factor. *(A) Immunostaining of VE-cadherin (green) at day 6. (B) Immunostaining of von Willebrand factor (red) at day 10. Nuclei were stained with Hoechst. Scale bars: 20 µm, 5 µm.*

endothelial cells derived from an AD patient. However, cells were sparsely seeded onto the plates, possibly due to increased stress and cell death during subculture, a phenomenon that was particularly pronounced in this specific AD patient-derived cell line.

3.3.8 Evaluation of barrier properties of AD patient-derived BECs by TEER.

In addition to BBB marker expression, AD patient-derived BECs were expected to exhibit tight barrier properties. Transendothelial electrical resistance (TEER) measurement is a key functional assay for assessing tight junction integrity between adjacent BECs. After purifying BECs onto collagen IV/fibronectin–coated transwell filters on day 6 (Figure 3.15A), TEER was measured daily (Fig. 3.15, B). In contrast to WT iPSC-derived BECs, the AD patient-derived BECs initially exhibited very low TEER values following subculture, consistent with phase-contrast

images showing sparse cell seeding at that time (Figure 3.13). However, by day 11, when cells reached confluency, TEER values exceeded 1000 Ωxcm², indicating the formation of a functional tight barrier.

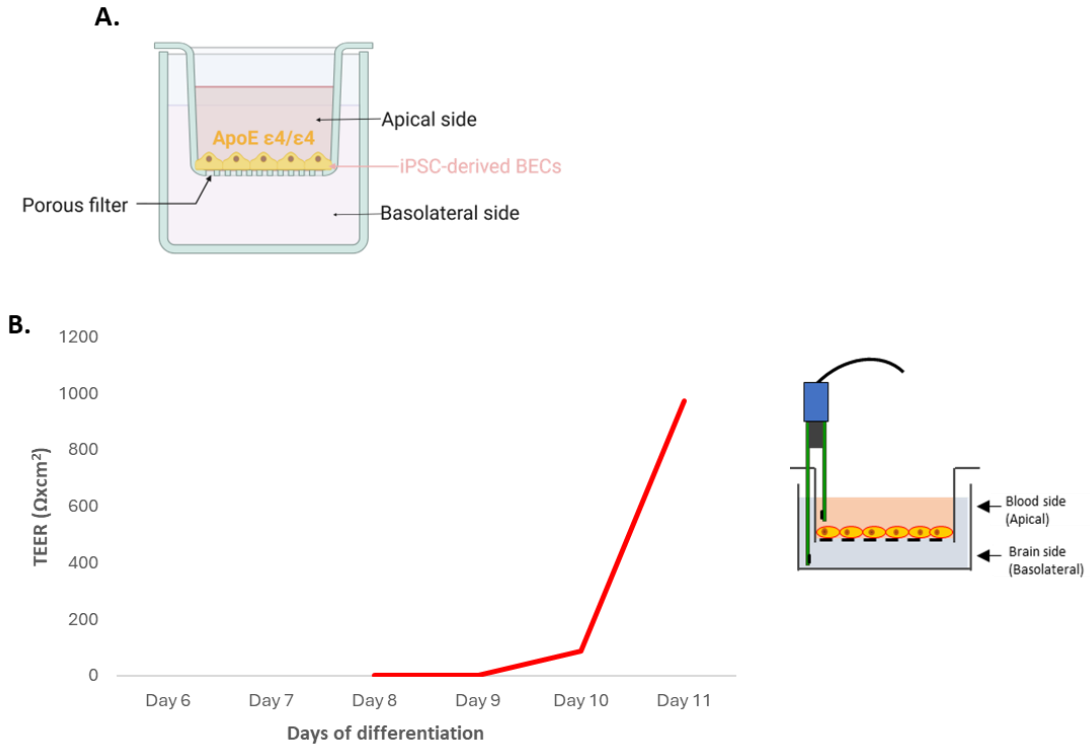

Figure 3.15: Evaluation of barrier integrity of ApoE ε4/ε4 iPSC-derived BECs by TEER measurement. *(A) At day 6 of differentiation, BECs were purified via replating onto collagen IV/fibronectin coated transwell inserts. (B) TEER was measured daily till day 11.*

These results demonstrate the successful differentiation of iPSCs derived from an AD patient carrying the ApoE ε4/ε4 genotype into BECs, as evidenced by the expression of key BBB marker and the achievement of high TEER values. This patient-specific BEC model provides a valuable human in vitro BBB model for investigating impaired endocytic pathways in Alzheimer's disease.

4. DISCUSSION

Aβ clearance from the brain is the primary mechanism preventing its accumulation and the formation of senile plaques, the hallmark of Alzheimer's disease (AD). Under physiological conditions, Aβ clearance is primarily mediated through endocytosis by brain endothelial cells (BECs) of the blood-brain-barrier (BBB), followed by transcytosis and subsequent release into the bloodstream for peripheral degradation. This pathway is frequently impaired in AD patients, leading to impaired efflux and progressive accumulation of Aβ in the brain parenchyma. To date, clathrin-mediated endocytosis has been the only identified route for Aβ uptake and transport by BECs (Zhao, Sagare et al. 2015). However, endothelial cells employ several distinct endocytic pathways for extracellular cargo uptake. Considering the increased level of VEGF in AD (Cho, Park et al. 2017) -a growth factor known to promote internalization

via macropinocytosis (Basagiannis, Zografou et al. 2016)- we hypothesized that Aβ may also be internalized through alternative pathways, particularly macropinocytosis.

The purpose of the present study was to investigate the role of macropinocytosis in Aβ uptake by BECs and its clearance from the brain, as well as to establish an in vitro, AD-relevant human BBB model derived from iPSCs. This model will enable further exploration of the entire range of unexplored endocytic pathways of BECs involved in Aβ clearance, as well as potential endocytic abnormalities and neurovascular unit dysfunction associated with AD pathology.

The first part of the study investigated the role of macropinocytosis in Aβ uptake by primary BECs. To test our hypothesis, we used RNA interference to silence specific molecular regulators of macropinocytosis (e.g. Rac1, Cdc42). Successful siRNA-mediated knockdown of these GTPases resulted in a significant reduction (approximately 50%) in exogenously added $A\beta_{42}$ uptake. These findings suggest that macropinocytosis contributes to Aβ uptake by BECs. Importantly, our siRNA-based approach provided higher specificity in targeting macropinocytosis compared to commonly used chemical inhibitors (e.g., EIPA, Dynasore), which are prone to off-target effects (Basagiannis, Zografou et al. 2021).

To validate these in vitro findings in an in vivo context, we employed the 5XFAD transgenic mouse model of AD, which develops early and aggressive Aβ deposition in the brain (Oakley, Cole et al. 2006). Chemical inhibition of macropinocytosis through intraperitoneal administration of EIPA between 1.5 and 3 months of age led to increased Aβ accumulation within the brain thereby highlighting the pivotal role of macropinocytosis in Aβ clearance. Nonetheless, some limitations must be acknowledged. EIPA inhibits macropinocytosis in multiple cell types rather than exclusively targeting BECs. Its potential effect on microglia makes it difficult to determine to what extent the observed effect stems from reduced Aβ transcytosis across the BBB or from impaired macropinocytosis-mediated internalization and degradation of Aβ by resident immune cells (Wildsmith, Holley et al. 2013). Nevertheless, given the limited permeability of EIPA across the BBB, it is reasonable to assume that the predominant effect arises from inhibition of macropinocytosis in BECs, which are directly exposed to circulating agents, rather than within parenchymal microglia. To address the specificity issue of systemic EIPA treatment, future studies could consider using endothelial-specific conditional knockouts, e.g. for the genes Rac1 or Cdc42.

Despite their widespread utility, animal models often lack consistent predictive value for humans, with about 50% of the findings not translating to human responses (Perel, Roberts et al. 2007). Interestingly, rodent BBB differs significantly from the human one in transporter expression, tight junction composition, and overall barrier tightness (Jamieson, Searson et al. 2017). This highlights the need to develop human in vitro models of the BBB to study its function in health and disease. The transwell platform is the most widely used model of BBB research, where BECs are seeded onto a porous membrane that separates the apical and basolateral chambers. To better mimic the in vivo environment, astrocytes, neurons, and pericytes are typically added to the basolateral chamber (Jamieson, Searson et al. 2017). Primary cells are commonly used to model BBB, but they exhibit several limitations. For instance, primary BECs display a poor BBB phenotype, that is rapidly lost after a few passages, while primary sources of other neurovascular unit cell types often face similar limitations and

are typically of animal origin (Jamieson, Searson et al. 2017). In contrast, human iPSCs provide an unlimited, self-renewable and scalable source of BECs for BBB research. Moreover, all neurovascular unit cell types can be derived from the same iPSC line, enabling the development of a fully human, syngeneic BBB model (Jamieson, Searson et al. 2017). Importantly, iPSCs can also be derived from AD patients, allowing the generation of disease-relevant BBB models that can be used to investigate potential endocytic abnormalities and BBB dysfunction associated with AD.

In the third part of this study, our aim was to establish an iPSC-derived in vitro model of the BBB through differentiation of iPSCs into BECs. For this purpose, we applied a facile, scalable and highly efficient differentiation protocol of iPSCs into a pure and mature population of BECs, using fully defined components. The method involved simultaneous endothelial and neural cell co-differentiation with culturing iPSCs for 4 days in E6 medium (Hollmann, Bailey et al. 2017), which is a derivative of E8 medium, lacking factors of pluripotency, that converts iPSCs to neuroectoderm (Lippmann, Estevez-Silva et al. 2014). By differentiating iPSCs into both neural and endothelial lineages, we recapitulate the in vivo embryonic brain environment, where developing neural progenitors secrete cues-such as regulators of Wnt/β-catenin pathway-that promote the BBB specification of endothelial cells (Stenman, Rajagopal et al. 2008, Daneman, Agalliu et al. 2009). By the end of the co-differentiation procedure (day 4), only a small percentage of the total population is expected to consist of brain endothelial cells (Lippmann, Azarin et al. 2012). At this point, the BEC population is expanded for 2 days in an endothelial cell medium supplemented with B27 (Neal, Marinelli et al. 2019), basic fibroblast growth factor (bFGF) and retinoic acid (RA), to facilitate BEC growth with selectivity (Lippmann, Azarin et al. 2012). RA is a key modulator of BBB-properties in BECs during differentiation, markedly enhancing physical barrier function-as demonstrated by elevated TEER- while also increasing junctional protein expression and BEC yield (Lippmann, Al-Ahmad et al. 2014). Subsequently, to stimulate the maturation and purification of BECs, the cells are subcultured onto plates coated with collagen IV-fibronectin extracellular matrix, which is commonly used in primary BEC cultures (Calabria, Weidenfeller et al. 2006). This selective passaging method facilitates the generation of a pure population of mature BECs with a robust BBB phenotype. Overall, this protocol achieves high brain endothelial differentiation efficiency, enables facile purification and ensures reproducible TEER values across independent differentiations. On the contrary, other iPSC differentiation strategies report lower endothelial cell differentiation efficiencies (1-43%), rely on antibody-based methods to yield pure endothelial cell populations(Levenberg, Golub et al. 2002, Wang, Li et al. 2004, Vodyanik, Bork et al. 2005, Wang, Au et al. 2007, Choi, Yu et al. 2009, Goldman, Feraud et al. 2009, Nakahara, Nakamura et al. 2009, Kane, Meloni et al. 2010), and fail to induce BBB properties (Choi, Yu et al. 2009, James, Nam et al. 2010)

Using this protocol, iPSCs derived from a healthy individual (WT) were successfully differentiated into BECs. Phase-contrast microscopy revealed a cobblestone-like endothelial morphology, and by the end of differentiation cells formed a confluent, dense monolayer of endothelial-like cells that appeared tightly sealed with a rounded morphology. Differentiation success was confirmed by the expression of BBB-specific tight junction proteins (e.g. ZO-1, claudin-5) and adherens junction proteins (e.g. VE-cadherin), and endothelial-specific markers (von-Willebrand factor), indicating the generation of mature endothelial cells. Following

purification of BECs onto collagen IV/fibronectin-coated transwells, the BEC monolayer exhibited TEER values above 1000 Ωxcm^2, demonstrating the formation of a functional barrier (Mantle, Min et al. 2016). TEER values above 1000 Ωxcm^2 are in line with values achieved by researchers that established this protocol (Neal, Marinelli et al. 2019). For comparison these TEER values are notably higher than those reported for other models: primary BECs from biopsies reach a maximum of 339 ± 107 Ωxcm^2 (Rubin, Hall et al. 1991), the immortalized human BEC line hCMEC/D3 reaches a maximum of 199 ± 5 Ωxcm^2 (Forster, Burek et al. 2008), while the peripheral endothelium exhibits much lower TEER values, in the range of 2–30 Ωxcm^2 (Lippmann, Azarin et al. 2012). Nevertheless, in vivo TEER values are estimated up to 8000 Ωxcm^2 based on radioactive ion permeability studies (Smith and Rapoport 1986). Although differentiation was successful, prolonged culture of differentiated cells led to a gradual loss of BBB phenotype, as evidenced by discontinuous membrane expression of VE-cadherin by day 10 and a decline in TEER values. These observations suggest that additional optimization may be required to maintain barrier integrity and endothelial phenotype over extended culture periods.

Next, we differentiated iPSCs derived from an AD patient carrying the ApoE ε4/ε4 genotype, the strongest known genetic risk factor for Alzheimer's disease. The differentiation process was largely successful, as indicated by the expression of BBB and endothelial-specific markers, including VE-cadherin and von Willebrand factor, as well as high TEER values (>1000 Ω·cm²). However, following the purification step at day 6, the yield of BECs seeded onto new plates was considerably lower than that observed in the WT line. This observation suggests that although patient-derived iPSCs can successfully differentiate into BECs, they may exhibit increased sensitivity to stress during replating. This highlights the need to optimize and standardize this step to minimize cell loss and enhance reproducibility, particularly by adjusting Accutase incubation time to balance efficient cell dissociation with maintained viability.

Following the successful differentiation of iPSCs to BECs, these cells can be utilized to develop a more physiologically relevant BBB model. To this end, co-culture of iPSC-derived BECs with astrocytes and pericytes is highly recommended. This approach can enhance the BBB properties of BECs, resulting in a more intact and functionally tight barrier. Notably, previous studies have reported that BECs co-cultured with astrocytes exhibit elevated TEER values exceeding 9000 Ω·cm² (Neal, Marinelli et al. 2019), closely approximating those observed *in vivo*.

Given the barrier tightness and the integrity of tight junction dynamics in iPSC-derived BECs, our BBB model is suitable for investigating the transcellular transport of Aβ across BECs. AD patient-derived BECs seeded on transwell inserts can be employed to examine potential impairments in Aβ uptake or transcytosis, in comparison with BECs derived from the age-matched healthy individual. Aβ can be exogenously added to either the luminal or abluminal compartment of the seeded BECs and we can quantitatively measure transcytosed Aβ using ELISA. In addition, BBB permeability assays following exposure to Aβ could be performed to examine whether Aβ increases paracellular permeability across the BBB and disrupts tight junctions. Moreover, iPSCs derived from the AD patient will be differentiated into mature neurons with amyloidogenic properties, using already established protocols (Mahairaki, Ryu

et al. 2014), and seeded at the bottom of the transwell. These neurons can generate and secrete Aβ protein at the abluminal side, enabling the investigation of Aβ transcytosis across disease-relevant or healthy BECs. This approach has the advantage of producing Aβ peptides with pathological conformations and patient-specific posttranslational modifications. Overall, comparing BECs derived from healthy individuals and AD patients can reveal cellular phenotypes associated with BBB dysfunction in AD, as well as potential endocytic abnormalities that contribute to impaired clearance of Aβ across the BBB.

REFERENCES

- Abbott, N. J., L. Ronnback and E. Hansson (2006). "Astrocyte-endothelial interactions at the blood-brain barrier." Nat Rev Neurosci **7**(1): 41-53.
- Apostolova, L. G. (2016). "Alzheimer Disease." Continuum (Minneap Minn) **22**(2 Dementia): 419-434.
- Armstrong, R. A. (2009). "The molecular biology of senile plaques and neurofibrillary tangles in Alzheimer's disease." Folia Neuropathol **47**(4): 289-299.
- Ashford, J. W. (2004). "APOE genotype effects on Alzheimer's disease onset and epidemiology." J Mol Neurosci **23**(3): 157-165.
- Bales, K. R., F. Liu, S. Wu, S. Lin, D. Koger, C. DeLong, J. C. Hansen, P. M. Sullivan and S. M. Paul (2009). "Human APOE isoform-dependent effects on brain beta-amyloid levels in PDAPP transgenic mice." J Neurosci **29**(21): 6771-6779.
- Bao, F., L. Wicklund, P. N. Lacor, W. L. Klein, A. Nordberg and A. Marutle (2012). "Different beta-amyloid oligomer assemblies in Alzheimer brains correlate with age of disease onset and impaired cholinergic activity." Neurobiol Aging **33**(4): 825 e821-813.
- Barker, W. W., C. A. Luis, A. Kashuba, M. Luis, D. G. Harwood, D. Loewenstein, C. Waters, P. Jimison, E. Shepherd, S. Sevush, N. Graff-Radford, D. Newland, M. Todd, B. Miller, M. Gold, K. Heilman, L. Doty, I. Goodman, B. Robinson, G. Pearl, D. Dickson and R. Duara (2002). "Relative frequencies of Alzheimer disease, Lewy body, vascular and frontotemporal dementia, and hippocampal sclerosis in the State of Florida Brain Bank." Alzheimer Dis Assoc Disord **16**(4): 203-212.
- Basagiannis, D., S. Zografou, E. Goula, D. Gkeka, E. Kolettas and S. Christoforidis (2021). "Chemical Inhibitors of Dynamin Exert Differential Effects in VEGF Signaling." Cells **10**(5).
- Basagiannis, D., S. Zografou, C. Murphy, T. Fotsis, L. Morbidelli, M. Ziche, C. Bleck, J. Mercer and S. Christoforidis (2016). "VEGF induces signalling and angiogenesis by directing VEGFR2 internalisation through macropinocytosis." J Cell Sci **129**(21): 4091-4104.
- Bell, R. D., A. P. Sagare, A. E. Friedman, G. S. Bedi, D. M. Holtzman, R. Deane and B. V. Zlokovic (2007). "Transport pathways for clearance of human Alzheimer's amyloid beta-peptide and apolipoproteins E and J in the mouse central nervous system." J Cereb Blood Flow Metab **27**(5): 909-918.
- Bicker, J., G. Alves, A. Fortuna and A. Falcao (2014). "Blood-brain barrier models and their relevance for a successful development of CNS drug delivery systems: a review." Eur J Pharm Biopharm **87**(3): 409-432.
- Borchelt, D. R., G. Thinakaran, C. B. Eckman, M. K. Lee, F. Davenport, T. Ratovitsky, C. M. Prada, G. Kim, S. Seekins, D. Yager, H. H. Slunt, R. Wang, M. Seeger, A. I. Levey, S. E. Gandy, N. G. Copeland, N. A. Jenkins, D. L. Price, S. G. Younkin and S. S. Sisodia (1996). "Familial Alzheimer's disease-linked presenilin 1 variants elevate Abeta1-42/1-40 ratio in vitro and in vivo." Neuron **17**(5): 1005-1013.
- Breijyeh, Z. and R. Karaman (2020). "Comprehensive Review on Alzheimer's Disease: Causes and Treatment." Molecules **25**(24).
- Brightman, M. W. and T. S. Reese (1969). "Junctions between intimately apposed cell membranes in the vertebrate brain." J Cell Biol **40**(3): 648-677.
- Brion, J. P. (1998). "Neurofibrillary tangles and Alzheimer's disease." Eur Neurol **40**(3): 130-140.
- Bryant, D. M., M. C. Kerr, L. A. Hammond, S. R. Joseph, K. E. Mostov, R. D. Teasdale and J. L. Stow (2007). "EGF induces macropinocytosis and SNX1-modulated recycling of E-cadherin." J Cell Sci **120**(Pt 10): 1818-1828.

- Buee, L., T. Bussiere, V. Buee-Scherrer, A. Delacourte and P. R. Hof (2000). "Tau protein isoforms, phosphorylation and role in neurodegenerative disorders." Brain Res Brain Res Rev **33**(1): 95-130.
- Butterfield, D. A. and D. Boyd-Kimball (2004). "Amyloid beta-peptide(1-42) contributes to the oxidative stress and neurodegeneration found in Alzheimer disease brain." Brain Pathol **14**(4): 426-432.
- Calabria, A. R., C. Weidenfeller, A. R. Jones, H. E. de Vries and E. V. Shusta (2006). "Puromycin-purified rat brain microvascular endothelial cell cultures exhibit improved barrier properties in response to glucocorticoid induction." J Neurochem **97**(4): 922-933.
- Campbell, H. K., J. L. Maiers and K. A. DeMali (2017). "Interplay between tight junctions & adherens junctions." Exp Cell Res **358**(1): 39-44.
- Canton, J., D. Schlam, C. Breuer, M. Gutschow, M. Glogauer and S. Grinstein (2016). "Calcium-sensing receptors signal constitutive macropinocytosis and facilitate the uptake of NOD2 ligands in macrophages." Nat Commun **7**: 11284.
- Cardoso, F. L., D. Brites and M. A. Brito (2010). "Looking at the blood-brain barrier: molecular anatomy and possible investigation approaches." Brain Res Rev **64**(2): 328-363.
- Castellano, J. M., J. Kim, F. R. Stewart, H. Jiang, R. B. DeMattos, B. W. Patterson, A. M. Fagan, J. C. Morris, K. G. Mawuenyega, C. Cruchaga, A. M. Goate, K. R. Bales, S. M. Paul, R. J. Bateman and D. M. Holtzman (2011). "Human apoE isoforms differentially regulate brain amyloid-beta peptide clearance." Sci Transl Med **3**(89): 89ra57.
- Chen, G. F., T. H. Xu, Y. Yan, Y. R. Zhou, Y. Jiang, K. Melcher and H. E. Xu (2017). "Amyloid beta: structure, biology and structure-based therapeutic development." Acta Pharmacol Sin **38**(9): 1205-1235.
- Cho, S. J., M. H. Park, C. Han, K. Yoon and Y. H. Koh (2017). "VEGFR2 alteration in Alzheimer's disease." Sci Rep **7**(1): 17713.
- Choi, K. D., J. Yu, K. Smuga-Otto, G. Salvagiotto, W. Rehrauer, M. Vodyanik, J. Thomson and I. Slukvin (2009). "Hematopoietic and endothelial differentiation of human induced pluripotent stem cells." Stem Cells **27**(3): 559-567.
- Commisso, C., S. M. Davidson, R. G. Soydaner-Azeloglu, S. J. Parker, J. J. Kamphorst, S. Hackett, E. Grabocka, M. Nofal, J. A. Drebin, C. B. Thompson, J. D. Rabinowitz, C. M. Metallo, M. G. Vander Heiden and D. Bar-Sagi (2013). "Macropinocytosis of protein is an amino acid supply route in Ras-transformed cells." Nature **497**(7451): 633-637.
- Coomber, B. L. and P. A. Stewart (1985). "Morphometric analysis of CNS microvascular endothelium." Microvasc Res **30**(1): 99-115.
- Corder, E. H., A. M. Saunders, N. J. Risch, W. J. Strittmatter, D. E. Schmechel, P. C. Gaskell, Jr., J. B. Rimmler, P. A. Locke, P. M. Conneally, K. E. Schmader and et al. (1994). "Protective effect of apolipoprotein E type 2 allele for late onset Alzheimer disease." Nat Genet **7**(2): 180-184.
- d'Uscio, L. V., T. He, A. V. Santhanam and Z. S. Katusic (2018). "Endothelium-specific amyloid precursor protein deficiency causes endothelial dysfunction in cerebral arteries." J Cereb Blood Flow Metab **38**(10): 1715-1726.
- Daneman, R., D. Agalliu, L. Zhou, F. Kuhnert, C. J. Kuo and B. A. Barres (2009). "Wnt/beta-catenin signaling is required for CNS, but not non-CNS, angiogenesis." Proc Natl Acad Sci U S A **106**(2): 641-646.
- Daneman, R. and A. Prat (2015). "The blood-brain barrier." Cold Spring Harb Perspect Biol **7**(1): a020412.
- Das, D., J. Li, S. Liu, E. Oh, L. Cheng, C. Lyketsos and V. Mahairaki (2020). "Generation and characterization of a novel human iPSC line from a resilient Alzheimer's disease patient." Stem Cell Res **48**: 101979.

- De-Paula, V. J., M. Radanovic, B. S. Diniz and O. V. Forlenza (2012). "Alzheimer's disease." Subcell Biochem **65**: 329-352.
- de Bruijn, R. F. and M. A. Ikram (2014). "Cardiovascular risk factors and future risk of Alzheimer's disease." BMC Med **12**: 130.
- Deane, R., A. Sagare, K. Hamm, M. Parisi, S. Lane, M. B. Finn, D. M. Holtzman and B. V. Zlokovic (2008). "apoE isoform-specific disruption of amyloid beta peptide clearance from mouse brain." J Clin Invest **118**(12): 4002-4013.
- Dharmawardhane, S., A. Schurmann, M. A. Sells, J. Chernoff, S. L. Schmid and G. M. Bokoch (2000). "Regulation of macropinocytosis by p21-activated kinase-1." Mol Biol Cell **11**(10): 3341-3352.
- Dore-Duffy, P., C. Owen, R. Balabanov, S. Murphy, T. Beaumont and J. A. Rafols (2000). "Pericyte migration from the vascular wall in response to traumatic brain injury." Microvasc Res **60**(1): 55-69.
- Dotiwala, A. K., C. McCausland and N. S. Samra (2025). Anatomy, Head and Neck: Blood Brain Barrier. StatPearls. Treasure Island (FL) ineligible companies. Disclosure: Cassidy McCausland declares no relevant financial relationships with ineligible companies. Disclosure: Navdeep Samra declares no relevant financial relationships with ineligible companies.
- Dragsten, P. R., R. Blumenthal and J. S. Handler (1981). "Membrane asymmetry in epithelia: is the tight junction a barrier to diffusion in the plasma membrane?" Nature **294**(5843): 718-722.
- Dubois, B., H. Hampel, H. H. Feldman, P. Scheltens, P. Aisen, S. Andrieu, H. Bakardjian, H. Benali, L. Bertram, K. Blennow, K. Broich, E. Cavedo, S. Crutch, J. F. Dartigues, C. Duyckaerts, S. Epelbaum, G. B. Frisoni, S. Gauthier, R. Genthon, A. A. Gouw, M. O. Habert, D. M. Holtzman, M. Kivipelto, S. Lista, J. L. Molinuevo, S. E. O'Bryant, G. D. Rabinovici, C. Rowe, S. Salloway, L. S. Schneider, R. Sperling, M. Teichmann, M. C. Carrillo, J. Cummings, C. R. Jack, Jr., G. Proceedings of the Meeting of the International Working, A. D. the American Alzheimer's Association on "The Preclinical State of, July and U. S. A. Washington Dc (2016). "Preclinical Alzheimer's disease: Definition, natural history, and diagnostic criteria." Alzheimers Dement **12**(3): 292-323.
- Engelhardt, B., R. O. Carare, I. Bechmann, A. Flugel, J. D. Laman and R. O. Weller (2016). "Vascular, glial, and lymphatic immune gateways of the central nervous system." Acta Neuropathol **132**(3): 317-338.
- Ertekin-Taner, N. (2007). "Genetics of Alzheimer's disease: a centennial review." Neurol Clin **25**(3): 611-667, v.
- Esparza, T. J., H. Zhao, J. R. Cirrito, N. J. Cairns, R. J. Bateman, D. M. Holtzman and D. L. Brody (2013). "Amyloid-beta oligomerization in Alzheimer dementia versus high-pathology controls." Ann Neurol **73**(1): 104-119.
- Farrer, L. A., L. A. Cupples, J. L. Haines, B. Hyman, W. A. Kukull, R. Mayeux, R. H. Myers, M. A. Pericak-Vance, N. Risch and C. M. van Duijn (1997). "Effects of age, sex, and ethnicity on the association between apolipoprotein E genotype and Alzheimer disease. A meta-analysis. APOE and Alzheimer Disease Meta Analysis Consortium." JAMA **278**(16): 1349-1356.
- Ferreira, S. T. and W. L. Klein (2011). "The Abeta oligomer hypothesis for synapse failure and memory loss in Alzheimer's disease." Neurobiol Learn Mem **96**(4): 529-543.
- Ferreira, S. T., M. V. Lourenco, M. M. Oliveira and F. G. De Felice (2015). "Soluble amyloid-beta oligomers as synaptotoxins leading to cognitive impairment in Alzheimer's disease." Front Cell Neurosci **9**: 191.
- Findeis, M. A. (2007). "The role of amyloid beta peptide 42 in Alzheimer's disease." Pharmacol Ther **116**(2): 266-286.

- Forster, C., M. Burek, I. A. Romero, B. Weksler, P. O. Couraud and D. Drenckhahn (2008). "Differential effects of hydrocortisone and TNFalpha on tight junction proteins in an in vitro model of the human blood-brain barrier." J Physiol **586**(7): 1937-1949.
- Goedert, M. and M. G. Spillantini (2006). "A century of Alzheimer's disease." Science **314**(5800): 777-781.
- Goldman, O., O. Feraud, J. Boyer-Di Ponio, C. Driancourt, D. Clay, M. C. Le Bousse-Kerdiles, A. Bennaceur-Griscelli and G. Uzan (2009). "A boost of BMP4 accelerates the commitment of human embryonic stem cells to the endothelial lineage." Stem Cells **27**(8): 1750-1759.
- Gonzalez-Mariscal, L., R. Tapia and D. Chamorro (2008). "Crosstalk of tight junction components with signaling pathways." Biochim Biophys Acta **1778**(3): 729-756.
- Gotz, J., A. Probst, M. G. Spillantini, T. Schafer, R. Jakes, K. Burki and M. Goedert (1995). "Somatodendritic localization and hyperphosphorylation of tau protein in transgenic mice expressing the longest human brain tau isoform." EMBO J **14**(7): 1304-1313.
- Guerreiro, R. and J. Bras (2015). "The age factor in Alzheimer's disease." Genome Med **7**: 106.
- Hardy, J. and D. J. Selkoe (2002). "The amyloid hypothesis of Alzheimer's disease: progress and problems on the road to therapeutics." Science **297**(5580): 353-356.
- Hardy, J. A. and G. A. Higgins (1992). "Alzheimer's disease: the amyloid cascade hypothesis." Science **256**(5054): 184-185.
- Harold, D., R. Abraham, P. Hollingworth, R. Sims, A. Gerrish, M. L. Hamshere, J. S. Pahwa, V. Moskvina, K. Dowzell, A. Williams, N. Jones, C. Thomas, A. Stretton, A. R. Morgan, S. Lovestone, J. Powell, P. Proitsi, M. K. Lupton, C. Brayne, D. C. Rubinsztein, M. Gill, B. Lawlor, A. Lynch, K. Morgan, K. S. Brown, P. A. Passmore, D. Craig, B. McGuinness, S. Todd, C. Holmes, D. Mann, A. D. Smith, S. Love, P. G. Kehoe, J. Hardy, S. Mead, N. Fox, M. Rossor, J. Collinge, W. Maier, F. Jessen, B. Schurmann, R. Heun, H. van den Bussche, I. Heuser, J. Kornhuber, J. Wiltfang, M. Dichgans, L. Frolich, H. Hampel, M. Hull, D. Rujescu, A. M. Goate, J. S. Kauwe, C. Cruchaga, P. Nowotny, J. C. Morris, K. Mayo, K. Sleegers, K. Bettens, S. Engelborghs, P. P. De Deyn, C. Van Broeckhoven, G. Livingston, N. J. Bass, H. Gurling, A. McQuillin, R. Gwilliam, P. Deloukas, A. Al-Chalabi, C. E. Shaw, M. Tsolaki, A. B. Singleton, R. Guerreiro, T. W. Muhleisen, M. M. Nothen, S. Moebus, K. H. Jockel, N. Klopp, H. E. Wichmann, M. M. Carrasquillo, V. S. Pankratz, S. G. Younkin, P. A. Holmans, M. O'Donovan, M. J. Owen and J. Williams (2009). "Genome-wide association study identifies variants at CLU and PICALM associated with Alzheimer's disease." Nat Genet **41**(10): 1088-1093.
- Hollmann, E. K., A. K. Bailey, A. V. Potharazu, M. D. Neely, A. B. Bowman and E. S. Lippmann (2017). "Accelerated differentiation of human induced pluripotent stem cells to blood-brain barrier endothelial cells." Fluids Barriers CNS **14**(1): 9.
- Hou, Y., X. Dan, M. Babbar, Y. Wei, S. G. Hasselbalch, D. L. Croteau and V. A. Bohr (2019). "Ageing as a risk factor for neurodegenerative disease." Nat Rev Neurol **15**(10): 565-581.
- Iadecola, C. (2017). "The Neurovascular Unit Coming of Age: A Journey through Neurovascular Coupling in Health and Disease." Neuron **96**(1): 17-42.
- Igarashi, Y., H. Utsumi, H. Chiba, Y. Yamada-Sasamori, H. Tobioka, Y. Kamimura, K. Furuuchi, Y. Kokai, T. Nakagawa, M. Mori and N. Sawada (1999). "Glial cell line-derived neurotrophic factor induces barrier function of endothelial cells forming the blood-brain barrier." Biochem Biophys Res Commun **261**(1): 108-112.
- Ittner, L. M., Y. D. Ke, F. Delerue, M. Bi, A. Gladbach, J. van Eersel, H. Wolfing, B. C. Chieng, M. J. Christie, I. A. Napier, A. Eckert, M. Staufenbiel, E. Hardeman and J. Gotz

(2010). "Dendritic function of tau mediates amyloid-beta toxicity in Alzheimer's disease mouse models." Cell **142**(3): 387-397.
- Ivanov, A. I. (2014). Pharmacological Inhibitors of Exocytosis and Endocytosis: Novel Bullets for Old Targets. Exocytosis and Endocytosis. A. I. Ivanov. New York, NY, Springer New York**:** 3-18.
- James, D., H. S. Nam, M. Seandel, D. Nolan, T. Janovitz, M. Tomishima, L. Studer, G. Lee, D. Lyden, R. Benezra, N. Zaninovic, Z. Rosenwaks, S. Y. Rabbany and S. Rafii (2010). "Expansion and maintenance of human embryonic stem cell-derived endothelial cells by TGFbeta inhibition is Id1 dependent." Nat Biotechnol **28**(2): 161-166.
- Jamieson, J. J., P. C. Searson and S. Gerecht (2017). "Engineering the human blood-brain barrier in vitro." J Biol Eng **11**: 37.
- Jiang, Q., C. Y. Lee, S. Mandrekar, B. Wilkinson, P. Cramer, N. Zelcer, K. Mann, B. Lamb, T. M. Willson, J. L. Collins, J. C. Richardson, J. D. Smith, T. A. Comery, D. Riddell, D. M. Holtzman, P. Tontonoz and G. E. Landreth (2008). "ApoE promotes the proteolytic degradation of Abeta." Neuron **58**(5): 681-693.
- Jones, A. R. and E. V. Shusta (2007). "Blood-brain barrier transport of therapeutics via receptor-mediation." Pharm Res **24**(9): 1759-1771.
- Kadry, H., B. Noorani and L. Cucullo (2020). "A blood-brain barrier overview on structure, function, impairment, and biomarkers of integrity." Fluids Barriers CNS **17**(1): 69.
- Kane, N. M., M. Meloni, H. L. Spencer, M. A. Craig, R. Strehl, G. Milligan, M. D. Houslay, J. C. Mountford, C. Emanueli and A. H. Baker (2010). "Derivation of endothelial cells from human embryonic stem cells by directed differentiation: analysis of microRNA and angiogenesis in vitro and in vivo." Arterioscler Thromb Vasc Biol **30**(7): 1389-1397.
- Kanekiyo, T. and G. Bu (2014). "The low-density lipoprotein receptor-related protein 1 and amyloid-beta clearance in Alzheimer's disease." Front Aging Neurosci **6**: 93.
- Kihara, T. and S. Shimohama (2004). "Alzheimer's disease and acetylcholine receptors." Acta Neurobiol Exp (Wars) **64**(1): 99-105.
- Knox, E. G., M. R. Aburto, G. Clarke, J. F. Cryan and C. M. O'Driscoll (2022). "The blood-brain barrier in aging and neurodegeneration." Mol Psychiatry **27**(6): 2659-2673.
- Koffie, R. M., B. T. Hyman and T. L. Spires-Jones (2011). "Alzheimer's disease: synapses gone cold." Mol Neurodegener **6**(1): 63.
- Krause, G., L. Winkler, C. Piehl, I. Blasig, J. Piontek and S. L. Muller (2009). "Structure and function of extracellular claudin domains." Ann N Y Acad Sci **1165**: 34-43.
- Kumar, A., J. Sidhu, F. Lui and J. W. Tsao (2025). Alzheimer Disease. StatPearls. Treasure Island (FL) ineligible companies. Disclosure: Jaskirat Sidhu declares no relevant financial relationships with ineligible companies. Disclosure: Forshing Lui declares no relevant financial relationships with ineligible companies. Disclosure: Jack Tsao declares no relevant financial relationships with ineligible companies.
- Langen, U. H., S. Ayloo and C. Gu (2019). "Development and Cell Biology of the Blood-Brain Barrier." Annu Rev Cell Dev Biol **35**: 591-613.
- Levenberg, S., J. S. Golub, M. Amit, J. Itskovitz-Eldor and R. Langer (2002). "Endothelial cells derived from human embryonic stem cells." Proc Natl Acad Sci U S A **99**(7): 4391-4396.
- Lippmann, E. S., A. Al-Ahmad, S. M. Azarin, S. P. Palecek and E. V. Shusta (2014). "A retinoic acid-enhanced, multicellular human blood-brain barrier model derived from stem cell sources." Sci Rep **4**: 4160.
- Lippmann, E. S., A. Al-Ahmad, S. P. Palecek and E. V. Shusta (2013). "Modeling the blood-brain barrier using stem cell sources." Fluids Barriers CNS **10**(1): 2.

- Lippmann, E. S., S. M. Azarin, J. E. Kay, R. A. Nessler, H. K. Wilson, A. Al-Ahmad, S. P. Palecek and E. V. Shusta (2012). "Derivation of blood-brain barrier endothelial cells from human pluripotent stem cells." Nat Biotechnol **30**(8): 783-791.
- Lippmann, E. S., M. C. Estevez-Silva and R. S. Ashton (2014). "Defined human pluripotent stem cell culture enables highly efficient neuroepithelium derivation without small molecule inhibitors." Stem Cells **32**(4): 1032-1042.
- Livingston, G., J. Huntley, A. Sommerlad, D. Ames, C. Ballard, S. Banerjee, C. Brayne, A. Burns, J. Cohen-Mansfield, C. Cooper, S. G. Costafreda, A. Dias, N. Fox, L. N. Gitlin, R. Howard, H. C. Kales, M. Kivimaki, E. B. Larson, A. Ogunniyi, V. Orgeta, K. Ritchie, K. Rockwood, E. L. Sampson, Q. Samus, L. S. Schneider, G. Selbaek, L. Teri and N. Mukadam (2020). "Dementia prevention, intervention, and care: 2020 report of the Lancet Commission." Lancet **396**(10248): 413-446.
- MacLeod, R., E. K. Hillert, R. T. Cameron and G. S. Baillie (2015). "The role and therapeutic targeting of alpha-, beta- and gamma-secretase in Alzheimer's disease." Future Sci OA **1**(3): FSO11.
- Mahairaki, V., J. Ryu, A. Peters, Q. Chang, T. Li, T. S. Park, P. W. Burridge, C. C. Talbot, Jr., L. Asnaghi, L. J. Martin, E. T. Zambidis and V. E. Koliatsos (2014). "Induced pluripotent stem cells from familial Alzheimer's disease patients differentiate into mature neurons with amyloidogenic properties." Stem Cells Dev **23**(24): 2996-3010.
- Mandel, L. J., R. Bacallao and G. Zampighi (1993). "Uncoupling of the molecular 'fence' and paracellular 'gate' functions in epithelial tight junctions." Nature **361**(6412): 552-555.
- Mann, D. M., T. Iwatsubo, S. M. Pickering-Brown, F. Owen, T. C. Saido and R. H. Perry (1997). "Preferential deposition of amyloid beta protein (Abeta) in the form Abeta40 in Alzheimer's disease is associated with a gene dosage effect of the apolipoprotein E E4 allele." Neurosci Lett **221**(2-3): 81-84.
- Mantle, J. L. and K. H. Lee (2019). "Immunoglobulin G transport increases in an in vitro blood-brain barrier model with amyloid-beta and with neuroinflammatory cytokines." Biotechnol Bioeng **116**(7): 1752-1761.
- Mantle, J. L., L. Min and K. H. Lee (2016). "Minimum Transendothelial Electrical Resistance Thresholds for the Study of Small and Large Molecule Drug Transport in a Human in Vitro Blood-Brain Barrier Model." Mol Pharm **13**(12): 4191-4198.
- Mawuenyega, K. G., W. Sigurdson, V. Ovod, L. Munsell, T. Kasten, J. C. Morris, K. E. Yarasheski and R. J. Bateman (2010). "Decreased clearance of CNS beta-amyloid in Alzheimer's disease." Science **330**(6012): 1774.
- Mayor, S. and R. E. Pagano (2007). "Pathways of clathrin-independent endocytosis." Nat Rev Mol Cell Biol **8**(8): 603-612.
- Mehta, D. and A. B. Malik (2006). "Signaling mechanisms regulating endothelial permeability." Physiol Rev **86**(1): 279-367.
- Michaux, G. and D. F. Cutler (2004). "How to roll an endothelial cigar: the biogenesis of Weibel-Palade bodies." Traffic **5**(2): 69-78.
- Morales, J. R., I. Ballesteros, J. M. Deniz, O. Hurtado, J. Vivancos, F. Nombela, I. Lizasoain, A. Castrillo and M. A. Moro (2008). "Activation of liver X receptors promotes neuroprotection and reduces brain inflammation in experimental stroke." Circulation **118**(14): 1450-1459.
- Moreira, P. I., C. Carvalho, X. Zhu, M. A. Smith and G. Perry (2010). "Mitochondrial dysfunction is a trigger of Alzheimer's disease pathophysiology." Biochim Biophys Acta **1802**(1): 2-10.
- Mylvaganam, S., S. A. Freeman and S. Grinstein (2021). "The cytoskeleton in phagocytosis and macropinocytosis." Curr Biol **31**(10): R619-R632.

- Nakahara, M., N. Nakamura, S. Matsuyama, Y. Yogiashi, K. Yasuda, Y. Kondo, A. Yuo and K. Saeki (2009). "High-efficiency production of subculturable vascular endothelial cells from feeder-free human embryonic stem cells without cell-sorting technique." Cloning Stem Cells **11**(4): 509-522.
- Neal, E. H., N. A. Marinelli, Y. Shi, P. M. McClatchey, K. M. Balotin, D. R. Gullett, K. A. Hagerla, A. B. Bowman, K. C. Ess, J. P. Wikswo and E. S. Lippmann (2019). "A Simplified, Fully Defined Differentiation Scheme for Producing Blood-Brain Barrier Endothelial Cells from Human iPSCs." Stem Cell Reports **12**(6): 1380-1388.
- Nian, K., I. C. Harding, I. M. Herman and E. E. Ebong (2020). "Blood-Brain Barrier Damage in Ischemic Stroke and Its Regulation by Endothelial Mechanotransduction." Front Physiol **11**: 605398.
- O'Brien, R. J. and P. C. Wong (2011). "Amyloid precursor protein processing and Alzheimer's disease." Annu Rev Neurosci **34**: 185-204.
- Oakley, H., S. L. Cole, S. Logan, E. Maus, P. Shao, J. Craft, A. Guillozet-Bongaarts, M. Ohno, J. Disterhoft, L. Van Eldik, R. Berry and R. Vassar (2006). "Intraneuronal beta-amyloid aggregates, neurodegeneration, and neuron loss in transgenic mice with five familial Alzheimer's disease mutations: potential factors in amyloid plaque formation." J Neurosci **26**(40): 10129-10140.
- Pardridge, W. M. (2002). "Drug and gene targeting to the brain with molecular Trojan horses." Nat Rev Drug Discov **1**(2): 131-139.
- Pardridge, W. M. (2012). "Drug transport across the blood-brain barrier." J Cereb Blood Flow Metab **32**(11): 1959-1972.
- Perel, P., I. Roberts, E. Sena, P. Wheble, C. Briscoe, P. Sandercock, M. Macleod, L. E. Mignini, P. Jayaram and K. S. Khan (2007). "Comparison of treatment effects between animal experiments and clinical trials: systematic review." BMJ **334**(7586): 197.
- Radde, R., T. Bolmont, S. A. Kaeser, J. Coomaraswamy, D. Lindau, L. Stoltze, M. E. Calhoun, F. Jaggi, H. Wolburg, S. Gengler, C. Haass, B. Ghetti, C. Czech, C. Holscher, P. M. Mathews and M. Jucker (2006). "Abeta42-driven cerebral amyloidosis in transgenic mice reveals early and robust pathology." EMBO Rep **7**(9): 940-946.
- Ramanathan, A., A. R. Nelson, A. P. Sagare and B. V. Zlokovic (2015). "Impaired vascular-mediated clearance of brain amyloid beta in Alzheimer's disease: the role, regulation and restoration of LRP1." Front Aging Neurosci **7**: 136.
- Recouvreux, M. V. and C. Commisso (2017). "Macropinocytosis: A Metabolic Adaptation to Nutrient Stress in Cancer." Front Endocrinol (Lausanne) **8**: 261.
- Redka, D. S., M. Gutschow, S. Grinstein and J. Canton (2018). "Differential ability of proinflammatory and anti-inflammatory macrophages to perform macropinocytosis." Mol Biol Cell **29**(1): 53-65.
- Riedel, B. C., P. M. Thompson and R. D. Brinton (2016). "Age, APOE and sex: Triad of risk of Alzheimer's disease." J Steroid Biochem Mol Biol **160**: 134-147.
- Ristori, E., S. Donnini and M. Ziche (2020). "New Insights Into Blood-Brain Barrier Maintenance: The Homeostatic Role of beta-Amyloid Precursor Protein in Cerebral Vasculature." Front Physiol **11**: 1056.
- Rubin, L. L., D. E. Hall, S. Porter, K. Barbu, C. Cannon, H. C. Horner, M. Janatpour, C. W. Liaw, K. Manning, J. Morales and et al. (1991). "A cell culture model of the blood-brain barrier." J Cell Biol **115**(6): 1725-1735.
- Santos, C. Y., P. J. Snyder, W. C. Wu, M. Zhang, A. Echeverria and J. Alber (2017). "Pathophysiologic relationship between Alzheimer's disease, cerebrovascular disease, and cardiovascular risk: A review and synthesis." Alzheimers Dement (Amst) **7**: 69-87.
- Scita, G. and P. P. Di Fiore (2010). "The endocytic matrix." Nature **463**(7280): 464-473.

- Shankar, G. M. and D. M. Walsh (2009). "Alzheimer's disease: synaptic dysfunction and Abeta." Mol Neurodegener **4**: 48.
- Shibata, M., S. Yamada, S. R. Kumar, M. Calero, J. Bading, B. Frangione, D. M. Holtzman, C. A. Miller, D. K. Strickland, J. Ghiso and B. V. Zlokovic (2000). "Clearance of Alzheimer's amyloid-ss(1-40) peptide from brain by LDL receptor-related protein-1 at the blood-brain barrier." J Clin Invest **106**(12): 1489-1499.
- Smith, Q. R. and S. I. Rapoport (1986). "Cerebrovascular permeability coefficients to sodium, potassium, and chloride." J Neurochem **46**(6): 1732-1742.
- Srinivasan, B., A. R. Kolli, M. B. Esch, H. E. Abaci, M. L. Shuler and J. J. Hickman (2015). "TEER measurement techniques for in vitro barrier model systems." J Lab Autom **20**(2): 107-126.
- Stamatovic, S. M., A. M. Johnson, R. F. Keep and A. V. Andjelkovic (2016). "Junctional proteins of the blood-brain barrier: New insights into function and dysfunction." Tissue Barriers **4**(1): e1154641.
- Stenman, J. M., J. Rajagopal, T. J. Carroll, M. Ishibashi, J. McMahon and A. P. McMahon (2008). "Canonical Wnt signaling regulates organ-specific assembly and differentiation of CNS vasculature." Science **322**(5905): 1247-1250.
- Sumbria, R. and M. Fisher (2017). Chapter 8 - Endothelium. Primer on Cerebrovascular Diseases (Second Edition). L. R. Caplan, J. Biller, M. C. Leary et al. San Diego, Academic Press**:** 47-51.
- Swanson, J. A. (2008). "Shaping cups into phagosomes and macropinosomes." Nat Rev Mol Cell Biol **9**(8): 639-649.
- Sweeney, M. D., Z. Zhao, A. Montagne, A. R. Nelson and B. V. Zlokovic (2019). "Blood-Brain Barrier: From Physiology to Disease and Back." Physiol Rev **99**(1): 21-78.
- Tabaton, M. and A. Piccini (2005). "Role of water-soluble amyloid-beta in the pathogenesis of Alzheimer's disease." Int J Exp Pathol **86**(3): 139-145.
- Tarasoff-Conway, J. M., R. O. Carare, R. S. Osorio, L. Glodzik, T. Butler, E. Fieremans, L. Axel, H. Rusinek, C. Nicholson, B. V. Zlokovic, B. Frangione, K. Blennow, J. Menard, H. Zetterberg, T. Wisniewski and M. J. de Leon (2015). "Clearance systems in the brain-implications for Alzheimer disease." Nat Rev Neurol **11**(8): 457-470.
- Tcw, J. and A. M. Goate (2017). "Genetics of beta-Amyloid Precursor Protein in Alzheimer's Disease." Cold Spring Harb Perspect Med **7**(6).
- Teixeira, M. I., C. M. Lopes, M. H. Amaral and P. C. Costa (2020). "Current insights on lipid nanocarrier-assisted drug delivery in the treatment of neurodegenerative diseases." Eur J Pharm Biopharm **149**: 192-217.
- Uddin, M. S., M. T. Kabir, P. Jeandet, B. Mathew, G. M. Ashraf, A. Perveen, M. N. Bin-Jumah, S. A. Mousa and M. M. Abdel-Daim (2020). "Novel Anti-Alzheimer's Therapeutic Molecules Targeting Amyloid Precursor Protein Processing." Oxid Med Cell Longev **2020**: 7039138.
- Uddin, M. S., M. T. Kabir, M. S. Rahman, T. Behl, P. Jeandet, G. M. Ashraf, A. Najda, M. N. Bin-Jumah, H. R. El-Seedi and M. M. Abdel-Daim (2020). "Revisiting the Amyloid Cascade Hypothesis: From Anti-Abeta Therapeutics to Auspicious New Ways for Alzheimer's Disease." Int J Mol Sci **21**(16).
- Van Uden, E., M. Mallory, I. Veinbergs, M. Alford, E. Rockenstein and E. Masliah (2002). "Increased extracellular amyloid deposition and neurodegeneration in human amyloid precursor protein transgenic mice deficient in receptor-associated protein." J Neurosci **22**(21): 9298-9304.
- Veltman, D. M., T. D. Williams, G. Bloomfield, B. C. Chen, E. Betzig, R. H. Insall and R. R. Kay (2016). "A plasma membrane template for macropinocytic cups." Elife **5**.

- Vestweber, D. (2008). "VE-cadherin: the major endothelial adhesion molecule controlling cellular junctions and blood vessel formation." Arterioscler Thromb Vasc Biol **28**(2): 223-232.
- Vodyanik, M. A., J. A. Bork, J. A. Thomson and Slukvin, II (2005). "Human embryonic stem cell-derived CD34+ cells: efficient production in the coculture with OP9 stromal cells and analysis of lymphohematopoietic potential." Blood **105**(2): 617-626.
- Wang, L. and S. M. Dudek (2009). "Regulation of vascular permeability by sphingosine 1-phosphate." Microvasc Res **77**(1): 39-45.
- Wang, L., L. Li, F. Shojaei, K. Levac, C. Cerdan, P. Menendez, T. Martin, A. Rouleau and M. Bhatia (2004). "Endothelial and hematopoietic cell fate of human embryonic stem cells originates from primitive endothelium with hemangioblastic properties." Immunity **21**(1): 31-41.
- Wang, Z. Z., P. Au, T. Chen, Y. Shao, L. M. Daheron, H. Bai, M. Arzigian, D. Fukumura, R. K. Jain and D. T. Scadden (2007). "Endothelial cells derived from human embryonic stem cells form durable blood vessels in vivo." Nat Biotechnol **25**(3): 317-318.
- Wattmo, C., L. Minthon and A. K. Wallin (2016). "Mild versus moderate stages of Alzheimer's disease: three-year outcomes in a routine clinical setting of cholinesterase inhibitor therapy." Alzheimers Res Ther **8**: 7.
- Weggen, S. and D. Beher (2012). "Molecular consequences of amyloid precursor protein and presenilin mutations causing autosomal-dominant Alzheimer's disease." Alzheimers Res Ther **4**(2): 9.
- Weibel, E. (2012). "Ewald Weibel: an organelle of his very own, and more. Interview by Caitlin Sedwick." J Cell Biol **197**(1): 4-5.
- Weibel, E. R. and G. E. Palade (1964). "New Cytoplasmic Components in Arterial Endothelia." J Cell Biol **23**(1): 101-112.
- Weksler, B. B., E. A. Subileau, N. Perriere, P. Charneau, K. Holloway, M. Leveque, H. Tricoire-Leignel, A. Nicotra, S. Bourdoulous, P. Turowski, D. K. Male, F. Roux, J. Greenwood, I. A. Romero and P. O. Couraud (2005). "Blood-brain barrier-specific properties of a human adult brain endothelial cell line." FASEB J **19**(13): 1872-1874.
- West, M. A., A. R. Prescott, E. L. Eskelinen, A. J. Ridley and C. Watts (2000). "Rac is required for constitutive macropinocytosis by dendritic cells but does not control its downregulation." Curr Biol **10**(14): 839-848.
- Wildsmith, K. R., M. Holley, J. C. Savage, R. Skerrett and G. E. Landreth (2013). "Evidence for impaired amyloid beta clearance in Alzheimer's disease." Alzheimers Res Ther **5**(4): 33.
- Wolburg, H., S. Noell, A. Mack, K. Wolburg-Buchholz and P. Fallier-Becker (2009). "Brain endothelial cells and the glio-vascular complex." Cell Tissue Res **335**(1): 75-96.
- Yiannopoulou, K. G. and S. G. Papageorgiou (2020). "Current and Future Treatments in Alzheimer Disease: An Update." J Cent Nerv Syst Dis **12**: 1179573520907397.
- Zelcer, N., N. Khanlou, R. Clare, Q. Jiang, E. G. Reed-Geaghan, G. E. Landreth, H. V. Vinters and P. Tontonoz (2007). "Attenuation of neuroinflammation and Alzheimer's disease pathology by liver x receptors." Proc Natl Acad Sci U S A **104**(25): 10601-10606.
- Zhao, Z., A. R. Nelson, C. Betsholtz and B. V. Zlokovic (2015). "Establishment and Dysfunction of the Blood-Brain Barrier." Cell **163**(5): 1064-1078.
- Zhao, Z., A. P. Sagare, Q. Ma, M. R. Halliday, P. Kong, K. Kisler, E. A. Winkler, A. Ramanathan, T. Kanekiyo, G. Bu, N. C. Owens, S. V. Rege, G. Si, A. Ahuja, D. Zhu, C. A. Miller, J. A. Schneider, M. Maeda, T. Maeda, T. Sugawara, J. K. Ichida and B. V. Zlokovic (2015). "Central role for PICALM in amyloid-beta blood-brain barrier transcytosis and clearance." Nat Neurosci **18**(7): 978-987.

- Zlokovic, B. V. (2013). "Cerebrovascular effects of apolipoprotein E: implications for Alzheimer disease." JAMA Neurol **70**(4): 440-444.